MycoKeys 76: 1–16 (2020)
doi: 10.3897/mycokeys.76.58628
https://mycokeys.pensoft.net

RESEARCH ARTICLE

A peer-reviewed open-access journal
MycoKeys
Launched to accelerate biodiversity research

# The insights into the evolutionary history of *Translucidithyrium*: based on a newly-discovered species

Xinhao Li[1], Hai-Xia Wu[1], Jinchen Li[1], Hang Chen[1], Wei Wang[1]

1 *International Fungal Research and Development Centre, The Research Institute of Resource Insects, Chinese Academy of Forestry, Kunming 650224, China*

Corresponding author: Hai-Xia Wu (aileen2008haixia@gmail.com, haixiawu@caf.ac.cn)

Academic editor: N. Wijayawardene | Received 15 September 2020 | Accepted 25 November 2020 | Published 17 December 2020

**Citation:** Li X, Wu H-X, Li J, Chen H, Wang W (2020) The insights into the evolutionary history of *Translucidithyrium*: based on a newly-discovered species. MycoKeys 76: 1–16. https://doi.org/10.3897/mycokeys.76.58628

## Abstract

During the field studies, a *Translucidithyrium*-like taxon was collected in Xishuangbanna of Yunnan Province, during an investigation into the diversity of microfungi in the southwest of China. Morphological observations and phylogenetic analysis of combined LSU and ITS sequences revealed that the new taxon is a member of the genus *Translucidithyrium* and it is distinct from other species. Therefore, *Translucidithyrium chinense* **sp. nov.** is introduced here. The Maximum Clade Credibility (MCC) tree from LSU rDNA of *Translucidithyrium* and related species indicated the divergence time of existing and new species of *Translucidithyrium* was crown age at 16 (4–33) Mya. Combining the estimated divergence time, paleoecology and plate tectonic movements with the corresponding geological time scale, we proposed a hypothesis that the speciation (estimated divergence time) of *T. chinense* was earlier than *T. thailandicum*. Our findings provided new insights into the species of *Translucidithyrium* about ecological adaptation and speciation in two separate areas.

## Keywords

Divergence time, morphological characteristics, new species, Phaeothecoidiellaceae, phylogeny, speciation, taxonomy

## Introduction

The sooty blotch and flyspeck fungi are widespread species and commonly occur on the surface of leaves, stems and fruits in tropical and subtropical zones (Yang et al. 2010; Gleason et al. 2011; Hongsanan et al. 2017; Zeng et al. 2018). Although these

fungi do not directly harm host plants, they may affect the economic value of fruit sales ability and reduce photosynthesis in plants (Gleason et al. 2011). Sooty blotch fungi can form dark mycelial mats, whereas flyspeck fungi lack mycelial mats, form shiny and small, black spots (Batzer et al. 2005; Yang et al. 2010; Gleason et al. 2011; Zhang et al. 2015; Singtripop et al. 2016; Hongsanan et al. 2017). However, these fungi are poorly known, because of the difficulty in obtaining the strain which grows slowly (Yang et al. 2010; Hongsanan et al. 2017; Zeng et al. 2018).

Phaeothecoidiellaceae K.D. Hyde & Hongsanan was introduced by Hongsanan et al. (2017) and accommodated three genera *Chaetothyrina*, *Houjia* and *Phaeothecoidiell*a in the order Capnodiales. Currently, it includes eight genera: *Chaetothyrina*, *Exopassalora*, *Houjia*, *Nowamyces*, *Phaeothecoidiella*, *Rivilata*, *Sporidesmajora* and *Translucidithyrium* (Hongsanan et al. 2020). Members of Phaeothecoidiellaceae are related to sooty blotch and flyspeck fungi and characterised by thyriothecia with setae, bitunicate asci and 1-septate ascospores (Singtripop et al. 2016; Hongsanan et al. 2017; Zeng et al. 2019; Hongsanan et al. 2020). *Chaetothyrina* is morphologically similar to the family Micropeltidaceae (Reynolds and Gilbert 2005), but is distinguishable by its brown upper wall of ascomata (Wu et al. 2019; Zeng et al. 2019). The genus *Rivilata* is placed in this family on the basis of morphological characters by Doilom et al. (2018). The *Nowamyces* was introduced as a new genus in the new family Nowamycetaceae by Crous et al. (2019) and Hongsanan et al. (2020) placed this genus into Phaeothecoidiellaceae by phylogenetic analysis. Hongsanan et al. (2020) listed *Houjia*, *Exopassalora*, *Sporidesmajora* and *Phaeothecoidiella* as asexual genera in Phaeothecoidiellaceae.

*Translucidithyrium* X.Y. Zeng & K.D. Hyde (2018) was introduced as a monotypic genus in Phaeothecoidiellaceae, which is represented by *T. thailandicum* X.Y. Zeng & K.D. Hyde (2018). It was characterised by epiphytes on the reverse of living leaves, semi-transparent ascomata, globose to subglobose asci and fusiform ascospores with verrucose and appendages. Ascospores germinated on MEA (Malt Extract Agar Medium) within 24 h. The colonies slowly grow on media, white to grey, circular and villiform (Zeng et al. 2018).

Liu et al. (2017) used the molecular clock approach to estimate the divergence time of the order Capnodiales crown age at 151–283 Mya (million years ago). Zeng et al. (2019) estimated the divergence time of the family Phaeothecoidiellaceae crown age at 40–60 Mya. The molecular clock approach for estimating divergence time might be used to predict speciation, historical climate change or other environmental events (Hélène and Arne 2014; Louca and Pennell 2020).

In this study, we collected an extraordinary new species of *Translucidithyrium* in Xishuangbanna, Yunnan Province, China. We described the morphological characteristics and built a phylogenetic tree to determine the classification of the new taxon. We compared and analysed the estimated divergence time of *Translucidithyrium* with the environmental changes around the corresponding time range to propose the evolutional history hypothesis of *Translucidithyrium* distributed in two different regions (China and Thailand).

## Methods

### Morphological

Fresh living leaves with olivaceous dots were collected at Xishuangbanna, China 21°55'51"N, 101°15'08"E, 540 m alt.) and delivered to the laboratory for observation. According to Wu et al. (2014), the collected samples were processed and examined by microscopes: the photos of ascomata were taken by using a compound stereomicroscope (KEYENCE CORPORATION V.1.10 with camera VH-Z20R). Hand sections were made under a stereomicroscope (OLYMPUS SZ61) and mounted in water and blue cotton and photomicrographs of fungal structures were taken with a compound microscope (Nikon ECLIPSE 80i). The single spore isolation was implemented by the methods of Choi et al. (1999) and Chomnunti et al. (2014). Germinated spores were individually transferred to PDA (Potato Dextrose Agar Medium) and incubated at 26 °C for 48 h. Colony characteristics were observed and measured after 4 weeks at 26 °C. Images used for figures were processed with Adobe Photoshop CC v. 2015.5.0 software (Adobe Systems, USA). The holotype was deposited at the herbarium of IFRD (International Fungal Research & Development Centre; Research Institute of Resource Insects, Kunming), reference number IFRD 9208. The ex-type strain was deposited at IFRDCC, reference number IFRDCC 3000.

### DNA isolation, amplification and sequencing

According to the manufacturer's instructions, genomic DNA was extracted from mycelium growing on PDA at room temperature by using the Forensic DNA Kit (OMEGA, USA). The primer pair LR0R and LR5 was used to amplify the large subunit (LSU) rDNA (Vilgalys and Hester 1990). The primer pair ITS5 and ITS4 was used to amplify the internal transcribed spacer (ITS) rDNA (White et al. 1990). The primer pair NS1 and NS4 was used to amplify the partial small subunit (SSU) rDNA (White et al. 1990). The PCR reactions were in accordance with instructions from Golden Mix, Beijing TsingKe Biotech Co. Ltd, Beijing, China: initial denaturation at 98 °C for 2 min, then 30 cycles of 98 °C denaturation for 10 s, 56 °C annealing for 10 s and 72 °C extension for 10 s (ITS and SSU) or 20 s (LSU) and a final extension at 72 °C for 1 min. All PCR products were sequenced by Biomed (Beijing, China).

### Sequences alignments and phylogenetic analysis

BioEdit version 7.0.5.3 (Hall 1999) was used to re-assemble sequences generated from forward and reverse primers for obtaining the integrated sequences. Sequences were downloaded from GenBank using data from the publications of Zeng et al.

(2018), Crous et al. (2019), Hongsanan et al. (2020) and Renard et al. (2020) and aligned using BioEdit version 7.0.5.3 (Hall 1999): in addition, sequences were adjusted manually.

Maximum Likelihood (ML) analysis was conducted by using RAxMLGUI v.1.0 (Silvestro and Michalak 2012). Aligned sequences were input into the software and *Dothidea sambuci* was selected as the outgroup taxon. One thousand non-parametric bootstrap iterations were employed with the "ML + rapid bootstrap" tools and "GTR-GAMMA" arithmetic.

For Bayesian analysis, MrModeltest 2.3 (Nylander 2004) was used to estimate the best-fitting model for the combined LSU and ITS genes. Posterior probabilities (Rannala and Yang 1996; Zhaxybayeva and Gogarten 2002) were determined by Markov Chain Monte Carlo (MCMC) sampling in MrBayes v.3.2 (Ronquist and Huelsenbeck 2003). Six simultaneous Markov chains were run for 2,000,000 generations; trees were printed every 1,000 generations; trees were sampled every 100 generations. The first 5,000 trees submitted to the burn-in phase and were discarded; the remaining trees were used for calculating posterior probabilities in the majority rule consensus tree (Cai et al. 2006, 2008; Liu et al. 2012).

## Fossil calibrations and divergence time estimations

The fossil *Protographum luttrellii* (Renard et al. 2020) was used to calibrate the divergence time of Asterotexiales and Aulographaceae (normal distribution, mean = 119.0, SD = 3.7). The secondary calibration from the family Phaeothecoidiellaceae with a crown age of 58 Mya (normal distribution, mean = 50.0, SD = 6.1) was used (Zeng et al. 2019). The additional secondary calibration of Capnodiales was used, based on the result from Liu et al. (2017) (normal distribution, mean = 217.0, SD = 40.0).

Divergence time analysis was carried out using BEAST v1.8.4 (Drummond et al. 2012). Aligned LSU sequence data were loaded into the BEAUti v1.10.4 for generating an XML file. An uncorrelated relaxed clock model (Drummond et al. 2006) with a lognormal distribution of rates was used for the analysis. We used a Yule Process tree prior (Yule 1925; Gernhard 2008), which assumes a constant speciation rate per lineage and a randomly-generated starting tree. The length of chain was set as 50 million generations and sampling parameters were set at every 5,000 generations in MCMC. Subsequent divergence time analysis was carried out using BEAST v.1.10.4 (Drummond et al. 2012). Tracer v.1.7.1 was used to check the effective sample sizes (ESS) and acceptable values were higher than 200. The .log files and .tree files generated by BEAST were combined in LogCombiner v1.10.4 after removing a proportion of states as burn-in. The Maximum Clade Credibility (MCC) tree was given by obtained data and was estimated in TreeAnnotator v.1.10.4 (Liu et al. 2017; Zeng et al. 2019, 2020; Renard et al. 2020).

The phylogenetic tree and MCC tree were visualized in FigTree v.1.4.3 (Rambaut 2012) and Adobe Illustrator CS6 v. 16.0.0 (Adobe Systems, USA).

**Table 1.** Selected taxa in this study with their corresponding GenBank accession numbers. The newly-generated sequences are shown in bold.

| No. | Species | Vouncher /strain no. | LSU | ITS |
|---|---|---|---|---|
| 1 | *Acidomyces acidophilus* | MH1085 | JQ172741 | JQ172741 |
| 2 | *Asterina phenacis* | TH 589 | GU586217 | – |
| 3 | *Asterotexiaceae sp.* | VUL.535 | MG844162 | – |
| 4 | *Aulographum sp.* | VUL.457 | MG844158 | – |
| 5 | *Batcheloromyces proteae* | CBS 110696 | JF746163 | JF746163 |
| 6 | *Baudoinia compniacensis* | CBS 123031 | GQ852580 | – |
| 7 | *Brunneosphaerella protearum* | CPC 16338 | GU214397 | GU214626 |
| 8 | *Buelliella minimula* | Lendemer 42237(NY) | KX244961 | – |
| 9 | *Camarosporula persooniae* | CBS 116258 | JF770461 | JF770449 |
| 10 | *Capnobotryella renispora* | CBS 214.90 | GU214398 | AY220612 |
| 11 | *Capnodium coffeae* | CBS 147.52 | GU214400 | DQ491515 |
| 12 | *Catenulostroma protearum* | CPC 15368 | GU214402 | GU214628 |
| 13 | *Chaetothyrina guttulata* | MFLUCC15–1080 | KU358917 | KX372277 |
| 14 | *Chaetothyrina guttulata* | MFLUCC15–1081 | KU358914 | KX372276 |
| 15 | *Chaetothyrina musarum* | MFLUCC 15–0383 | KU710171 | – |
| 16 | *Cladosporium herbarum* | CBS 121621 | KJ564331 | EF679363 |
| 17 | *Cladosporium hillianum* | CBS 125988 | KJ564334 | HM148097 |
| 18 | *Cladosporium ramotenellum* | CBS 170.54 | DQ678057 | AY213640 |
| 19 | *Colletogloeum sp.* | NY1_3.2F1c | FJ031986 | FJ425193 |
| 20 | *Conidiocarpus*(*Phragmocapnias*) *betle* | MFLUCC 10–0050 | JN832605 | – |
| 21 | *Devriesia staurophora* | ATCC 200934 | KF901963 | AF393723 |
| 22 | *Dissoconium aciculare* | CBS 204.89 | GU214419 | AY725520 |
| 23 | *Dothidea sambuci* | AFTOL-ID 274 | AY544681 | DQ491505 |
| 24 | *Dothistroma pini* | CBS 121011 | JX901821 | JX901734 |
| 25 | *Elasticomyces elasticus* | CCFEE 5547 | KF309991 | – |
| 26 | *Exopassalora zambiae* | YHJN13 | GQ433631 | GQ433628 |
| 27 | *Extremus adstrictus* | TRN96 | KF310022 | – |
| 28 | *Friedmanniomyces endolithicus* | CCFEE 5199 | KF310007 | JN885547 |
| 29 | *Hispidoconidioma alpinum* | L2–1/2 | FJ997286 | FJ997285 |
| 30 | *Hortaea werneckii* | CBS 100496 | GU301817 | AY128703 |
| 31 | *Houjia yanglingensis* | YHJN13 | GQ433631 | GQ433628 |
| 32 | *Lecanosticta pini* | CBS 871.95 | GQ852598 | – |
| 33 | *Lembosia albersii* | MFLUCC 13–0377 | KM386982 | – |
| 34 | *Lembosina sp.* | VUL.644 | MG844165 | – |
| 35 | *Leptoxyphium cacuminum* | MFLUCC 10–0049 | JN832602 | – |
| 36 | *Melanodothis caricis* | CBS 860.72 | GU214431 | GU214638 |
| 37 | *Microcyclosporella mali* | CPC 16171 | GU570545 | GU570528 |
| 38 | *Microxyphium citri* | CBS 451.66 | KF902094 | – |
| 39 | *Morenoina calamicola* | MFLUCC 14–1162 | NG059779 | NR154210 |
| 40 | *Mycosphaerella pneumatophorae* | AFTOL-ID 762 | KJ176856 | – |
| 41 | *Neodevriesia coryneliae* | CPC 23534 | KJ869211 | KJ869154 |
| 42 | *Neodevriesia hilliana* | CPC 15382 | GU214414 | GU214633 |
| 43 | *Neodevriesia xanthorrhoeae* | CBS 128219 | HQ599606 | HQ599605 |
| 44 | *Neopseudocercosporella capsellae* | CBS 127.29 | KF251830 | KF251326 |
| 45 | *Nowamyces globulus* | CBS 144598 | MN162196 | MN161935 |
| 46 | *Nowamyces piperitae* | CBS 143490 | MN162200 | MN161944 |
| 47 | *Parapenidiella tasmaniensis* | CBS 124991 | KF901844 | KF901522 |
| 48 | *Passalora eucalypti* | CBS 111318 | KF901938 | KF901613 |
| 49 | *Penidiella columbiana* | CBS 486.80 | EU019274 | KF901630 |
| 50 | *Periconiella velutina* | CBS 101950 | EU041840 | EU041783 |
| 51 | *Petrophila incerta* | TRN 77 | GU323963 | – |
| 52 | *Phaeophleospora eugeniae* | CPC 15159 | KF902095 | KF901742 |

| No. | Species | Vouncher /strain no. | LSU | ITS |
|---|---|---|---|---|
| 53 | *Phaeothecoidea eucalypti* | CBS 120831 | KF901848 | KF901526 |
| 54 | *Phaeothecoidiella illinoisensis* | CBS 125223 | GU117901 | GU117897 |
| 55 | *Phaeothecoidiella missouriensis* | CBS 125222 | AY598917 | AY598878 |
| 56 | *Phloeospora maculans* | CBS 115123 | GU214670 | GU214670 |
| 57 | *Piedraia hortae* | CBS 480.64 | GU214466 | GU214647 |
| 58 | *Piedraia quintanilhae* | CBS 327.63 | GU214468 | – |
| 59 | *Pseudocercospora vitis* | CPC 11595 | GU214483 | GU269829 |
| 60 | *Pseudoramichloridium henryi* | CBS 124775 | KF442561 | KF442521 |
| 61 | *Pseudotaeniolina globosa* | CCFEE 5734 | KF310010 | KF309976 |
| 62 | *Pseudoveronaea obclavata* | CBS 132086 | JQ622102 | – |
| 63 | *Racodium rupestre* | L346 | EU048583 | GU067666 |
| 64 | *Racodium rupestre* | L424 | EU048582 | GU067669 |
| 65 | *Ramichloridium apiculatum* | CBS 156.59 | EU041848 | EU041791 |
| 66 | *Ramularia endophylla* | CBS 113265 | AY490776 | AY490763 |
| 67 | *Ramularia pusilla* | CBS 124973 | KP894141 | KP894248 |
| 68 | *Ramulispora sorghi* | CBS 110578 | GQ852653 | - |
| 69 | *Readeriella mirabilis* | CBS 125000 | KF251836 | KF251332 |
| 70 | *Recurvomyces mirabilis* | CBS 119434 | GU250372 | FJ415477 |
| 71 | *Repetophragma zygopetali* | VIC42946 | KT732418 | |
| 72 | *Schizothyrium pomi* | CBS 486.50 | EF134948 | EF134948 |
| 73 | *Scolecostigmina mangiferae* | CBS 125467 | GU253877 | GU269870 |
| 74 | *Scorias spongiosa* | CBS 325.33 | GU214696 | GU214696 |
| 75 | *Septoria cytisi* | USO 378994 | JF700954 | JF700932 |
| 76 | *Septoria lysimachiae* | CBS 123794 | KF251972 | KF251468 |
| 77 | *Sonderhenia eucalyptorum* | CBS 120220 | KF901822 | KF901505 |
| 78 | *Sphaerulina myriadea* | CBS 124646 | JF770468 | JF770455 |
| 79 | *Sporidesmajira pennsylvaniensis* | CBS 125229 | MH874965 | MF951287 |
| 80 | *Stenella araguata* | CBS 105.75 | EU019250 | EU019250 |
| 81 | *Teratoramularia kirschneriana* | CBS 113093 | GU214669 | GU214669 |
| 82 | *Teratosphaeria fibrillosa* | CBS 1217.07 | GU323213 | KF901728 |
| 83 | *Toxicocladosporium irritans* | CBS 185.58 | EU040243 | EU040243 |
| 84 | *Toxicocladosporium rubrigenum* | CBS 124158 | FJ790305 | FJ790287 |
| 85 | ***Transluciditbyrium chinense*** | **IFRDCC 3000** | **MT659404** | **MT659671** |
| 86 | *Transluciditbyrium thailandicum* | MFLUCC 16–0362 | MG993048 | MG993045 |
| 87 | *Tripospermum myrti* | CBS 437.68 | GU323216 | – |
| 88 | *Trochophora simplex* | CBS 124744 | GU253880 | GU269872 |
| 89 | *Uwebraunia communis* | CBS 114238 | EU019267 | AY725541 |
| 90 | *Vermiconia foris* | CCFEE 5459 | GU250390 | KF309981 |
| 91 | *Xenoconiothyrium catenatum* | CMW 22113 | JN712570 | JN712502 |
| 92 | *Zasmidium cellare* | CBS 146.36 | EU041878 | EU041821 |
| 93 | *Zygophiala cryptogama* | OH4_1A1a | FJ147157 | FJ425208 |
| 94 | *Zygophiala tardicrescens* | MWA1a | EF164901 | AY598856 |
| 95 | *Zygophiala wisconsinensis* | OH4_9A1c | FJ147158 | FJ425209 |

# Results

## Phylogenetic study

The dataset of combined LSU and ITS sequences comprised 1350 characters after alignment. Bayesian Inference, in total, generated 20,001 trees and the average standard deviation of split frequencies reached 0.0096. A total of 15,001 trees were finally used to calculate posterior probabilities. Phylogenetic analysis showed that the new collection clusters with *T. thailandicum* with 100% Maximum Likelihood bootstrap support and 1.00 posterior probabilities (Fig. 1).

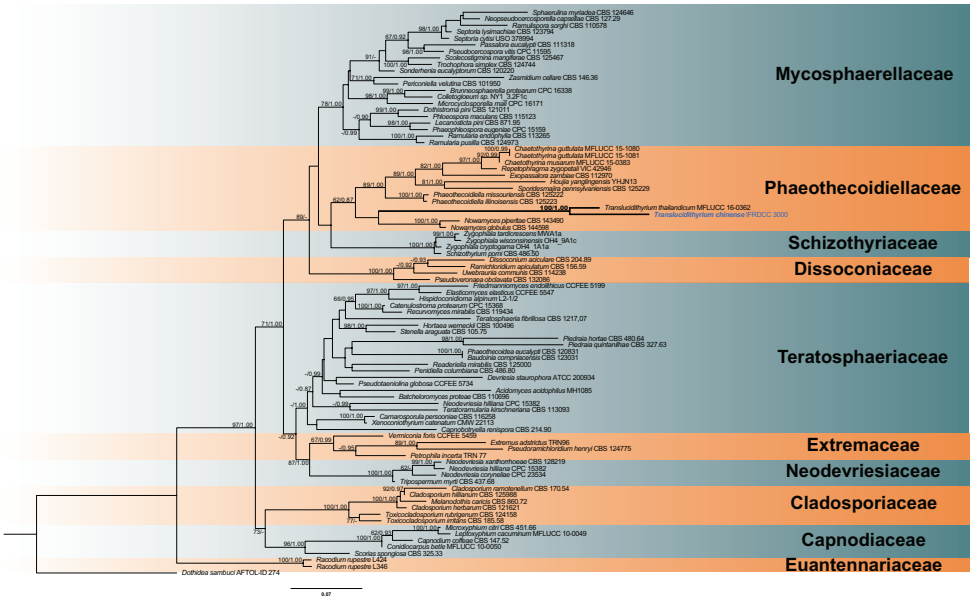


**Figure 1.** The topology shows family relationships of Capnodiales, based on combined LSU and ITS dataset analysis. Bootstrap values of Maximum Likelihood higher than 60% are shown on the left, while values of Bayesian posterior probabilities above 80% are shown on the right. New species is given in bold. Clades of the key species or family are given in bold. The tree is rooted with *Dothidea sambuci* (Dothideaceae, Dothideales).

## Taxonomy

***Translucidithyrium chinense* H. X. Wu & X. H. Li, sp. nov.**
Index Fungorum number: IF 557843
Facesoffungi number: FoF 09429
Figures 2, 3

**Etymology.** Refer to the location of species, China.

**Holotype.** IFRD9208

**Description.** *Epiphytic* on living leaves, ascomata with papillate. *Superficial hyphae* absent. **Sexual morph:** *Ascomata* solitary or scattered, 480–870 µm diam. ($\bar{x}$ = 741 µm, n = 6), 65–82 µm high ($\bar{x}$ = 72 µm, n = 8), olivaceous to brown, slightly semi-transparent under highlighted background, circular to suborbicular, with slightly prominent papilla, membranous, without ostiole (Fig. 2A–C). *Peridium* 8.3–10 µm thick, ($\bar{x}$ = 9 µm, n = 11), composed of irregular, meandering, interwoven arranged cells, two layers: from brown to hyaline, outer layer composed of closely-arranged cells, brown; inner layer composed of hyaline, oblong, subdense arranged cells, poorly developed at the base (Fig. 2D–F). *Asci* evenly distributed and parallel arranged in hamathecium (Fig. 2D–F), 65–90 × 51–81 µm ($\bar{x}$ = 77 × 60 µm, n = 10), 8-spored, bitunicate, hyaline, with an ocular chamber, ovoid at immature state, globose to subglobose at mature

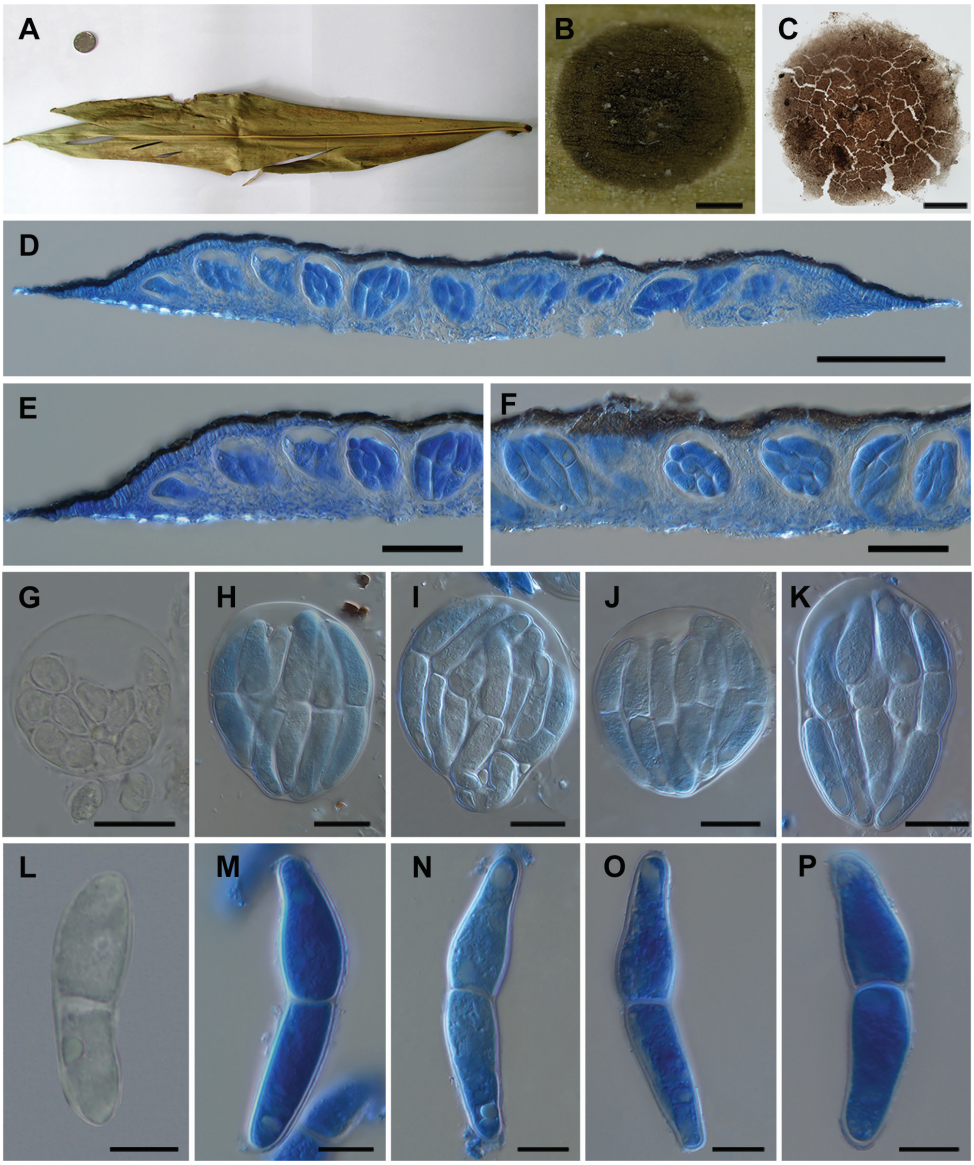


**Figure 2.** *Translucidithyrium chinense* (IFRD 9208, holotype) **A** plant leaves **B** acscoma on leaves surface **C** squash of ascoma at 20 times amplification **D** cross section of ascoma in blue cotton at 20 times amplification **E, F** cross section of ascoma in blue cotton at 40 times amplification **G** asci at 100 times amplification **H–K** asci in blue cotton at 100 times amplification **L** ascospore at 100 times amplification **M–P** ascospore in blue cotton at 100 times amplification. Scale bars: 200 µm (**B**); 100 µm (**C, D**); 50 µm (**E, F**); 20 µm (**G–K**); 10 µm (**L–P**). We slightly adjusted the contrast, saturation and hue of images and removed the contaminants around main object in images in PS software without obscuration, erasure or distortion of any information existing in the original document.

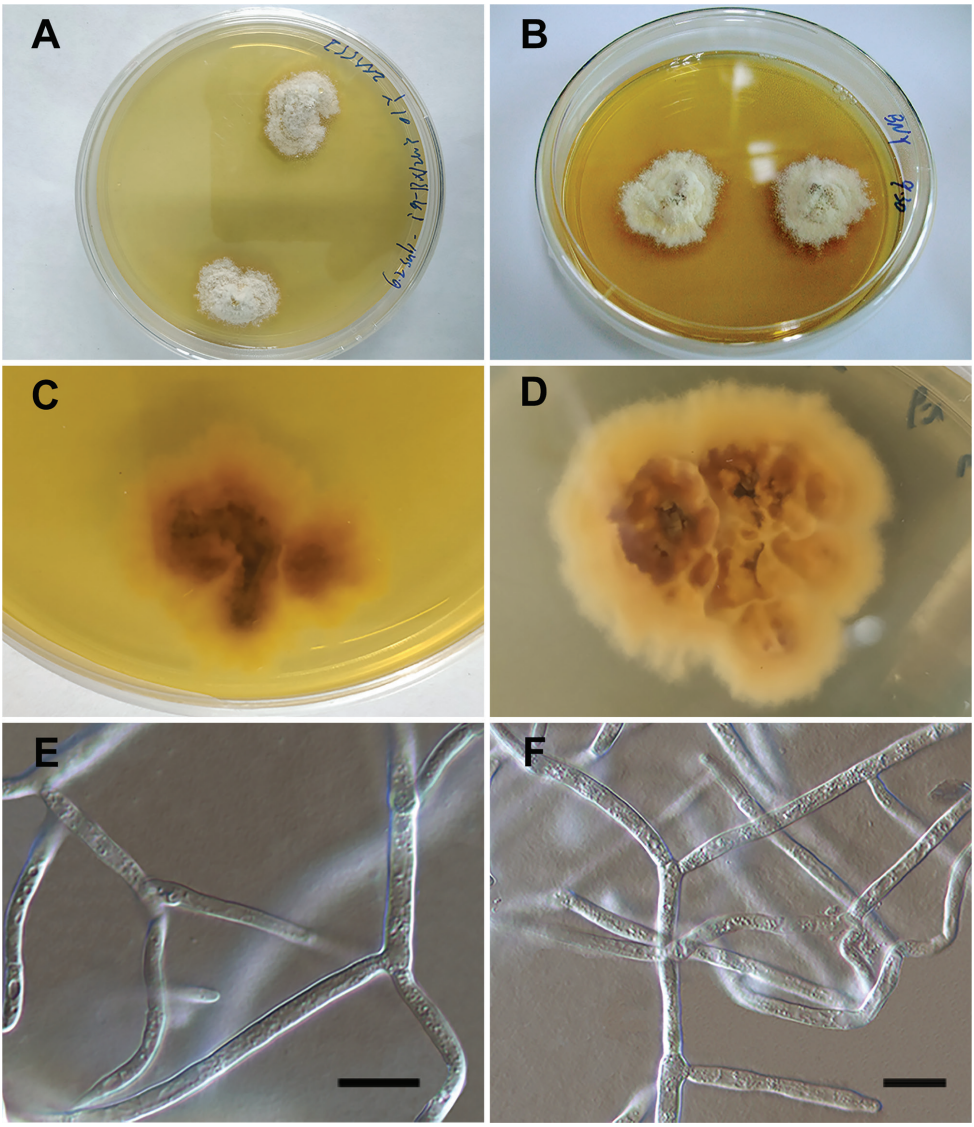


**Figure 3.** Culture of *Translucidithyrium chinense* (IFRDCC3000) **A, B** culture growing on the medium **C, D** the bottom of the medium with culture growing **E, F** the mycelium of culture at 100 times amplification. Scale bars: 10 μm (**E, F**).

state, lacking pedicel, paraphyses absent (Fig. 2G–K). *Ascospores* 41–65 × 10–13 μm ($\bar{x}$ = 50 × 11 μm, n = 20), irregularly overlapping, hyaline, ovoid at young state, fusiform with both ends tapered at mature state, 1-septate, constricted at the septum, upper cell a little larger than lower, with guttules at both ends, verrucose (Fig. 2L–P). **Asexual morph:** Undetermined.

**Culture characteristics.** Ascospores germinating on MEA at 36 h after spore-isolation, germinating on PDA at 48 h after spore-isolation. Colonies slow growing on MEA and PDA, irregular, villiform, convex, white on surface, yellow to brown at base. After a long period of growth, the pigments produced by culture discolour the medium, roots generate at the bottom (Fig. 3A–D). Culture hyphae hyaline, branched, constricted at the septum, 3 µm wide (Fig. 3E, F).

**Material examined.** China, Yunnan Province, Xishuangbanna Dai Autonomous Prefecture, Xishuangbanna Botanical Garden; 21°55'51"N, 101°15'08"E, 540 m alt.; 21 Apr 2019; Haixia Wu and Xinhao Li leg; collected on living leaves of *Alpinia blepharocalyx* (IFRD 9208, holotype), ex-type living culture (IFRDCC 3000).

**Notes.** This new species is morphologically similar to *Translucidithyrium thailandicum* in having semi-transparent and largish ascomata, globose asci and hyaline ascospores with 1-septate. However, *Translucidithyrium chinense* has a slightly papilla thyriothecium with weaker transmittance and ascospores with guttules at both ends, while *T. thailandicum* has a flattened thyriothecium with higher transmittance and ascospores with appendages at both ends; besides, the size of ascomata and asci of *T. chinense* are slightly larger than those of *T. thailandicum* (795 µm vs. 621 µm; 77 µm vs. 64 µm). The culture characteristics of both species are different: the culture of *T. chinense* grows more slowly, has roots inserting into medium and turn the bottom brown. Phylogenetically, *T. chinense* clusters with *T. thailandicum* as a distinct clade with high support (100% ML / 1.00 PP, Fig. 1).

**Divergence times estimates.** The Maximum Clade Credibility (MCC) tree was similar to the major lineages in the Bayesian and ML trees. The crown age of

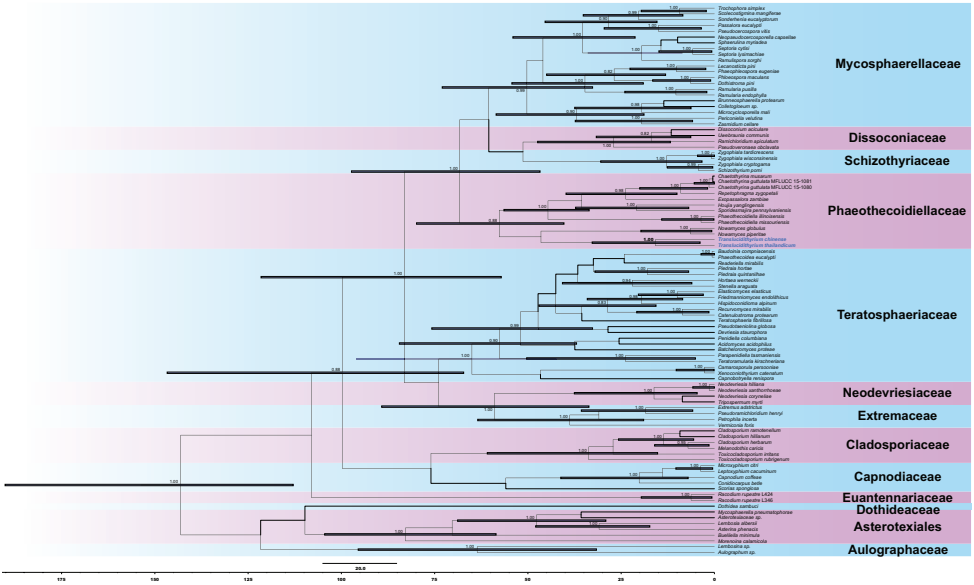


**Figure 4.** The MCC tree with divergence times estimates of Phaeothecoidiellaceae obtained from a Bayesian approach (BEAST). Numbers at nodes indicate posterior probabilities (pp) for node support; bars correspond to the 95% highest posterior density (HPD) intervals. The key species are given in blue.

*Translucidithyrium* showed 16 Mya (4–33), which was earlier than the divergence time of most genera in Phaeothecoidiellaceae. The estimated divergence time of Phaeothecoidiellaceae from Zeng et al. (2019) is 58 Mya, which corresponds to our results.

## Discussion

*Translucidithyrium thailandicum* was found in the north of Thailand (Zeng et al. 2018). *Translucidithyrium chinense* was found in the Xishuangbanna Region, southwest of China, which lies on the northern border of a rainforest with rich microfungal resources. The new species is characterised by brown to olivaceous ascomata and slightly semi-transparent, subglobose asci without pedicel and fusiform ascospores with verrucose and guttules (Fig. 2). *T. chinense* is introduced as a new species in *Translucidithyrium* by morphological and phylogenetic studies (Figs 1–3).

The ascomata of *Translucidithyrium* are different from related genera of Phaeothecoidiellaceae: *Nowamyces* has immersed ascomata, *Chaetothyrina* has ascomata with setae and *Rivilata* has subcuticular ascomata (Singtripop et al. 2016; Doilom et al. 2018; Zeng et al. 2018; Crous et al. 2019; Hongsanan et al. 2020). *Translucidithyrium* is similar to the family Schizothyriaceae in having semi-transparent ascomata, globose to subglobose asci and hyaline ascospores with guttules. Schizothyriaceae includes *Schizothyrium*, *Plochmopeltis*, *Hexagonella*, *Lecideopsella*, *Mycerema*, *Kerniomyces*, *Metathyriella*, *Myriangiella*, *Amazonotheca* and *Vonarxella* (Phookamsak et al. 2016; Wijayawardene et al. 2020). The morphology of *T. chinense* is most similar to *Lecideopsella* by having globose asci and 1-septate ascospores, but *Lecideopsella* has a short pedicel at the bottom of the asci (Phookamsak et al. 2016; Zeng et al. 2018). Phylogenetically, *Translucidithyrium* formed a long clade and clustered within the family Phaeothecoidiellaceae. It indicated the existing certain genetic distance amongst *Translucidithyrium*, Phaeothecoidiellaceae and Schizothyriaceae. Phaeothecoidiellaceae and Schizothyriaceae are poorly studied families (Batzer et al. 2008; Phookamsak et al. 2016; Singtripop et al. 2016; Hongsanan et al. 2017; Zeng et al. 2018). Therefore, more fresh specimens with molecular data are needed to confirm the classification of *Translucidithyrium*, Phaeothecoidiellaceae and Schizothyriaceae.

Zuckerkandl and Pauling (1962) suggested that the number of differences amongst amino acids was proportional to species divergence time. We estimated the divergence time using BEAST analysis. The divergence time of *Translucidithyrium* crown age was estimated at 16 Mya (4–33), which was earlier than the crown ages of *Chaetothyrina* at 2 Mya (0–5), the crown ages of *Repetophragma* at 9 Mya (2–20), the crown ages of *Nowamyces* at 7 Mya (1–20) and the crown ages of *Phaeothecoidiella* at 4 Mya (0–14) within Phaeothecoidiellaceae (Fig. 4). The divergence time of *Translucidithyrium* is earlier than other genera in Phaeothecoidiellaceae. We estimate that the long divergence time should affect the genetic variation (Pauling 1964; Hall and Hallgrímsson 2008). Additionally, the evolutionary molecular clock approach confirmed the long clades of *Translucidithyrium* in the phylogenetic tree (Fig. 1).

Historical events amongst different biological groups could then be compared with the dates of plate tectonic movements and paleoecology, according to the corresponding geological time scale (Lomolino et al. 2006; Berbee and Taylor 2010). Through relevant studies on the Qinghai-Tibet Plateau, it was found that the time of intense tectonic uplift and denudation is concentrated in 60–35 Mya, 25–17 Mya, 12–8 Mya and 5 Mya. Global cooling might have an impact on climate change in East Asia, especially at 15 Mya and 8 Mya (Lu et al. 2010). Rising plateaus and global cooling were drying up Asia (Liu 2000; Garzione et al. 2015). The time of the Qinghai-Tibet Plateau uplift and global cooling corresponded to the interval of the species in *Translucidithyrium* divergence time. We predict that the speciation of *T. chinense* was earlier than the speciation of *T. thailandicum*, as the divergence of *Translucidithyrium* was related to the Qinghai-Tibet Plateau uplift and global cooling. According to the evolution history of *Translucidithyrium*, it could be speculated that the speciation of *T. chinense* was earlier than *T. thailandicum*. With the climate becoming colder and with increased drought, *T. chinense* migrated from China to Thailand gradually to find a suitable area, then *T. thailandicum* formed. Due to the end of global cooling, the distribution pattern of *Translucidithyrium* in two different countries formed. Increasing fresh collections and application of new methodologies may result in modified conclusions.

## Acknowledgements

Funds for research were provided by the Grant for Essential Scientific Research of National Nonprofit Institute (no. CAFYBB2019QB005), the Yunnan Province Ten Thousand Plan of Youth Top Talent Project (no. YNWR-QNBJ-2018-267) and the Yunnan Fundamental Research Projects (grant NO. 202001AT070014). The authors are deeply grateful to Prof. K.D. Hyde (Mae Fah Luang University, Thailand, MFU) for editing the English language of the manuscript, to Dr. Xiang-Yu Zeng and Dr. Nawaz Haider for revising this manuscript and to Dr. Rungtiwa Phookamsak for guiding experiment operation.

## References

Batzer JC, Gleason ML, Harrington TC, Tiffany LH (2005) Expansion of the sooty blotch and flyspeck complex on apples based on analysis of ribosomal DNA gene sequences and morphology. Mycologia 97(6): 1268–1286. https://doi.org/10.1080/15572536.2006.11832735

Batzer JC, Arias MMD, Harrington TC, Gleason ML, Groenewald JZ, Crous PW (2008) Four species of *Zygophiala* (Schizothyriaceae, Capnodiales) are associated with the sooty blotch and flyspeck complex on apple. Mycologia 100: 246–258. https://doi.org/10.1080/15572536.2008.11832480

Berbee ML, Taylor JW (2010) Dating the molecular clock in fungi – how close are we? Fungal Biology Reviews 24: 1–16. https://doi.org/10.1016/j.fbr.2010.03.001

Cai L, Jeewon R, Hyde KD (2006) Phylogenetic investigations of Sordariaceae based on multiple gene sequences and morphology. Mycological Research 110: 137–150. https://doi.org/10.1016/j.mycres.2005.09.014

Cai L, Guo XY, Hyde KD (2008) Morphological and molecular characterisation of a new anamorphic genus Cheirosporium, from freshwater in China. Persoonia 20: 53–58. https://doi.org/10.3767/003158508X314732

Choi Y, Hyde KD, Ho W (1999) Single spore isolation of fungi. Fungal Diversity 3: 29–38.

Chomnunti P, Hongsanan S, Aguirre-Hudson B, Tian Q, Alias AS (2014) The sooty moulds. Fungal Diversity 66: 1–36. https://doi.org/10.1007/s13225-014-0278-5

Crous PW, Wingfield MJ, Cheewangkoon R, Carnegie AJ, Burgess TI, Summerell BA, Edwards J, Taylor PWJ, Groenewald JZ (2019) Foliar pathogens of eucalypts. Studies in Mycology 94, 125–298. https://doi.org/10.1016/j.simyco.2019.08.001

Doilom M, Hyde KD, Phookamsak R, Dai DQ, Tang LZ, Hongsanan S, Chomnunti P, Boonmee S, Dayarathne MC, Li WJ, Thambugala KM, Perera RH, Daranagama DA, Norphanphoun C, Konta S, Dong W, Ertz D, Phillips AJL, McKenzie EHC, Vinit K, Ariyawansa HA, Jones EBG, Mortimer PE, Xu JC, Promputtha I (2018) Mycosphere Notes 225–274: types and other specimens of some genera of *Ascomycota*. Mycosphere 9(4): 647–754.

Drummond AJ, Ho SYW, Phillips MJ, Rambaut A (2006) Relaxed phylogenetics and dating with confidence. PLoS Biology 4: e88. https://doi.org/10.1371/journal.pbio.0040088

Drummond AJ, Suchard MA, Xie D, Rambaut A (2012) Bayesian phylogenetics with BEAUti and the BEAST 1.7. Molecular Biology and Evolution 29(8): 1969–1973. https://doi.org/10.1093/molbev/mss075

Garzione CN, Quade J, Decelles PG, English NB (2015) Predicting paleo-elevation of Tibet and the Himalaya from δ18O vs. altitude gradients in meteoric water across the Nepal Himalaya. Earth & Planetary Ence Letters 183: 215–229. https://doi.org/10.1016/S0012-821X(00)00252-1

Gernhard T (2008) The conditioned reconstructed process. Journal of Theoretical Biology 253: 769–778. https://doi.org/10.1016/j.jtbi.2008.04.005

Gleason ML, Batzer JC, Sun GY, Zhang R, Arias MMD, Sutton TB, Crous PW, Ivanović M, McManus PS, Cooley DR, Mayr U, Weber RWS, Yoder KS, Ponte EMD, Biggs AR, Oertel B (2011) A new view of sooty blotch and flyspeck. Plant Disease 95(4): 368–383. https://doi.org/10.1094/PDIS-08-10-0590

Hall BK, Hallgrímsson B (2008) Strickberger's evolution. Sudbury, Jones and Bartlett.

Hall TA (1999) BioEdit: A user-friendly biological sequence alignment program for Windows 95/98/NT. Nucleic Acids Symposium Series 41: 95–98.

Hélène M, Arne M (2014) Phylogenetic approaches for studying diversification. Ecology Letters 17: 508–525. https://doi.org/10.1111/ele.12251

Hongsanan S, Hyde KD, Phookamsak R, Wanasinghe DN, McKenzie EHC, Sarma VV, Boonmee S, Lücking R, Bhat DJ, Liu NG, Tennakoon DS, Pem D, Karunarathna A, Jiang SH, Jones EBG, Phillips AJL, Manawasinghe IS, Tibpromma S, Jayasiri SC, Sandamali DS, Jayawardena RS, Wijayawardene NN, Ekanayaka AH, Jeewon R, Lu YZ, Dissanayake AJ, Zeng XY, Luo ZL, Tian Q, Phukhamsakda C, Thambugala KM, Dai DQ, Chethana KWT, Samarakoon MC, Ertz D, Bao DF, Doilom M, Liu JK, PérezOrtega S, Suija A, Senwanna

C, Wijesinghe SN, Konta S, Niranjan M, Zhang SN, Ariyawansa HA, Jiang HB, Zhang JF, Norphanphoun C, de Silva NI, Thiyagaraja V, Zhang H, Bezerra JDP, Miranda-González R, Aptroot A, Kashiwadani H, Harishchandra D, Sérusiaux E, Aluthmuhandiram JVS, Abeywickrama PD, Devadatha B, Wu HX, Moon KH, Gueidan C, Schumm F, Bundhun D, Mapook A, Monkai J, Chomnunti P, Suetrong S, Chaiwan N Dayarathne MC, Yang J, Rathnayaka AR, Bhunjun CS, Xu JC, Zheng JS, Liu G, Feng Y, Xie N (2020) Refined families of Dothideomycetes: Dothideomycetidae and Pleosporomycetidae. Mycosphere 11(1): 1553–2107. https://doi.org/10.5943/mycosphere/11/1/13

Hongsanan S, Zhao RL, Hyde KD (2017) A new species of *Chaetothyrina* on branches of mango, and introducing Phaeothecoidiellaceae fam. nov. Mycosphere 8: 137–146.

Liu JK, Hyde KD, Jeewon R, Phillips AJL, Maharachchikumbura SSN, Ryber, M, Liu ZY, Zhao Q (2017) Ranking higher taxa using divergence times: a case study in Dothideomycetes. Fungal Diversity 84(1): 75–99. https://doi.org/10.1007/s13225-017-0385-1

Liu JK, Phookamsak R, Doilom M, Wikee S, Li YM, Ariyawansha H, Boonmee S, Chomnunti P, Dai DQ, Bhat JD, Romero AI, Zhuang WY, Monkai J, Jones EBG, Chukeatirote E, Ko TWK, Zhao YC, Wang Y, Hyde KD (2012) Towards a natural classification of Botryosphaeriales. Fungal Diversity 57: 149–210. https://doi.org/10.1007/s13225-012-0207-4

Liu X (2000) Sensitivity of East Asian monsoon climate to the uplift of the Tibetan Plateau. Palaeogeography Palaeoclimatology Palaeoecology 183: 223–245. https://doi.org/10.1016/S0031-0182(01)00488-6

Lomolino MV, Riddle BR, Whittaker RH, Brown JH (2006) Biogeography. Inc. Publishers, Sunderland.

Louca S, Pennell MW (2020) Extant timetrees are consistent with a myriad of diversification histories. Nature 580: 502–505. https://doi.org/10.1038/s41586-020-2176-1

Lu H, Wang X, Li L (2010) Aeolian sediment evidence that global cooling has driven late cenozoic stepwise aridification in central Asia. Geological Society London Special Publications 342: 29–44. https://doi.org/10.1144/SP342.4

Nylander JAA (2004) MrModeltest v2. Program distributed by the author. Evolutionary Biology Centre, Uppsala University.

Pauling L (1964) Molecular disease and evolution. Bulletin of the New York Academy of Medicine 40(5): 334–342. https://doi.org/10.1159/000405851

Phookamsak R, Boonmee S, Norphanphoun C, Wanasinghe D, de Silva N, Dayarathne M, Hongsanan S, Bhat DJ, Hyde KD (2016) Schizothyriaceae. Mycosphere 7: 154–189. https://doi.org/10.5943/mycosphere/7/2/7

Rambaut A (2012) FigTree version 1.4.0. Computer program and documentation distributed by the author. http://treebioedacuk/software/figtree

Rannala B, Yang Z (1996) Probability distribution of molecular evolutionary trees: a new method of phylogenetic inference. Journal of Molecular Evolution 43: 304–311. https://doi.org/10.1007/BF02338839

Renard LL, Stockey RA, Upchurch G, Berbee ML (2020) A new epiphyllous fly-speck fungus from the Early Cretaceous Potomac group of Virginia (125–112 Ma): Protographum luttrellii, gen. et sp. nov. Mycologia 112: 504–518. https://doi.org/10.1080/00275514.2020.1718441

Reynolds DR, Gilbert GS (2005) Epifoliar fungi from Queensland, Australia. Australian Systematic Botany 18(3): 265–289. https://doi.org/10.1071/SB04030

Ronquist F, Huelsenbeck JP (2003) MrBayes 3: Bayesian phylogenetic inference under mixed models. Bioinformatics 19: 1572–1574. https://doi.org/10.1093/bioinformatics/btg180

Silvestro D, Michalak I (2012) raxmlGUI: a graphical front-end for RAxML. Organisms Diversity & Evolution 12: 335–337. https://doi.org/10.1007/s13127-011-0056-0

Singtripop C, Hongsanun S, Li J, De Silva NI, Phillips AJL, Jones GEB, Bahkali AH, Hyde KD (2016) *Chaetothyrina mangiferae* sp. nov., a new species of *Chaetothyrina*. Phytotaxa 255(1): 21–33. https://doi.org/10.11646/phytotaxa.255.1.2

Vilgalys R, Hester M (1990) Rapid genetic identification and mapping of enzymatically amplified ribosomal DNA from several Cryptococcus species. Journal of Bacteriology 172: 4238–4246. https://doi.org/10.1128/JB.172.8.4238-4246.1990

von Höhnel FXR (1909) Fragmente zur Mykologie: VIII. Mitteilung (Nr. 354 bis 406). Sitzungsberichte der Kaiserlichen Akademie der Wissenschaften Math.-naturw. Klasse Abt. I. 118: 1157–1246.

White TJ, Bruns T, Lee S, Taylor J (1990) Amplification and direct sequencing of fungal ribosomal RNA genes for phylogenetics. In: Innis MA, Gelfand DH, Sninsky JJ, White TJ (Eds) PCR protocols: a guide to methods and applications. Academic Press, New York, 315–322. https://doi.org/10.1016/B978-0-12-372180-8.50042-1

Wijayawardene NN, Hyde KD, Al-Ani LKT, Tedersoo L, Haelewaters D, Rajeshkumar KC, Zhao RL, Aptroot A, Leontyev DV, Saxena RK, Tokarev YS, Dai DQ, Letcher PM, Stephenson SL, Ertz D, Lumbsch HT, Kukwa M, Issi IV, Madrid H, Phillips AJL, Selbmann L, Pfliegler WP, Horváth E, Bensch K, Kirk PM, Kolaříková K, Raja HA, Radek R, Papp V, Dima B, Ma J, Malosso E, Takamatsu S, Rambold G, Gannibal PB, Triebel D, Gautam AK, Avasthi S, Suetrong S, Timdal E, Fryar SC, Delgado G, Réblová M, Doilom M, Dolatabadi S, Pawłowska JZ, Humber RA, Kodsueb R, Sánchez-Castro I, Goto BT, Silva DKA, de Souza FA, Oehl F, da Silva GA, Silva IR, Błaszkowski J, Jobim K, Maia LC, Barbosa FR, Fiuza PO, Divakar PK, Shenoy BD, Castañeda-Ruiz RF, Somrithipol S, Lateef AA, Karunarathna SC, Tibpromma S, Mortimer PE, Wanasinghe DN, Phookamsak R, Xu J, Wang Y, Tian F, Alvarado P, Li DW, Kušan I, Matočec N, Mešić A, Tkalčec Z, Maharachchikumbura SSN, Papizadeh M, Heredia G, Wartchow F, Bakhshi M, Boehm E, Youssef N, Hustad VP, Lawrey JD, Santiago ALC, Bezerra JDP, Souza-Motta CM, Firmino AL, Tian Q, Houbraken J, Hongsanan S, Tanaka K, Dissanayake AJ, Monteiro JS, Grossart HP, Suija A, Weerakoon G, Etayo J, Tsurykau A, Vázquez V, Mungai P, Damm U, Li QR, Zhang H, Boonmee S, Lu YZ, Becerra AG, Kendrick B, Brearley FQ, Motiejūnaitė J, Sharma B, Khare R, Gaikwad S, Wijesundara DSA, Tang LZ, He MQ, Flakus A, Rodriguez-Flakus P, Zhurbenko MP, McKenzie EHC, Stadler M, Bhat DJ, Liu JK, Raza M, Jeewon R, Nassonova ES, Prieto M, Jayalal RGU, Erdoğdu M, Yurkov A, Schnittler M, Shchepin ON, Novozhilov YK, Silva-Filho AGS, Gentekaki E, Liu P, Cavender JC, Kang Y, Mohammad S, Zhang LF, Xu RF, Li YM, Dayarathne MC, Ekanayaka AH, Wen TC, Deng CY, Pereira OL, Navathe S, Hawksworth DL, Fan XL, Dissanayake LS, Kuhnert E, Grossart HP, Thines M (2020) Outline of Fungi and fungi-like taxa. Mycosphere 11(1): 1060–1456. https://doi.org/10.5943/mycosphere/11/1/8

Wu HX, Chen H, Rong K, Yi CS (2019) Type studies in Micropeltidaceae and suggested transfer of three excluded genera. Nova Hedwigia 108: 517–526. https://doi.org/10.1127/nova_hedwigia/2019/0517

Wu HX, Li Y, Ariyawansa HA, Li W, Yang H, Hyde KD (2014) A new species of *Microthyrium* from Yunnan, China. Phytotaxa 176(1): 213–218. https://doi.org/10.11646/phytotaxa.176.1.21

Yang HL, Sun GY, Batzer JC, Crous PW, Groenewald JZ, Gleason ML (2010) Novel fungal genera and species associated with the sooty blotch and flyspeck complex on apple in China and the USA. Persoonia 24: 29–37. https://doi.org/10.3767/003158510X492101

Yule GU (1925) A mathematical theory of evolution, based on the conclusions of Dr. J.C. Willis. Philosophical Transactions of the Royal Society B – Biological Sciences 213: 21–87. https://doi.org/10.1098/rstb.1925.0002

Zeng XY, Hongsanan S, Hyde KD, Putarak C, Wen TC (2018) *Translucidithyrium thailandicum* gen. et sp. nov.: a new genus in Phaeothecoidiellaceae. Mycological Progress 17: 1087–1096. https://doi.org/10.1007/s11557-018-1419-0

Zeng XY, Jeewon R, Hongsanan S, Hyde KD, Wen TC (2020) Unravelling evolutionary relationships between epifoliar Meliolaceae and angiosperms. Journal of Systematics and Evolution. https://doi.org/10.1111/jse.12643

Zeng XY, Wu HX, Hongsanan S, Jeewon R, Wen TC, Maharachchikumbura SSN, Chomnunti P, Hyde KD (2019) Taxonomy and the evolutionary history of Micropeltidaceae. Fungal Diversity 97: 393–436. https://doi.org/10.1007/s13225-019-00431-8

Zhang M, Gao L, Shang S, Han X, Zhang R, Latinović J, Latinović N, Batzer JC, Gleason ML, Sun GY (2015) New species and record of *Zygophiala* (Capnodiales, Mycosphaerellaceae) on apple from Montenegro. Phytotaxa 195: 227–235. https://doi.org/10.11646/phytotaxa.195.3.2

Zhaxybayeva O, Gogarten JP (2002) Bootstrap, Bayesian probability and maximum likelihood mapping: exploring new tools for comparative genome analyses. BMC Genomics 3: e4. https://doi.org/10.1186/1471-2164-3-4

Zuckerkandl E, Pauling LB (1962) Molecular disease, evolution, and genetic heterogeneity. In: Kasha M, Pullman B (Eds) Horizons in Biochemistry. Academic Press, New York, 189–225.

MycoKeys 76: 17–30 (2020)
doi: 10.3897/mycokeys.76.57410
https://mycokeys.pensoft.net

RESEARCH ARTICLE

A peer-reviewed open-access journal
MycoKeys
Launched to accelerate biodiversity research

# *Phialolunulospora vermispora* (Chaetosphaeriaceae, Sordariomycetes), a novel asexual genus and species from freshwater in southern China

Hua Zheng[1*], Yake Wan[1*], Jie Li[1], Rafael F. Castañeda-Ruiz[2], Zefen Yu[1]

**1** *Laboratory for Conservation and Utilization of Bio-resources, Key Laboratory for Microbial Resources of the Ministry of Education, School of Life Sciences, Yunnan University, Kunming, Yunnan, 650091, China*
**2** *Instituto de Investigaciones Fundamentales en Agricultura Tropical "Alejandro de Humboldt" (INIFAT), 17200, La Habana, Cuba*

Corresponding author: Zefen Yu (zfyuqm@hotmail.com)

Academic editor: H. Raja | Received 9 August 2020 | Accepted 6 December 2020 | Published 22 December 2020

**Citation:** Zheng H, Wan Y, Li J, Castañeda-Ruiz RF, Yu Z (2020) *Phialolunulospora vermispora* (Chaetosphaeriaceae, Sordariomycetes), a novel asexual genus and species from freshwater in southern China. MycoKeys 76: 17–30. https://doi.org/10.3897/mycokeys.76.57410

## Abstract

The asexual taxon *Phialolunulospora vermispora* **gen. et sp. nov.**, collected from submerged dicotyledonous leaves in Hainan, China, is described and illustrated herein. *Phialolunulospora* **gen. nov.** is characterized by macronematous, semimacronematous, septate and pigmented conidiophores and acrogenous, long lunate, vermiform to sigmoid, hyaline conidia with an eccentric basal appendage. Complete sequences of internal transcribed spacer (ITS) and partial sequences of nuclear large subunits ribosomal DNA (LSU) genes are provided. Phylogenetic analyses of combined ITS and LSU sequences revealed its placement in the Chaetosphaeriaceae. The new fungus is compared with morphologically similar genera.

## Keywords

Biodiversity, Chaetosphaeriales, phylogeny, taxonomy

## Introduction

China is considered an important Asian reservoir of biodiversity. The southern area of China ranks 34th in biodiversity hotspots (Myers et al. 2000; Williams et al. 2001).

* These authors contributed equally to this work.

Hainan Island, located in the south of China, harbors an incredibly high diversity of fungi. Its humid, subtropical climate, with an average annual temperature of 22 to 27 °C and an average annual precipitation of 1000–2600 mm, favors development of fungi. Our group has conducted investigations of freshwater fungi to increase knowledge of this important ecological group in China (Qiao et al. 2017a, b, 2018a, b, 2019a, b, 2020).

During our present investigation of freshwater fungi in Hainan Island, South China, an interesting species was collected on dead leaves of an unidentified dicotyledonous tree. This species is characterized by unbranched and septate conidiophores, phialidic conidiogenous cells and vermiform to sigmoid and aseptate conidia with an eccentric basal appendage. Based on preliminary analysis of morphological data, we place this unknown fungus in Chaetosphaeriaceae, but a literature search found that it did not belong to any known genus. To further confirm the position of the species, phylogenetic analyses with related taxa within Chaetosphaeriaceae were carried out based on complete sequences of internal transcribed spacer (ITS) and partial sequences of nuclear large subunits ribosomal DNA (LSU) genes.

## Materials and methods

### Isolation and morphological study

Submerged dicotyledonous leaves were collected from Limu Mountain Nature Reserve in Hainan Province. Samples were preserved in zip-lock plastic bags, labelled, and transported to the laboratory. The decomposed leaves were cut into several 2–4 × 2–4 cm sized fragments and then spread on to the surface of corn meal agar (CMA, 20 g cornmeal, 18 g agar, 40 mg streptomycin, 30 mg ampicillin, 1000 ml distilled water) medium for 10 days; single conidium was isolated with a sterilized needle and transferred to CMA plates while viewing with an Olympus BX51 microscope. The pure strain was further transferred to potato dextrose agar (PDA, 200 g potato, 20 g dextrose, 18 g agar, 40 mg streptomycin, 30 mg ampicillin, 1000 ml distilled water) medium. Colony morphology and microscopic characteristics were examined, and photographs were taken with an Olympus BX51 microscope connected to a DP controller digital camera. Measurement data were based on 30 random conidia and 10 conidiophores.

Pure cultures were deposited in the Herbarium of the Laboratory for Conservation and Utilization of Bio resources, Yunnan University, Kunming, Yunnan, China (**YMF**, formerly Key Laboratory of Industrial Microbiology and Fermentation Technology of Yunnan) and at the China General Microbiological Culture Collection Center (**CGMCC**).

### DNA extraction, PCR amplification, and sequencing

Pure cultures were grown on PDA medium for 5 days at 25 °C. Actively growing mycelium was scraped off from the surface of the culture and transferred to 2 ml Eppendorf

micro-centrifuge tubes. Total genomic DNA was extracted according to the procedures in Turner et al. (1997). Primers used for PCR amplification and sequencing of the nuclear large subunits ribosomal DNA (LSU) and the internal transcribed spacer (ITS) were LROR-LR7 and ITS1-ITS4, respectively (Vilgalys and Hester 1990; White et al. 1990). PCR products were purified and stored at -20 °C until sequencing. The same pairs of primers were used to obtain sequences, which was performed by Macrogen Europe (Macrogen Inc. Amsterdam, The Netherlands). Finally, the sequences were assembled and edited using SeqMan v. 7.0.0 (DNAStar Lasergene, Madison, WI, USA) to obtain the consensus sequences. The newly obtained sequences were submitted to GenBank nucleotide database (Table 1).

## Sequence alignment and phylogenetic analysis

Preliminary BLAST searches with the ITS and LSU sequences of our strain against the GenBank nucleotide database determined the closely related species (Altschul et al. 1990). BLAST search showed that our strain has homology to species in Chaetosphaeriaceae. Based on this information, related sequences of the two marker loci, which include 72 representatives belonging to Chaetosphaeriaceae, 4 representatives of Helminthosphaeriaceae, 2 representatives of Linocarpaceae and 2 representatives of Leptosporellaceae, were downloaded according to recent studies (Yang et al. 2016, 2018; Wei et al. 2018; Lin et al. 2019). Sordaria fimicola (Roberge ex Desm.) Ces. & De Not, *Gelasinospora tetrasperma* Dowding and *Lasiosphaeria ovina* (Pers.) Ces. & De Not were used as the outgroup. These, together with the newly generated sequences, were aligned with ClustalX 1.83 (Thompson et al. 1997) with default parameters, and the consensus sequences were manually adjusted and linked through BioEdit v.7.0 (Hall 1999). Manual gap adjustments were done to improve the alignment and ambiguously aligned regions were excluded. Then, the combined alignment was converted to a NEXUS file using the program MEGA6 (Tamura et al. 2013) and a PHY files using the program ClustalX 1.83. The resulting combined sequence matrix included 1475 nucleotide positions (with alignment gaps) from two regions (607 from ITS, 868 from LSU). GenBank accession numbers of downloaded sequences are given in Table 1.

Maximum-likelihood (ML) analysis was computed with RAxML (Stamatakis 2006) with the PHY files generated with CLUSTAL_X version 1.83, using the GTR-GAMMA model. ML bootstrap proportions (MLBPs) were computed with 1000 replicates. Bayesian inference (BI) analysis was conducted with MrBayes version 3.2.2 (Ronquist and Huelsenbeck 2003). The Akaike information criterion (AIC) implemented in jModelTest version 2.0 was used to select the best fit models after likelihood score calculations were done (Posada 2008). The base tree for likelihood calculations was ML-optimized. HKY+I+G was estimated as the best-fit model under the output strategy of the AIC. Metropolis-coupled Markov chain Monte Carlo (MCMCMC) searches were run for 5 000 000 generations, sampling every 500$^{th}$ generation.

**Table 1.** List of strains analyzed in this study, with GenBank accession numbers.

| Species | Strain | ITS | LSU |
|---|---|---|---|
| *Adautomilanezia caesalpiniae* | LAMIC 010212 | NR_153560 | NG_058594 |
| *Anacacumisporium appendiculatum* | HMAS 245593$^{T}$ | KT001555 | KT001553 |
| *Anacacumisporium appendiculatum* | HMAS 245602 | KT001556 | KT001554 |
| *Bahusutrabeeja dwaya* | CBS 261.77$^{T}$ | MH861059 | MH872829 |
| *Brunneodinemasporium brasiliense* | CBS 112007$^{T}$ | JQ889272 | JQ889288 |
| *Brunneodinemasporium jonesii* | GZCC 16–0050$^{T}$ | KY026058 | KY026055 |
| *Cacumisporium capitulatum* | FMR 11339 | HF677176 | HF677190 |
| *Cacumisporium capitulatum* | SMH 3766 | – | AY017374 |
| *Calvolachnella guaviyunis* | CBS 134695 | NR_153892 | NG_058879 |
| *Chaetosphaeria ciliata* | CBS 122131$^{T}$ | MH863180 | MH874726 |
| *Chaetosphaeria ciliata* | ICMP 18253 | – | GU180637 |
| *Chloridium chloroconium* | FMR 11940 | KY853435 | KY853495 |
| *Chloridium* sp. | HGUP 1806 | MK372070 | MK372068 |
| *Codinaea lambertiae* | CBS 143419$^{T}$ | NR_156389 | NG_059053 |
| *Codinaea pini* | CBS 138866$^{T}$ | NR_137943 | NG_058902 |
| *Conicomyces pseudotransvaalensis* | HHUF 29956$^{T}$ | NR_138015 | LC001708 |
| *Cryptophiale hamulata* | MFLUCC 180098 | – | MG386756 |
| *Cryptophiale udagawae* | MFLUCC 180422 | MH758198 | MH758211 |
| *Cryptophialoidea fasciculata* | MFLUCC 172119 | MH758195 | MH758208 |
| *Dendrophoma cytisporoides* | CBS 223.95$^{T}$ | JQ889273 | JQ889289 |
| *Dictyochaeta ellipsoidea* | MFLUCC 181574$^{T}$ | MK828628 | MK835828 |
| *Dictyochaeta lignicola* | DLUCC 0899$^{T}$ | MK828630 | MK835830 |
| *Dictyochaeta assamica* | CBS 242.66 | MH858788 | MH870426 |
| *Dictyochaetopsis gonytrichoides* | CBS 593.93 | AF178556 | AF178556 |
| *Dinemasporium morbidum* | CBS 129.66$^{T}$ | JQ889280 | JQ889296 |
| *Dinemasporium polygonum* | CBS 516.95$^{T}$ | NR_137786 | NG_059109 |
| *Echinosphaeria canescens* | SMH 4791 | – | AY436403 |
| *Eucalyptostroma eucalypti* | CBS 142074$^{T}$ | NR_154027 | NG_059257 |
| *Eucalyptostroma eucalyptorum* | CPC 31800$^{T}$ | NR_159834 | MH327838 |
| *Exserticlava vasiformis* | TAMA 450 | – | AB753846 |
| *Gelasinospora tetrasperma* | CBS 178.33 | NR_077163 | DQ470980 |
| *Helminthosphaeria clavariarum* | SMH 4609$^{T}$ | – | AY346283 |
| *Infundibulomyces cupulata* | BCC 11929$^{T}$ | EF113976 | EF113979 |
| *Infundibulomyces oblongisporus* | BCC 13400$^{T}$ | EF113977 | EF113980 |
| *Kionochaeta castaneae* | GZCC 18–0025$^{T}$ | MN104610 | MN104621 |
| *Kionochaeta microspora* | GZCC 18–0036$^{T}$ | MN104607 | MN104618 |
| *Lasiosphaeria ovina* | SMH 4605 | AY587923 | AY436413 |
| *Lecythothecium duriligni* | CBS 101317 | – | AF261071 |
| *Leptosporella arengae* | MFLUCC 150330$^{T}$ | MG272255 | MG272246 |
| *Leptosporella gregaria* | SMH 4290$^{T}$ | – | AY346290 |
| *Linocarpon arengae* | MFLUCC 150331$^{T}$ | – | MG272247 |
| *Linocarpon cocois* | MFLUCC 150812$^{T}$ | MG272257 | MG272248 |
| *Menispora glauca* | FMR 12089 | HF678528 | HF678538 |
| *Menispora tortuosa* | DAOM 231154 | KT225527 | AY544682 |
| *Menispora tortuosa* | CBS 214.56 | AF178558 | AF178558 |
| *Menisporopsis breviseta* | GZCC 18–0071$^{T}$ | MN104612 | MN104623 |
| *Menisporopsis dushanensis* | GZCC 18–0084$^{T}$ | MN104615 | MN104626 |
| *Morrisiella indica* | HKUCC 10827 | – | DQ408578 |
| *Multiguttulispora sympodialis* | MFLUCC 180153$^{T}$ | MN104606 | MN104617 |
| *Nawawia filiformis* | MFLUCC 160853 | – | MH758206 |
| *Nawawia filiformis* | MFLUCC 172394 | MH758196 | MH758209 |
| *Neonawawia malaysiana* | CBS 125544$^{T}$ | GU229886 | GU229887 |
| *Paliphora intermedia* | CBS 896.97$^{T}$ | NR_160203 | NG_057766 |
| *Paliphora intermedia* | CBS 199.95 | – | EF204500 |
| *Phaeostalagmus cyclosporus* | CBS 663.70 | MH859892 | MH871680 |

| Species | Strain | ITS | LSU |
|---|---|---|---|
| *Phaeostalagmus cyclosporus* | CBS 312.75 | – | MH872661 |
| ***Phialolunulospora vermispora*** | YMF 1.04260[T] | **MK165444** | **MK165442** |
| *Phialosporostilbe scutiformis* | MFLUCC 170227[T] | MH758194 | MH758207 |
| *Phialosporostilbe scutiformis* | MFLUCC 181288 | MH758199 | MH758212 |
| *Pseudodinemasporium fabiforme* | MAFF 244361[T] | AB934068 | AB934044 |
| *Pseudolachnea fraxini* | CBS 113701[T] | JQ889287 | JQ889301 |
| *Pseudolachnea hispidula* | MAFF 244364 | AB934071 | AB934047 |
| *Pseudolachnella longiciliata* | HHUF 29962 | AB934081 | AB934057 |
| *Pseudolachnella yakushimensis* | HHUF 29683[T] | AB934087 | AB934063 |
| *Pseudolachnella pachyderma* | HHUF 29955 | AB934085 | AB934061 |
| *Pyrigemmula aurantiaca* | CBS 126743[T] | HM241692 | HM241692 |
| *Pyrigemmula aurantiaca* | CBS 126744 | HM241693 | HM241693 |
| *Rattania setulifera* | GUFCC 15501 | GU191794 | HM171322 |
| *Ruzenia spermoides* | SMH 4606 | – | AY436422 |
| *Sordaria fimicola* | CBS 508.50 | MH856730 | MH868251 |
| *Sporoschisma hemipsilum* | SMH 2125 | – | AF466083 |
| *Sporoschisma hemipsilum* | SMH 3251 | – | AF466084 |
| *Stanjehughesia vermiculata* | HKUCC 10840 | – | DQ408570 |
| *Striatosphaeria codinaeaphora* | MR 1230 | AF178546 | AF178546 |
| *Striatosphaeria codinaeaphora* | SMH 1524 | – | AF466088 |
| *Synaptospora plumbea* | SMH 3962 | – | KF765621 |
| *Tainosphaeria jonesii* | GZCC 16–0053 | KY026059 | KY026056 |
| *Tainosphaeria jonesii* | GZCC 16–0065 | KY026060 | KY026057 |
| *Tainosphaeria monophialidica* | MFLUCC 180146[T] | – | MN104616 |
| *Thozetella pandanicola* | MFLUCC 160253[T] | MH388366 | MH376740 |
| *Thozetella tocklaiensis* | CBS 378.58[T] | MH857817 | MH869349 |
| *Verhulstia trisororum* | CBS 143234[T] | MG022181 | MG022160 |
| *Zanclospora iberica* | CBS 130426[T] | KY853480 | KY853544 |
| *Zanclospora iberica* | FMR 12186 | KY853481 | KY853545 |

*Sequences generated in this study are emphasized in bold face. [T]ex-type cultures.

Two independent analyses with four chains each (one cold and three heated) were run until the average standard deviation of the split frequencies dropped below

0.01. The initial 25% of the generations of MCMC sampling were discarded as burn-in. The refinement of the phylogenetic tree was used for estimating BI posterior probability (BIPP) values. The tree was viewed in FigTree version 1.4 (Rambaut 2012).

## Results

### Phylogenetic analyses

The combined dataset comprised 71 taxa (including our strain) representing 52 genera, which include 60 species in the family Chaetosphaeriaceae, 4 species in Helminthosphaeriaceae, 2 species in Linocarpaceae and 2 species in Leptosporellaceae, with *Gelasinospora tetrasperma* CBS 178.33, *Sordaria fimicola* CBS 508.50 and *Lasiosphaeria ovina* SMH 4605 as the outgroup. The final alignment comprised a total of 1475 base pairs, containing the ITS and LSU sequences, and were analyzed by BI and ML method. The topology of the tree is shown in Fig. 1, with the Bayesian posterior probabilities above 95% and ML bootstrap support greater than 70% indicated for respective clades. In this tree, our strain occurred

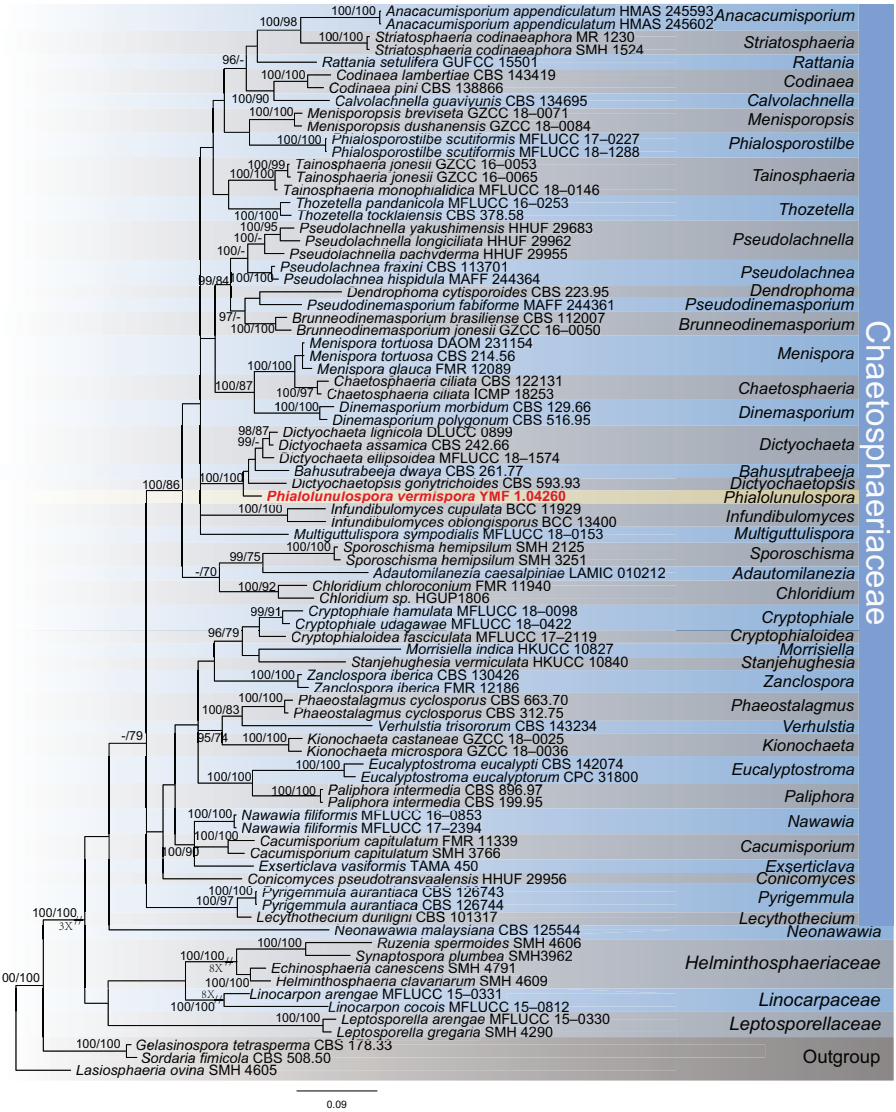


**Figure 1.** Phylogenetic tree derived from Bayesian analysis based on ITS and LSU sequences, depicting the relationships of the new taxon *Phialolunulospora vermispora* with closely related taxa. The numbers above branches represent BIPP (left) and MLBPs (right). BIPP over 95% and MLBPs greater than 70% are shown on the respective branches, and the bar represents the substitutions per nucleotide position. *Gelasinospora tetrasperma* CBS 178.33, *Sordaria fimicola* CBS 508.50 and *Lasiosphaeria ovina* SMH 4605 were used as outgroup.

on an isolated clade within Chaetosphaeriaceae, and clustered together with *Dictyochaetopsis* Aramb. & Cabello, *Bahusutrabeeja* Subram. & Bhat and *Dictyochaeta* Speg. with good Bayesian posterior probabilities (100%) and ML bootstrap proportions (100%). Considering distinct morphological characters with these three genera, we propose to describe our unknown isolate as a new genus and species, *Phialolunulospora vermispora*.

## Taxonomy

***Phialolunulospora* Z. F. Yu & R. F. Castaneda, gen. nov.**
MycoBank No: 828716

**Type species.** *Phialolunulospora vermispora* Z. F, Yu & R. F. Castañeda

**Etymology.** *Phialo*-Prefix, *Phia. lis* N.L fem. S. Phialide referring to the phialidic conidiogenous cells, and *lunulospora*, (*lu.nu.la.tus* N.L. adj. mean crescent-shaped + *spo.ra* N.L. fem. S. spora, referred to the conidia), referring to the genus *Lunulospora*.

**Description.** Asexual fungus. *Conidiophores* macronematous, semimacronematous, mononematous, septate, prostrate or erect, straight or flexuous, pigmented. *Conidiogenous cells* integrated, terminal, cylindrical to subulate, pale brown to brown, monophialidic or polyphialidic, enteroblastic. Conidial secession schizolytic. *Conidia* solitary, acrogenous, long lunate, vermiform to sigmoid, unicellular, hyaline, truncate at the conspicuous or inconspicuous basal frill, with a cellular, unbranched, eccentric basal appendage.

***Phialolunulospora vermispora* Z. F. Yu & R. F. Castaneda, sp. nov.**
MycoBank No: 828717
Figures 2–4

**Type.** China, Hainan province, Limu Mountain, 19°29'40"N, 107°80'45"E, ca. 350 m alt., from leaves of an unidentified dicotyledonous plant submerged in a stream, Apr 2015, Zefen Yu, YMF 1.04260 – ***holotype***; CGMCC 3.19632 – culture ex-type.

**Etymology.** *ver.mi-* (from *vermiformis*), NL fem. adj mean worm-shaped + *spo.ra* N.L. fem. S. spora, referred to worm-shaped conidia.

**Description.** Mycelium partly superficial and partly immersed, composed of septate, branched, smooth, hyaline, 1–2 µm wide hyphae. *Conidiophores* solitary, macronematous, semimacronematous, erect or prostrate, straight or flexuous, unbranched, up to 4-septate, cylindrical, up to 150 µm long, 3–4 µm wide, pale brown to brown, smooth, sometimes reduced to conidiogenous cells. *Conidiogenous cells* integrated, terminal, cylindrical to subulate, sometimes lageniform, determinate, smooth, pale brown to brown, mostly darker than conidiophores, phialidic, after secession leaving an inconspicuous basal frill, 12–47 × 2.6–3 µm. *Conidia* solitary, acrogenous, long lunate, vermiform to sigmoid, unicellular, guttulate, hyaline, smooth-walled, 31–55 × 2.5–3.5 µm, acute at the apex and narrow truncate at the base bearing minute marginal frills and a cellular, single, unbranched, somewhat attenuated or acuminate, eccentric basal appendage, 1.5–4.6 µm long.

**Culture characteristics.** Colonies attain 2.4 cm diameter on PDA and 2.8 cm diameter on CMA after 10 days at 25 °C. On PDA, colonies flat to slightly raised, aerial mycelium abundant, margin entire to undulate, surface white initially, then become buff and grey with age, reverse same color. Colonies on CMA, center with aerial my-

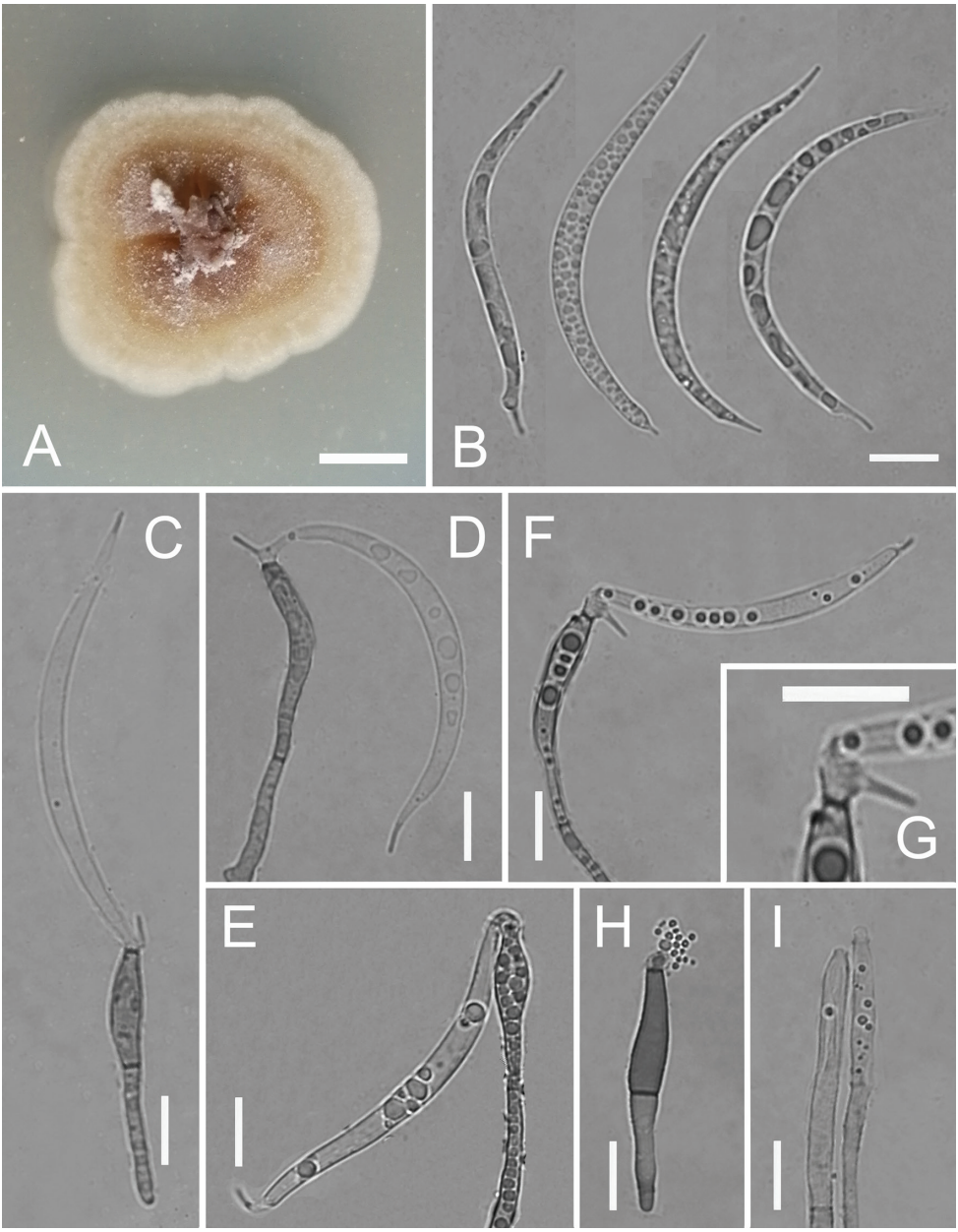


**Figure 2.** *Phialolunulospora vermispora* (YMF 1.04260) **A** colony on PDA at day 10 **B** conidia **C–F** conidiophores, conidiogenous cells and conidia **G** conidiogenous cells **H, I** conidiophores and conidiogenous cells. Scale bars: 10 mm (**A**); 10 μm (**B–I**).

celium cottony, periphery with scarce aerial mycelium, olivaceous grey, dark green exudate and soluble pigment produced, reverse same color.

**Distribution and ecology.** The species occurs on submerged leaves in stream. This species is currently known only from the type locality.

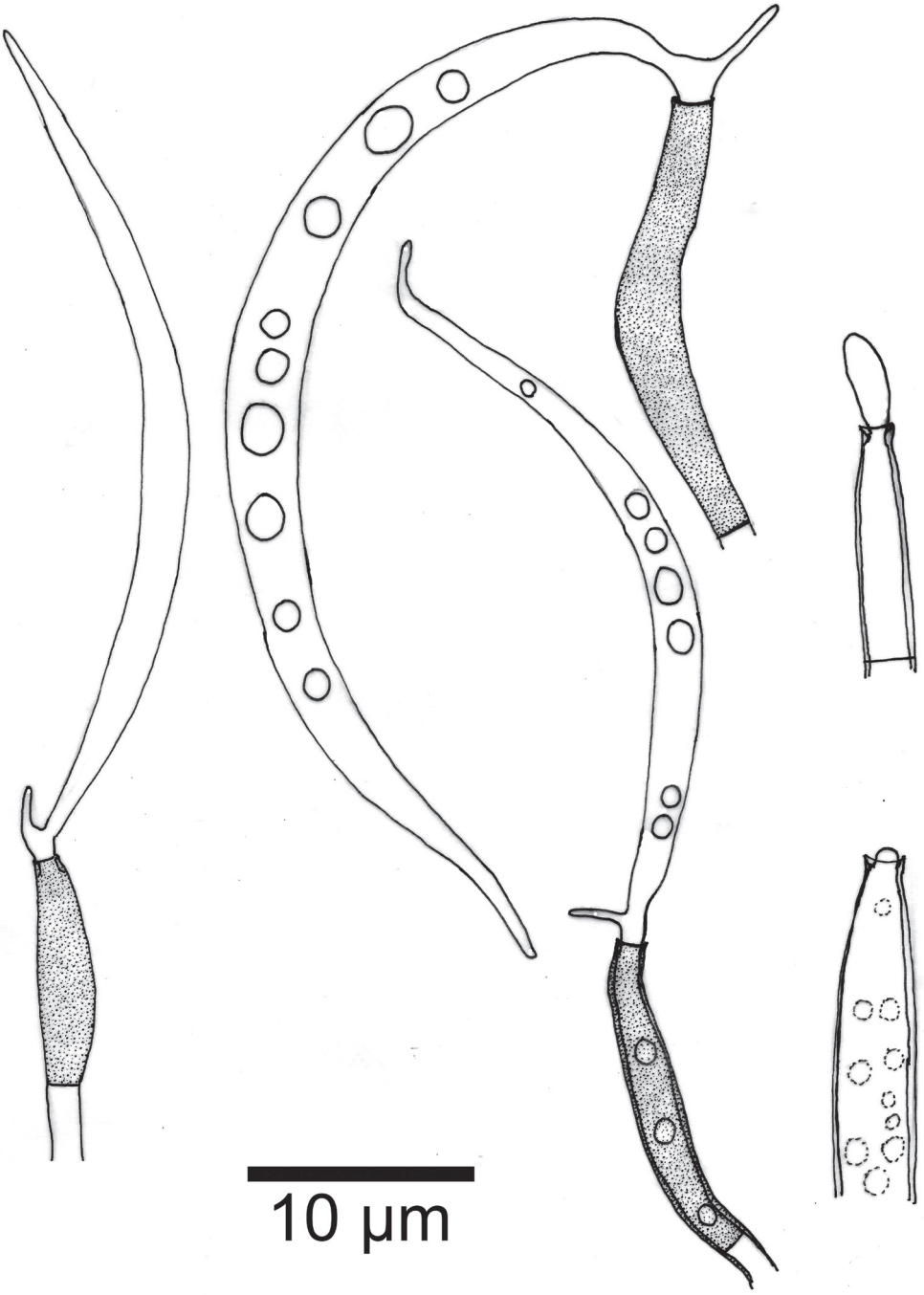


**Figure 3.** *Phialolunulospora vermispora* conidiogenous cells and conidia.

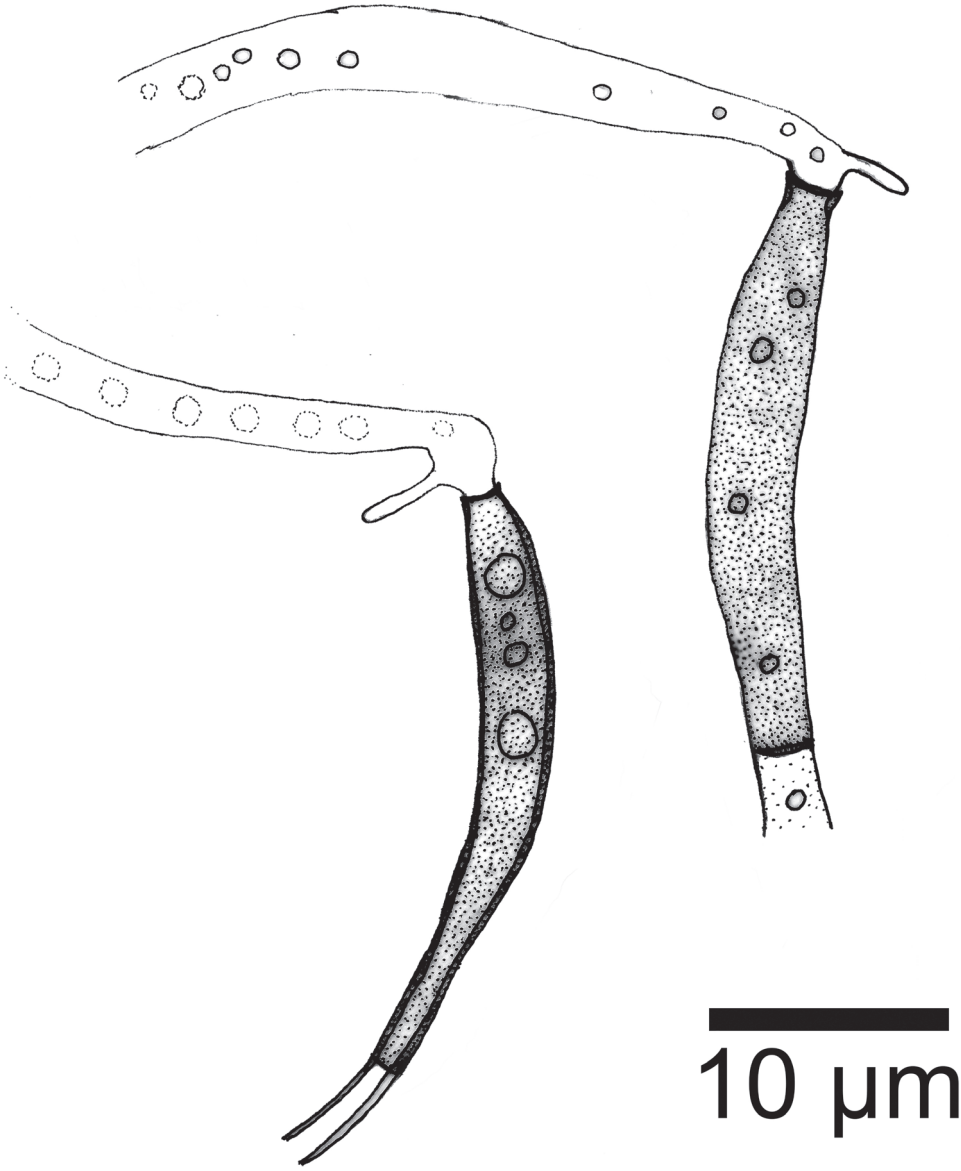


**Figure 4.** *Phialolunulospora vermispora* conidiogenous cells.

## Discussion

The family Chaetosphaeriaceae was firstly introduced by Réblová et al. (1999) to accommodate *Chaetosphaeria* and its allies. Réblová et al. (1999) also suggested that Chaetosphaeriaceae should be placed in the Sordariales. However, based on the nuclear large subunit ribosomal RNA gene (LSU) sequence, Huhndorf et al. (2004) placed Chaetosphaeriaceae in order Chaetosphaeriales. In a recent review of the family Chaetosphaeriaceae based on morphology and phylogenetic analysis, Lin et al. (2019)

accepted 49 genera (including three uncertain genera) within the family, among which 44 were asexual genera.

The asexual morph of the Chaetosphaeriaceae is hyphomycetous taxa. It is characterized by septate, branched or unbranched conidiophores with the conidiogenous cell monophialidic or polyphialidic, holoblastic or enteroblastic, smoothwalled (Réblová et al. 1999, 2011). Our new fungus, *Phialolunulospora vermispora*, fits the general description of asexual hyphomycetous Chaetosphaeriaceae well. *Phialolunulospora* is mainly distinguished from other species in the Chaetosphaeriaceae in having vermiform to sigmoid conidia. Conidia of typical members of the family, including *Dictyochaeta* and *Codinaea* Maire (Réblová 2000; Whitton et al. 2000; Cruz et al. 2008; Crous et al. 2014), are aseptate or 1-septate; they may be setulose or not. In this study, the phylogenetic analyses combining ITS and LSU sequences showed that *P. vermispora* is close to three asexual genera in Chaetosphaeriaceae (Fig. 1), *Dictyochaetopsis*, *Bahusutrabeeja* and *Dictyochaeta*. Morphologically, *Bahusutrabeeja* and *Dictyochaeta* are superficially similar to *P. vermispora* in septate and cylindrical conidiophores, but can be distinguished from the new genus in having globose conidia without appendages and long fusiform conidia with long appendage (Subramanian and Bhat 1977; Li et al. 2014; Liu et al. 2016; Lin et al. 2019), respectively. *P. vermispora* is clearly different from *Dictyochaetopsis* species in morphology, such as smooth and pale brown or brown conidiophores and long lunate, vermiform to sigmoid conidia (Arambarri and Cabello 1990; Whitton et al. 2000; Castañeda-Ruíz et al. 2008).

*Phialolunulospora* is morphologically similar to some other genera species of Chaetosphaeriaceae in hyaline conidia with basal eccentric cellular appendages, including *Neopseudolachnella* A. Hashim. & Kaz. Tanaka, *Pseudolachnea* Ranoj., *Pseudolachnella* Teng and *Rattania* Prabhug. & Bhat. Of these, species of *Neopseudolachnella*, *Pseudolachnea* and *Pseudolachnella* are different from *Phialolunulospora* in acervular, setose and stromatic conidiomata (Ranojevic 1910; Teng and Ling 1936; Hashimoto et al. 2015). The genus *Rattania* is distinguished from *Phialolunulospora* in having seta and smaller septate conidia (Prabhugaonkar and Bhat 2009). In addition, the type species of *Lunulospora* Ingold, *L. curvula* Ingold (Sordariomycetes, Sordariales incertae sedis), also has resemblance to *Phialolunulospora* in conidial shape (Ingold 1942; Seifert et al. 2011), but it has obviously bigger size of conidia, 70–90 × 4–5 µm vs. 12–47 × 2.6–3 µm, in *Lunulospora*.

Many freshwater species occur in the family Chaetosphaeriaceae. So far, approximately 16 genera in this family have been reported from fresh water, such as *Codinaea* (Luo et al. 2019). In this study, *Phialolunulospora vermispora* was also collected from freshwater habitats.

## Acknowledgements

This work was financed by the National Natural Science Foundation Program of PR China (31770026, 31970013). We are grateful to two reviewers for critically reviewing the manuscript and for providing helpful suggestions to improve this paper.

## References

Altschul SF, Gish W, Miller W, Myers EW, Lipman DJ (1990) Basic local alignment search tool. Journal of Molecular Biology 215: 403–410. https://doi.org/10.1016/S0022-2836(05)80360-2

Arambarri AM, Cabello MN (1990) Considerations about *Dictyochaeta*, *Codinaeopsis* and a new genus *Dictyochaetopsis*. Mycotaxon 38: 11–14. https://doi.org/10.1007/BF02277306

Castañeda-Ruíz RF, Gusmão LFP, Guarro J, Stchigel AM, Stadler M, Saikawa M, Leão-Ferreira SM (2008) Two new anamorphic fungi from Brazil: *Dictyochaetopsis polysetosa* and *Myrothecium compactum*. Mycotaxon 103: 1–8. https://doi.org/10.1007/BF02277306

Crous PW, Wingfield MJ, Schumacher RK, Summerell BA, Giraldo A, Gené J, Guarro J, Wanasinghe DN, Hyde KD, Camporesi E, Garethjones EB, Thambugala KM, Malysheva EF, Malysheva VF, Acharya K, Álvarez J, Alvarado P, Assefa A, Barnes CW, Bartlett JS, Blanchette RA, Burgess TI, Carlavilla JR, Coetzee MPA, Damm U, Decock CA, Denbreeÿen A, Devries B, Dutta AK, Holdom DG, Rooney-Latham S, Manjón JL, Marincowitz S, Mirabolfathy M, Moreno G, Nakashima C, Papizadeh M, Shahzadehfazeli SA, Amoozegar MA, Romberg MK, Shivas RG, Stalpers JA, Stielow B, Stukely MJC, Swart WJ, Tan YP, Vanderbank M, Wood AR, Zhang Y, Groenewald JZ (2014) Fungal Planet description sheets: 281–319. Persoonia 33: 212–289. https://doi.org/10.3767/003158514X685680

Cruz ACR, Leáo-ferreira SM, Barbosa FR, Gusmão LFP (2008) Conidial fungi from semi-arid Caatinga biome of Brazil. New and interesting *Dictyochaeta* species. Mycotaxon 106: 15–27.

Hall TA (1999) BioEdit: a user-friendly biological sequence alignment editor and analysis program for Windows 95/98/NT. Nucleic Acids Symposium Series 41: 95–98. https://doi.org/10.1021/bk-1999-0734.ch008

Hashimoto A, Sato G, Matsuda T, Matsumura M, Hatakeyama S, Harada Y, Ikeda H, Tanaka K (2015) Taxonomic revision of *Pseudolachnea* and *Pseudolachnella* and establishment of *Neopseudolachnella* and *Pseudodinemasporium* gen. nov. Mycologia 107(2): 383–408. https://doi.org/10.3852/14-171

Huhndorf SM, Miller AN, Fernandez FA (2004) Molecular systematics of the Sordariales: the order and the family Lasiosphaeriaceae redefined. Mycologia 96: 368–387. https://doi.org/10.2307/3762068

Ingold CT (1942) Aquatic hyphomycetes of decaying alder leaves. Transactions of the British Mycological Society 25(4): 339–417. [IN1–IN6] https://doi.org/10.1016/S0007-1536(42)80001-7

Li XX, Xia JW, Ma LG, Castaneda-Ruiz RF, Zhang XG (2014) A new species of *Bahusutrabeeja* from Guangxi, China. Mycotaxon 126: 227–230. https://doi.org/10.5248/126.227

Lin CG, McKenzie EHC, Liu JK, Jones EBG, Hyde KD (2019) Hyaline-spored chaetosphaeriaceous hyphomycetes from Thailand and China, with a review of the family Chaetosphaeriaceae. Mycosphere 10(1): 655–700. https://doi.org/10.5943/mycosphere/10/1/14

Liu J, Yang J, Maharachchikumbura SS, Mckenzie EH, Jones EB, Hyde KD, Liu ZY (2016) Novel chaetosphaeriaceous hyphomycetes from aquatic habitats. Mycological Progress 15(10–11): 1157–1167. https://doi.org/10.1007/s11557-016-1237-1

Luo Z, Hyde KD, Liu J, Maharachchikumbura SSN, Jeewon R, Bao D-F, Bhat DJ, Lin C-G, Li W-L, Yang J, Liu N-G, Lu Y-Z, Jayawardena RS, Li J-F, Su H-Y (2019) Freshwater

Sordariomycetes. Fungal Diversity 99: 451–660. https://doi.org/10.1007/s13225-019-00438-1

Myers N, Mittermeier RA, Mittermeier CG, da Fonseca GAB, Kent J (2000) Biodiversity hotspots for conservation priorities. Nature 403: 853–858. https://doi.org/10.1038/35002501

Posada D (2008) jModelTest: phylogenetic model averaging. Molecular Biology and Evolution 25: 1253–1256. https://doi.org/10.1093/molbev/msn083

Prabhugaonkar A, Bhat DJ (2009) *Rattania setulifera*, an undescribed endophytic hyphomycete on rattans from Western Ghats, India. Mycotaxon 108: 217–222. https://doi.org/10.5248/108.217

Qiao M, Du X, Bian ZH, Peng J, Yu ZF (2017a) *Ellisembia pseudokaradkensis* sp. nov. from Hainan, China. Mycotaxon 132: 813–817. https://doi.org/10.5248/132.813

Qiao M, Huang Y, Deng C, Yu ZF (2017b) *Tripospermum sinense* sp. nov. from China. Mycotaxon 132(3): 513–517. https://doi.org/10.5248/132.513

Qiao M, Guo JS, Tian WG, Yu ZF (2018a) *Ellisembia hainanensis* sp. nov. from Hainan, China. Mycotaxon 133: 97–101. https://doi.org/10.5248/133.97

Qiao M, Li WJ, Huang Y, Xu JP, Zhang L, Yu ZF (2018b) *Classiculasinensis*, a new species of basidiomycetous aquatic hyphomycetes from southwest China. MycoKeys 40: 1–12. https://doi.org/10.3897/mycokeys.40.23828

Qiao M, Tian WG, Castañeda-Ruiz RF, Xu JP, Yu ZF (2019a) Two new species of *Verruconis* from Hainan, China. MycoKeys 48: 41–53. https://doi.org/10.3897/mycokeys.48.32147

Qiao M, Zheng H, Zhang Z, Yu ZF (2019b) *Seychellomyces sinensis* sp. nov. from China. Mycotaxon 134(2): 391–398. https://doi.org/10.5248/134.161

Qiao M, Zheng H, Lv RL, Yu ZF (2020) Neodactylariales, Neodactylariaceae (Dothideomycetes, Ascomycota): new order and family, with a new species from China. MycoKeys 73: 69–85. https://doi.org/10.3897/mycokeys.73.54054

Rambaut A (2012) FigTree v1.4.2. http://tree.bio.ed.ac.uk/software/figtree/

Ranojevic N (1910) Zweiter Beitrag zur Pilzflora Serbiens. Annales Mycologici 8: 347–402.

Réblová M (2000) The genus *Chaetosphaeria* and its anamorphs. Studies in Mycology 143: 149–168. https://doi.org/10.1007/s005720050286

Réblová M, Barr ME, Samuels GJ (1999) Chaetosphaeriaceae, a new family for *Chaetosphaeria* and its relatives. Sydowia 51: 49–70.

Réblová M, Gams W, Seifert K (2011) *Monilochaetes* and allied genera of the Glomerellales, and a reconsideration of families in the Microascales. Studies in Mycology 68: 163–191. https://doi.org/10.3114/sim.2011.68.07

Ronquist F, Huelsenbeck JP (2003) MrBayes 3: Bayesian phylogenetic inference under mixed models. Bioinformatics 19: 1572–1574. https://doi.org/10.1093/bioinformatics/btg180

Seifert KA, Morgan-Jones G, Gams W, Kendrick B (2011) The genera of Hyphomycetes. CBS Biodiversity Series 9, CBSKNAW Fungal Biodiversity Centre, Utrecht.

Stamatakis A (2006) RAxML-VI-HPC: maximum likelihood-based phylogenetic analyses with thousands of taxa and mixed models. Bioinformatics 22: 2688–2690. https://doi.org/10.1093/bioinformatics/btl446

Subramanian CV, Bhat DJ (1977) *Bahusutrabeeja*, a new genus of the hyphomycetes. Botany 55(16): 2202–2206. https://doi.org/10.1139/b77-249

Tamura K, Stecher G, Peterson D, Filipski A, Kumar S (2013) MEGA6: molecular evolutionary genetics analysis version 6.0. Molecular Biology and Evolution 30: 2725–2729. https://doi.org/10.1093/molbev/mst197

Teng SC, Ling L (1936) Additional fungi from China IV. Sinensia 7: 752–823.

Thompson JD, Gibson TJ, Plewniak F, Jeanmougin F, Higgins DG (1997) The CLUSTAL_X windows interface: flexible strategies for multiple sequence alignment aided by quality analysis tools. Nucleic Acids Research 25: 4876–4882. https://doi.org/10.1093/nar/25.24.4876

Turner D, Kovacs W, Kuhls K, Lieckfeldt E, Peter B, Arisan-Atac I, Strauss J, Samuels GJ, Börner T, Kubicek CP (1997) Biogeography and phenotypic variation in *Trichoderma* sect. *Longibrachiatum* and associated *Hypocrea* species. Mycological Research 101(4): 449–459. https://doi.org/10.1017/S0953756296002845

Vilgalys R, Hester M (1990) Rapid genetic identification and mapping of enzymatically amplified ribosomal DNA from several *Cryptococcus* species. Journal of Bacteriology 172: 4238–4246. https://doi.org/10.1128/JB.172.8.4238-4246.1990

Wei M, Zhang H, Dong W, Boonmee S, Zhang D (2018) Introducing *Dictyochaeta aquatica* sp. nov. and two new species of *Chloridium* (Chaetosphaeriaceae, Sordariomycetes) from aquatic habitats. Phytotaxa 362(2): 187–199. https://doi.org/10.11646/phytotaxa.362.2.5

White TJ, Bruns T, Lee S, Taylor J (1990) Amplification and direct sequencing of fungal ribosomal RNA genes for phylogenetics. PCR Protocols: a guide to methods and applications 18(1): 315–322. https://doi.org/10.1016/B978-0-12-372180-8.50042-1

Whitton SR, Mckenzie EHC, Hyde KD (2000) *Dictyochaeta* and *Dictyochaetopsis* species from the Pandanaceae. Fungal Diversity 4: 133–158.

Williams J, Read C, Norton A, Dovers S, Burgman M, Proctor W, Anderson H (2001) Biodiversity, Australia State of the Environment Report 2001 (Theme Report). CSIRO Publishing on behalf of the Department of the Environment and Heritage, Canberra, 217 pp.

Yang J, Liu JK, Hyde KD, Bhat DJ, Jones EBG, Liu Z-Y (2016) New species of *Sporoschisma* (Chaetosphaeriaceae) from aquatic habitats in Thailand. Phytotaxa 289(2): 147–157. https://doi.org/10.11646/phytotaxa.289.2.4

Yang J, Liu NG, Liu J, Hyde KD, Jones EB, Liu ZY (2018) Phylogenetic placement of *Cryptophiale*, *Cryptophialoidea*, *Nawawia*, *Neonawawia* gen. nov. and *Phialosporostilbe*. Mycosphere 9(6): 1132–1150. https://doi.org/10.5943/mycosphere/9/6/5

MycoKeys 76: 31–47 (2020)
doi: 10.3897/mycokeys.76.58179
https://mycokeys.pensoft.net

RESEARCH ARTICLE

A peer-reviewed open-access journal
MycoKeys
Launched to accelerate biodiversity research

# New *Cantharellus* species from South Korea

Bart Buyck[1], Valérie Hofstetter[2], Rhim Ryoo[3], Kang-Hyeon Ka[3], Vladimír Antonín[4]

**1** *Institut de Systématique, Écologie, Biodiversité (ISYEB), Muséum national d'histoire naturelle, CNRS, Sorbonne Université, EPHE, 57 rue Cuvier, CP 39, F-75005, Paris, France* **2** *Département fédéral de l'économie, de la formation et de la recherche DEFR, Agroscope Domaine de recherche Protection des végétaux, Route de Duillier 60, CP 1012, 1260, Nyon 1, Switzerland* **3** *Department of Forest Bioresources, National Institute of Forest Science, Suwon 16631, South Korea* **4** *Department of Botany, Moravian Museum, Zelný trh 6, CZ-659 37, Brno, Czech Republic*

Corresponding author: Vladimír Antonín (vantonin@mzm.cz)

Academic editor: B-K Cui | Received 31 August 2020 | Accepted 24 November 2020 | Published 22 December 2020

**Citation:** Buyck B, Hofstetter V, Ryoo R, Ka K-H, Antonín V (2020) New *Cantharellus* species from South Korea. MycoKeys 76: 31–47. https://doi.org/10.3897/mycokeys.76.58179

**Abstract**

In this third contribution involving new *Cantharellus* species from South Korea, two new species are introduced. In addition, we document a first report of the recently described Japanese *Cantharellus anzutake* outside of Japan based on identical ITS sequence data. *Cantharellus citrinus* **sp. nov.** is introduced as a new member of subg. *Cinnabarini*, to which the closely related Korean *C. albovenosus* and Chinese *C. phloginus* also belong. *Cantharellus curvatus* **sp. nov.** is introduced as a new member of subg. *Parvocantharellus*, in which the Korean *C. koreanus* was recently placed. The respective placements of the new taxa are significantly supported by a phylogenetic analysis of sequences from the transcription elongation factor (*tef*-1).

**Keywords**

ITS, morphology, new species, phylogeny, *tef*-1

## Introduction

In our previous contributions reporting the biodiversity of *Cantharellus* Adans.:Fr. in Korea (Antonín et al. 2017; Buyck et al. 2018), we have reviewed the still limited taxonomic knowledge on *Cantharellus* species in Asia. During the past two years two more new chanterelles have been described from Asia: *C. anzutake* W. Ogawa, N. Endo, M. Fukuda and A. Yamada from Japan (Ogawa et al. 2018) and *C. hainanensis* N.K. Zeng, Zhi Q. Liang & S. Jiang from China (An et al. 2017). In the present paper, we

describe two more new species from South Korea supported by morphological features and in particular by sequence data obtained for the transcription elongation factor (*tef*-1) gene. In addition, identical ITS sequence data also document the presence, in South Korea, of the recently described *C. anzutake* from Japan, a species belonging to subg. *Cantharellus* and based on a 100 base pair deletion in the internal transcribed spacer 1 (ITS1) of the rDNA (Ogawa et al. 2018). Obtained *tef*-1 sequence data from all of our recent collections of chanterelles in South Korea could not confirm the presence of any of the European or North American *Cantharellus* previously reported from South Korea (Park and Lee 1991; Kim 2004; Kim et al. 2006; Lee 2011) nor any of the chanterelles already described from India (Das et al. 2015; Kumari et al. 2011, 2013), neighbouring China (Shao et al. 2011, 2014, 2016a, b; Tian et al. 2012; An et al. 2017), Japan (Suhara and Kurogi 2015; Ogawa et al. 2018) or Malaysia (Corner 1966; Eyssartier et al. 2009)

## Materials and methods

### Field work

Collections for this work were made during field trips of the last author in collaboration with colleagues from the National Institute of Forest Science (former Korea Forest Research Institute) in the margin of two larger inventory projects: "Diversity and molecular taxonomy of marasmielloid and gymnopoid fungi (Basidiomycota, Omphalotaceae) in South Korea" and "Phylogeny of litter decomposing fungi in South Korea". The various localities in which *Cantharellus* specimens were collected are shown below (Fig. 1).

### Morphology

Macroscopic descriptions of collected specimens were based on fresh basidiomata. Colour abbreviations follow Kornerup and Wanscher (1983). Microscopic features were studied using dried material mounted in $H_2O$, approximately 5% KOH, Melzer's reagent and Congo Red, using an Olympus BX-50 light microscope (Tokyo, Japan) at 1000× magnification. For the hymenophore, "L" refers to the number of whole gill folds, while "l" refers to the number of shorter gill folds between each pair of entire gill folds. For basidiospores, the factor E indicates the quotient of the length and width in any one basidiospore and Q is the mean of the E-values; the basidiospore values are based on 20 measurements in each collection. Specimens are preserved in the herbarium of the Moravian Museum, Brno, Czech Republic (**BRNM**) and duplicates deposited in the fungarium of the Natural History Museum in Paris, France (**PC**).

### Taxon sampling, sequence data and phylogenetic analyses

Translation elongation factor 1-alpha (*tef*-1) sequence data were produced following Buyck et al. (2014) for the newly described species from dried materials: four

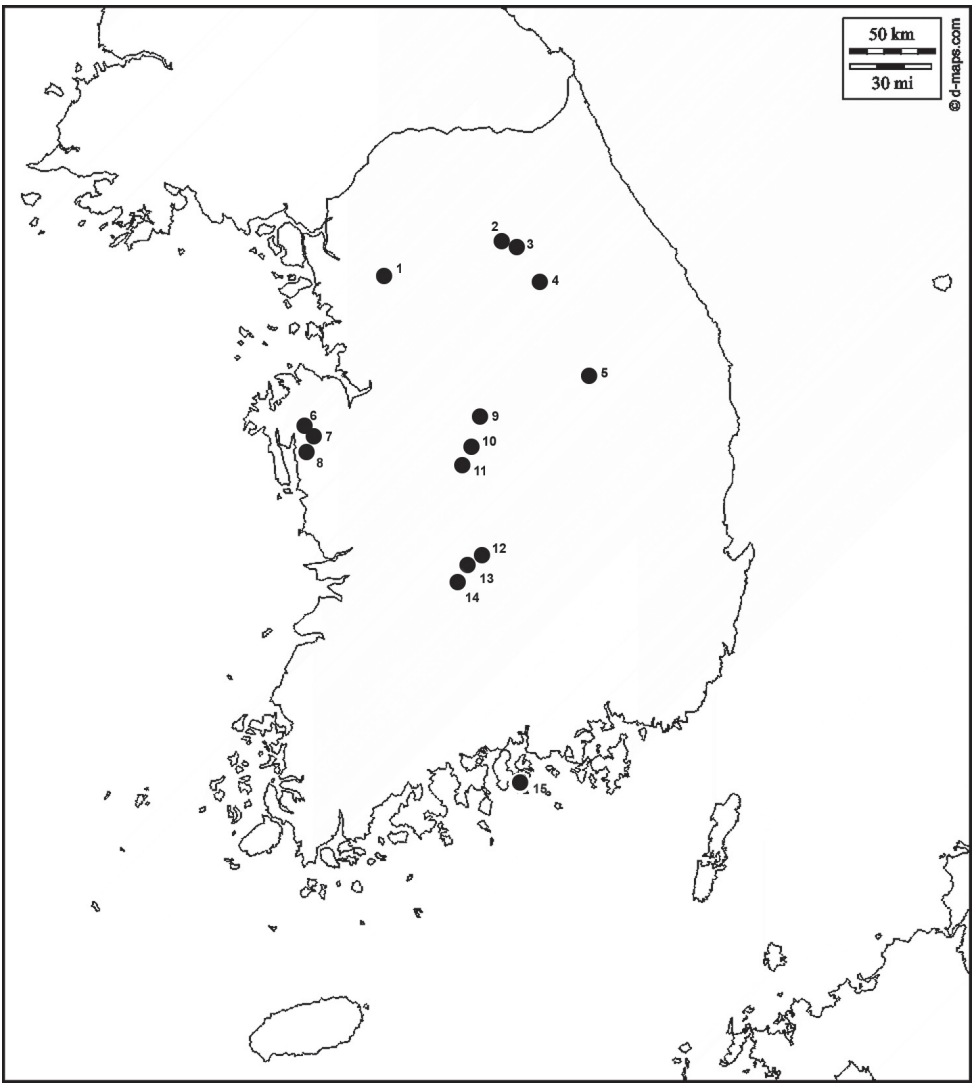


**Figure 1.** Map of localities of the *Cantharellus* species **1** Hongneung Arboretum, Seoul **2** Suta-sa, Dong-myeon, Hongcheon **3** Experimental Forest, Dong-myeon, Hongcheon **4** Mts. Chiaksan, Haggok-ri, Wonju **5** Guin-sa, Mts. Sobaek, Danyang **6** Yonghyeon National Natural Recreation Forest, Unsan-myeon, Seosan **7** Mts.Gaya, Deoksan-myeon, Yesan **8** Sudeok-sa, Deoksan-myeon, Yesan **9** Mt. Gunjusan, Chilseon-myeon, Goeisan **10** Cheoncheon-myeon, Geoisan **11** Songnisan National Park, Boeun **12** Mulan Valley, Sangcheon-myeon, Yeongdong **13** Minjoojisan Recreational Forest, Yonghwa-myeon, Yeongdong **14** Unjangsan Recreational Forest, Jeongcheon-myeon, Jinan **15** Pyunbaeg Recreational Forest, Samdong-myeon, Namhae.

sequences for four collections of *Cantharellus citrinus* sp. nov and one sequence from a collection of *C. curvatus* sp. nov. Additional *tef*-1 sequences were obtained for two previously described species: for two collections of *C. koreanus* Buyck, Antonín & V. Hofst. and for one collection of *C. albovenosus* Buyck, Antonín & V. Hofst. We

introduced these newly produced *tef*-1 sequences in the alignment obtained by Antonín et al. (2017). Species of subg. *Pseudocantharellus* Eyssart. & Buyck were used as outgroup sequences. GenBank submissions numbers are given in Fig. 2. Alignment of sequence data was performed manually in MacClade (Maddison and Maddison 2003). Three independent searches for the most likely tree were conducted in PhyML v. 3.0 (Guindon and Gascuel 2003) to check for convergence toward the same likelihood value. These searches used the GTR evolutionary model (Abadi et al. 2019) with the proportion of invariable sites, the gamma shape parameter and the number of substitution categories estimated during the search. Branches were considered as significantly supported when maximum likelihood bootstrap support (ML-bs) was ≥ 70%.

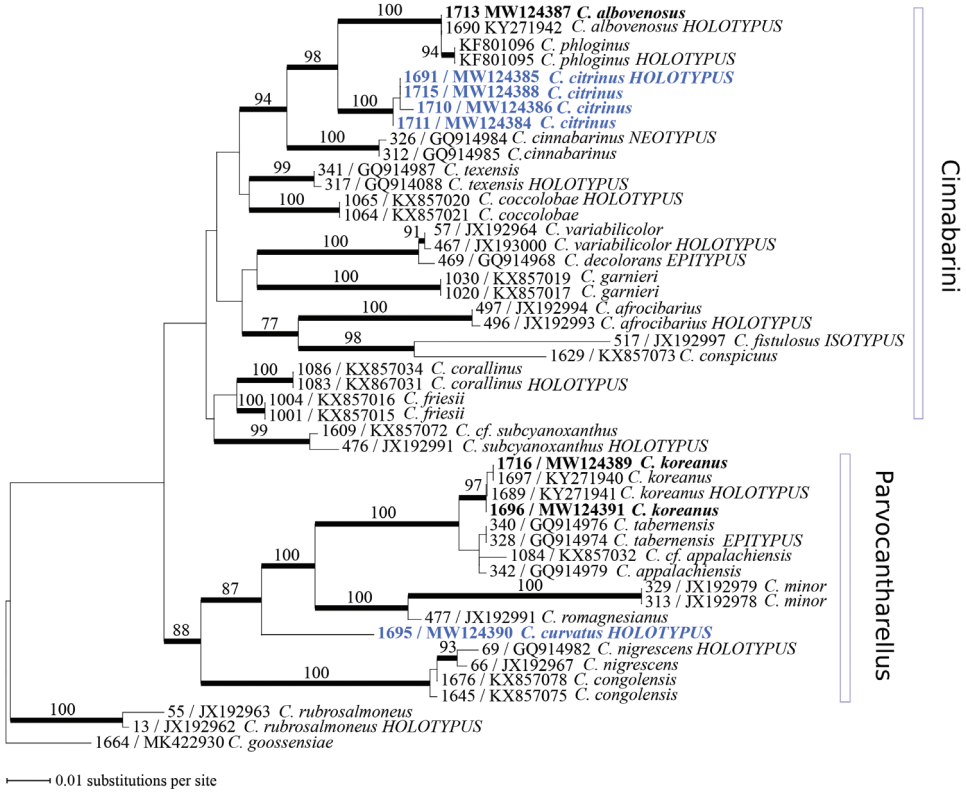


**Figure 2.** Most likely tree (-ln = 3254.82124) obtained by phylogenetic analyses of 48 *tef*-1 *Cantharellus* sequences. Supported branches are in bold with bootstrap values, when significant (≥ 70%), indicated along the branches. Sequences newly obtained for this study are in bold and highlighted in blue for the new species described in the present study. Extraction numbers and GenBank accession numbers for *tef*-1 sequences are reported before taxon names. Delimitation of *Cantharellus* subgenera *Cinnabarini* and *Parvocantharellus* (sensu lato) are indicated and *C. goossensiae* Heinem. and *C. rubrosalmoneus* (Buyck & V. Hofst.) Buyck & V. Hofst. (both in *C.* subg. *Pseudocantharellus*) are used as outgroup.

## Results

### Phylogeny

The final alignment of *tef*-1sequences included 837 characters. After the removal of three spliceosomal introns, the alignment used for phylogenetic analyses included 629 characters. The most likely tree (Fig. 2) suggests that *C. citrinus* sp. nov. is part of subgenus *Cinnabarini* Buyck & V. Hofst. This species has a sister relationship (ML-bs = 98%) with the subclade (ML-bs =100%) including *C. albovenosus* and *C. phloginus* S.C. Shao & P.G. Liu. Our phylogeny further suggests that *C. curvatus* sp. nov. nests in the significantly supported subgenus *Parvocantharellus* Eyssart. & Buyck (ML-bs = 88%). The new species occupies a basal position in a subclade (ML-bs = 87%) composed of *C. romagnesianus* Eyssart. & Buyck, *C. minor* Peck, *C. appalachiensis* R.H. Petersen, *C. tabernensis* Feibelman & Cibula and *C. koreanus* and is clearly separated (ML-bs = 100%) from these other species. The only other subclade (ML-bs 100%) in the subgenus is composed of the blackening *Cantharellus* from tropical Africa, *C. nigrescens* Buyck & V. Hofst. and *C. congolensis* Beeli.

### Taxonomy

***Cantharellus citrinus* Buyck, R. Ryoo & Antonín, sp. nov.**
MycoBank No: 837726
Figs 3, 4

**Diagnosis.** Differs from its closest Asian and North American relatives in the variously coloured but often bright lemon yellow pileus, similarly tinted stipe and smaller size, as well as in differences in sequence data produced for the transcription elongation factor (*tef*-1).

**Holotype.** South Korea. Geoi-san, Cheong-cheon-myeon, alt. 330 m, 36°37'02.99"N, 127°49'36.56"E, 14 Aug 2013, V. Antonín, R. Ryoo & K.-H. Ka, 1691 / VA 13.156 (holotype: BRNM 825748; isotype: PC 0142457).

**Description.** Basidiomata dispersed in small groups or fascicles. Pileus 4–20 mm broad, convex, with involute margin when young, then plane or infundibuliform with depressed centre and inflexed to straight, smooth margin, irregularly undulate when old, hygrophanous, finely tomentose when very young, soon glabrescent and smooth or slightly rugulose, uniformly coloured, light yellow, orange yellow to light orange (3–4A6, 4–5A5–7), sometimes with greyish yellow tinge when old. Hymenophore composed of thick vein-like folds, sometimes strongly decurrent in a reticulate pattern on upper stipe, often not reaching the pileus margin, forking or with rare lamellulae, transversely anastomosed in between, white to whitish (3A2); edges concolorous. Stipe 4–22 × 1–3(–4) mm, slightly tapering towards base when young, then cylindrical, sometimes curved, finely pubescent when young, later glabrescent, smooth, concolorous with pileus or slightly paler. Context thin, yellowish, fibrillose-hollow and yellow-

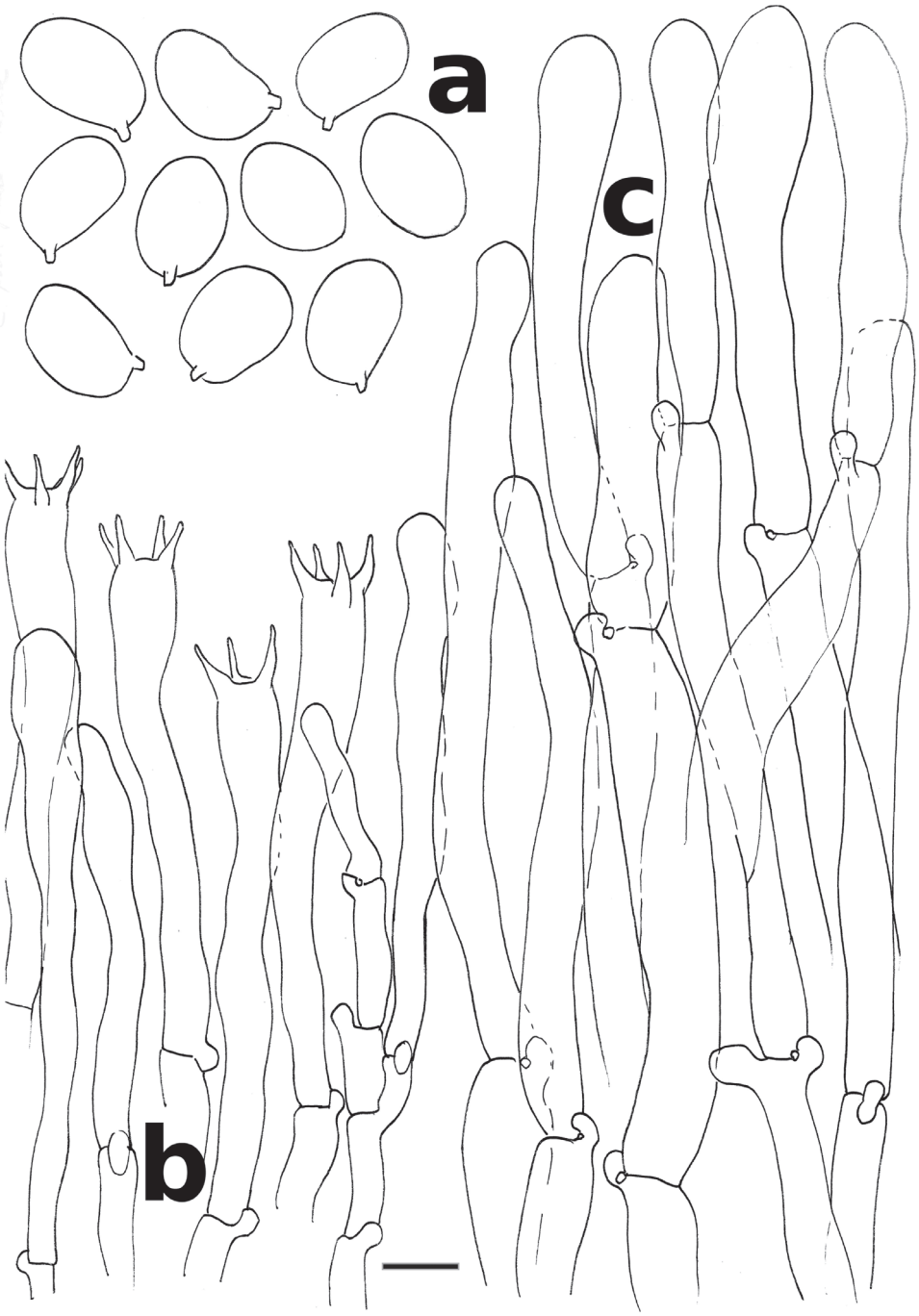


**Figure 3.** *Cantharellus citrinus* (holotype) **a** spores **b** basidia and basidiola **c** hyphal extremities of the pileipellis near mid-radius. Scale bar: 10 µm, but only 5 µm for spores. Drawings B. Buyck.

ish whitish in stipe when old, with a spicy apricot smell and mild taste. Spore print not obtained.

Basidiospores ellipsoid, (7.3–)7.6–**8.24**–8.4(–8.8) × (5.1–)5.4–**5.67**–5.9(–6.1) µm, Q = (1.32–)1.34–**1.42**–1.50(–1.56), smooth, thin-walled. Basidia mostly (42–)66–80 × 8 µm, 4–5(–6)-spored, narrowly clavate; basidiola subcylindrical and slender when young, undulate-wavy in outline, later becoming narrowly clavate, subfusoid, sometimes irregular, rarely submoniliform, thin-walled. Cystidia not observed. Subhymenium composed of narrow, filamentous and cylindrical cells. Pileipellis a cutis composed of cylindrical, ± thin-walled, smooth or minutely incrusted, sparsely septate, (4–)8–12 µm wide hyphae; terminal cells (36–)50–110 × 4.0–15 µm, appressed to suberect, mostly slightly clavate, some with a subapical weak constriction, obtuse, thin-walled. Stipitipellis a cutis of cylindrical, slightly thick-walled, 2.5–6.0(–7.0) µm wide hyphae with isolated terminal cells distinct only in a narrow zone at very top, otherwise rare to absent, 20–51 × 4.0–11 µm, (narrowly) clavate, cylindrical or subfusoid, thin-walled. Clamp connections everywhere and distinct.

**Habitat.** On soil near *Quercus mongolica* Fisch. ex Ledeb., *Q. acutissima* Carruth., *Quercus* sp., *Castanea crenata* Siebold & Zucc., *Carpinus laxiflora* (Siebold & Zucc.) Blume and *Abies koreana* E.H. Wilson.

**Etymology.** The name refers to the frequent bright lemon yellow colour of pileus and stipe surface of the most common form.

**Other specimens examined.** Jinan, Jeongcheon-myeon, Unjangsan Recreational Forest, alt. 390 m, 35°54'01.13"N, 127°24'59.41"E, 7 Sep 2016, V. Antonín, R. Ryoo, K.-H. Wang & Y.-S. Jang, 1710 / VA 16.169 (BRNM 825753, PC 0142467). Ibid., 1711 / VA 16.170 (BRNM 825754, PC 0142468). Yeongdong, Yonghwa-myeon, Minjoojisan Recreational Forest, alt. 540 m, 36°03'14.57"N, 127°49'43.15"E, 26 Aug 2015, V. Antonín, K.-H. Ka, K.S. Kim & J.A. Kang, 1715 / VA 15.93 (PC 0142472).

**Remarks.** The description is based on the type specimen, but examination of the other specimens shows that variation of morphological features includes a rather wide amplitude of the overall colour, which seems – based on identical *tef1* sequences – to extend from entirely and predominantly pale lemon yellow to an overall deep orange. Collection from Jinan (VA 16.169, BRNM 825753, PC 0142467) differs from other collections of this species by an orange (5–6A7) pileus, light yellow to light orange (4–5A5) lamellae and a stipe more or less concolorous with the pileus.

This new species is here placed in *Cantharellus* subg. *Cinnabarini* (Fig. 2), a subgenus that comprises several species exhibiting a similarly wide colour range, e.g. the Malagasy *C. variabilicolor* Buyck & V. Hofst. (in Ariyawansa et al. 2015) or the North American *C. cinnabarinus* (Schwein.) Schwein. *Cantharellus citrinus* is here shown to be part of a well-supported clade composed of two other Asian species, the Chinese *C. phloginus* and Korean *C. albovenosus*. The latter two species are very different in general aspect, but, except for a single mutation in the coding part, the *tef*-1 sequences of both species are identical, even including the introns. Yet, their

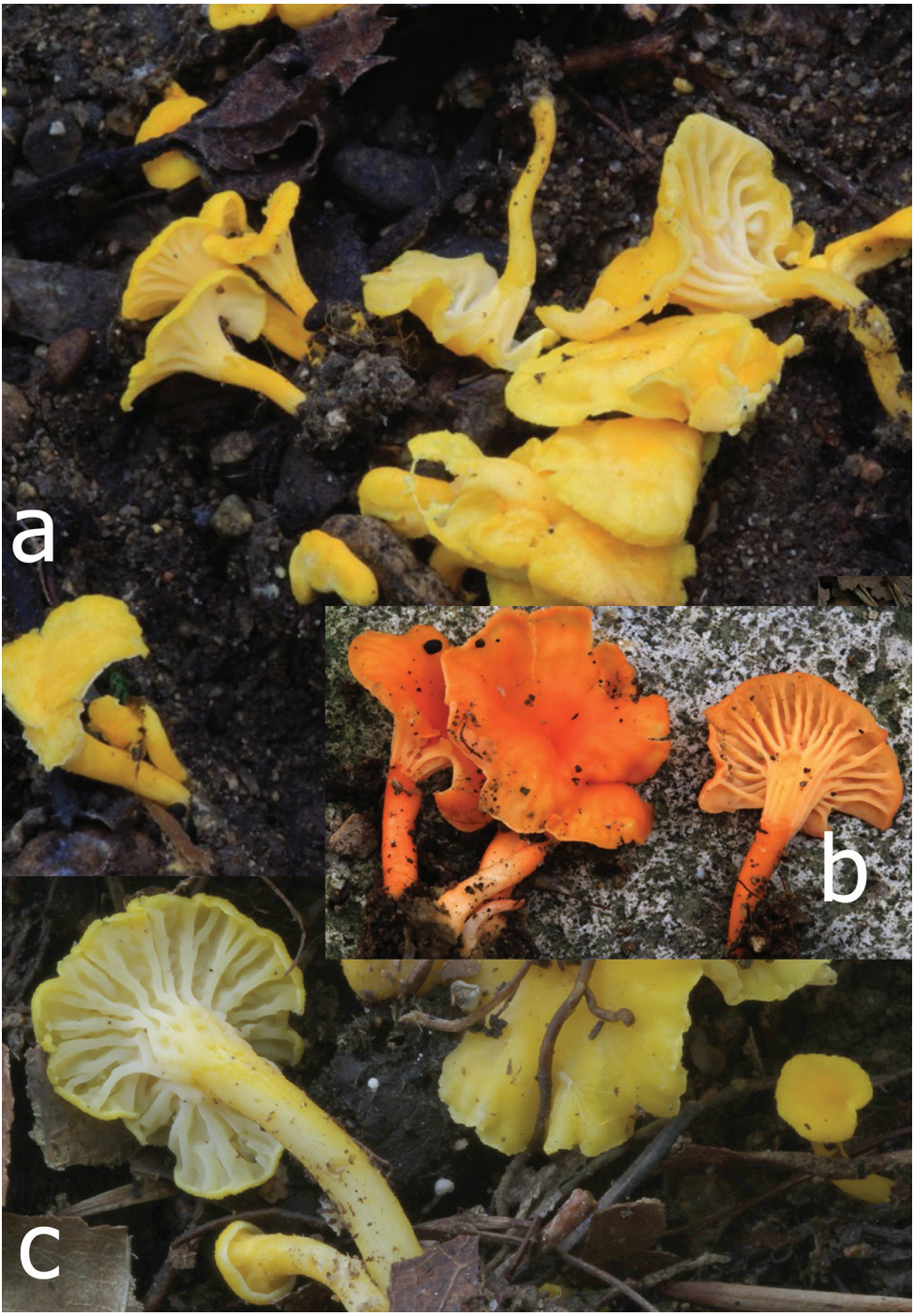


**Figure 4. a–c** *Cantharellus citrinus*, yellow, more common form **a** (VA 13.170) **b** *C. citrinus*, reddish orange form (VA 16.169) **c** (VA 13.156, holotype). Photos V. Antonín.

very different general habitus justifies us in our view that we should accept them as a separate species. The clade comprising these Asian species is sister to a clade composed of North American species.

Because of its very small overall size and comparable overall colour, *C. citrinus* could also easily be mistaken for some species in *Cantharellus* subg. *Parvocantharellus* Eyssart. & Buyck, in particular the European *C. romagnesianus* (= *C. pseudominimus* Eyssart. & Buyck, see Olariaga et al. 2015). Under the microscope, *C. citrinus* differs hardly from its Asian relatives and identification relies principally on field characters or sequence data.

***Cantharellus curvatus*** **Buyck, R. Ryoo & Antonín, sp. nov.**
MycoBank No: 837727
Figs 5, 6

**Diagnosis.** Differs from the European *C. romagnesianus* in the distinctly smaller spores and shorter basidia (see Olariaga et al. 2016), the strongly veined hymenophore and sequence data obtained from the transcription elongation factor one alpha (*tef-1*).

**Holotype.** South Korea. Yesan, Deoksan-myeon, Sudeok-sa, alt. 220 m, 36°39'57.40"N, 126°37'20.91"E, 8 Jul 2014, V. Antonín & K.-H. Ka, 1695 / VA 14.57 (holotype: BRNM 825749; isotype: PC0142461)

**Description.** Basidiomata in groups. Pileus 20–30 mm broad, low convex with a low broad central umbo and involute margin, then irregularly applanate or shallowly infundibuliform with an undulate, often uplifted margin, hygrophanous, not translucently striate, smooth, glabrous, watery dull yellow when moist, drying out to orangish yellow (± slightly more yellow than 4A5). Hymenophore composed of distant gill folds [L = 37–40], shortly decurrent, thick, sometimes furcate when young, furcate-anastomosed in upper half when old, pale yellow (± 3A3), ± dirty (greyish) yellow at the end; edge concolorous. Stipe 25–30 × 3.5–4 mm, cylindrical and tapering towards base, longitudinally fibrillose, yellow (± concolorous with pileus). Context pale whitish-yellowish, with cantharelloid smell.

Basidiospores (7.25–)7.5–**8.05**–9.0 × 5.0–**5.25**–6.0(–6.25) µm, Q =1.40–**1.52**–1.66, ellipsoid, rarely broadly ellipsoid, ventrical applanate or suballantoid, thin-walled, smooth. Basidia 42–55 × 9.5–12 µm, (4–)6-spored, narrowly clavate, clamped. Basidiola 15–42 × 3.0–11 µm, clavate, cylindrical, subfusoid, irregularly curved or undulate. Trama hyphae of cylindrical to fusoid, clamped, ± thin-walled, 4.0–20 µm wide cells. Pileipellis a cutis composed of cylindrical, clamped, mostly thin-walled, 4.0–10 µm wide hyphae; terminal cells appressed to suberect, mostly cylindrical, slightly thick-walled, up to 80 µm long and 5.0–10(–15) µm wide. Stipitipellis a cutis of cylindrical, parallel, slightly thick-walled, clamped, 3.0–6.0 µm wide hyphae. Terminal cells appressed to suberect, clavate or cylindrical.

**Habitat.** On soil under *Pinus densiflora* Siebold & Zucc. and *Castanea crenata*.

**Figure 5.** *Cantharellus curvatus* (VA 14.57, holotype). Scale bar: 15 mm. Photos V. Antonín.

**Etymology.** Referring to the curved-undulate hymenial cells, viz. basidia and particularly basidiola.

**Remarks.** This Asian species differs from the European *C. romagnesianus*, presently the most similar chanterelle, in the distinctly smaller spores and shorter basidia (see Olariaga et al. 2016), further also in the strongly anastomosing hymenophore and in sequence data obtained from the transcription elongation factor one alpha (*tef-1*).

***Cantharellus anzutake*** **W. Ogawa, N. Endo, M. Fukada & A. Yamada, Mycoscience 59(2): 158 (2018)**
Figs 7–9

**Description.** Pileus 10–40 mm broad, convex-conical when young, soon plane to broadly funnel-shaped, sometimes with a low obtuse umbo at centre, margin involute then inflexed to straight and undulate, pruinose when young then ± glabrous, greasy when moist, smooth or slightly uneven, not translucently striate, yellow (4A7–8), sometimes with darker ("dirty") centre. Lamellae moderately close, L = c. 25–30, decurrent, often furcate, rarely branched, whitish to pale cream from ± half radius toward the stipe attachment, then yellow towards pileus margin. Stipe 20–40 × 3.5–6 mm, cylindrical, not broadened towards base, finely pruinose when young, then glabrous, white, not hollowing. Context yellow beneath pileipellis, white otherwise. Smell slight, cantharelloid. Taste mild with slightly sharp aftertaste. Spore print not obtained.

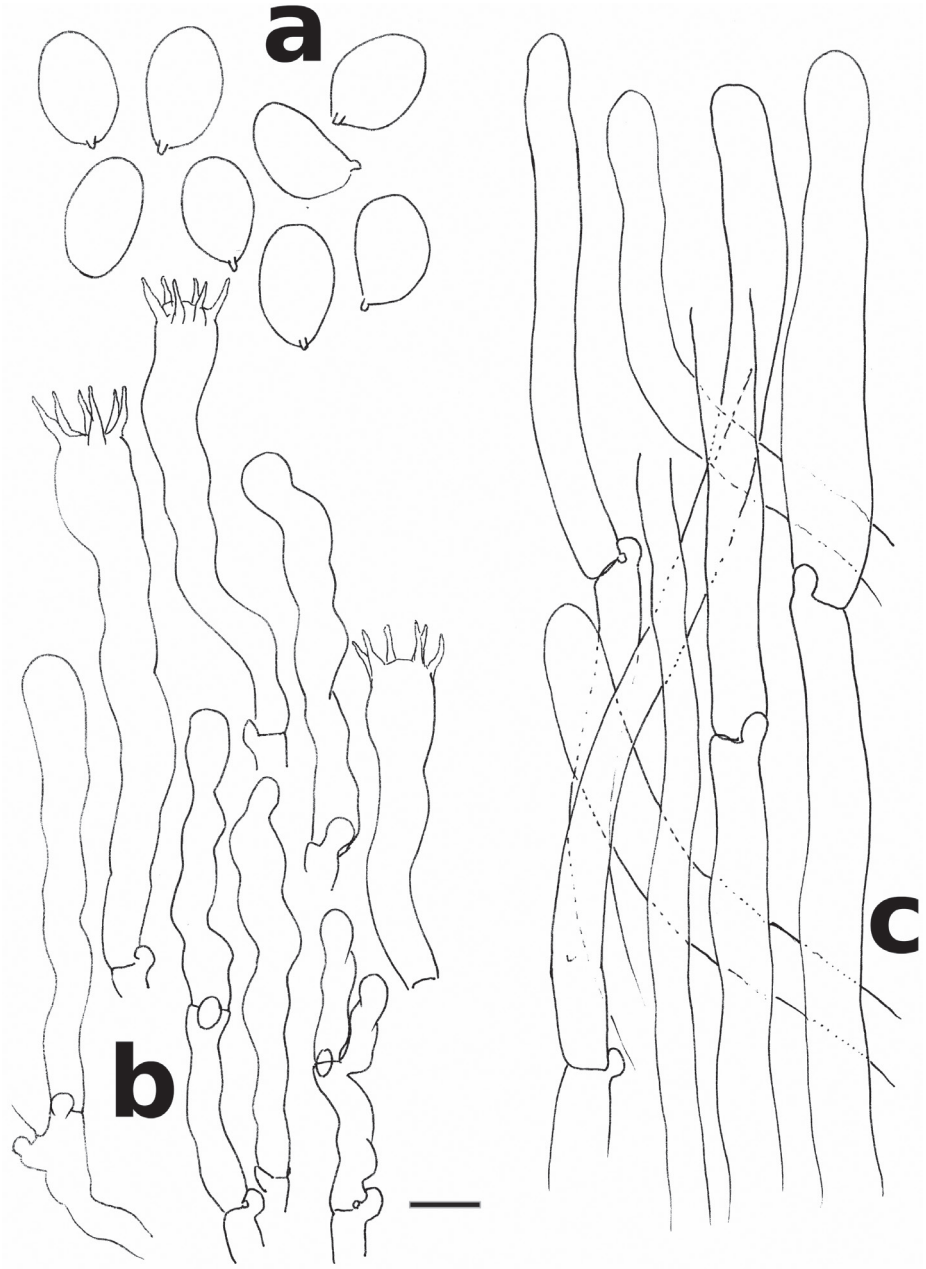


**Figure 6.** *Cantharellus curvatus* (holotype) **a** spores **b** basidia and basidiola **c** hyphal extremities of the pileipellis near mid-radius. Scale bar: 10 µm, but only 5 µm for spores. Drawings B. Buyck.

Basidiospores ellipsoid to ovoid, (6.9–)7.2–**7.56**–8.0(–8.3) × (4.6–)4.8–**5.10**–5.4(–5.6) µm, Q = (1.31–)1.39–**1.49**–1.58(–1.68), smooth, with a small apiculus. Basidia clavate-pedicellate, (60–)70–80 × 7–8 µm, long and slender, mostly 6(–5)-spored

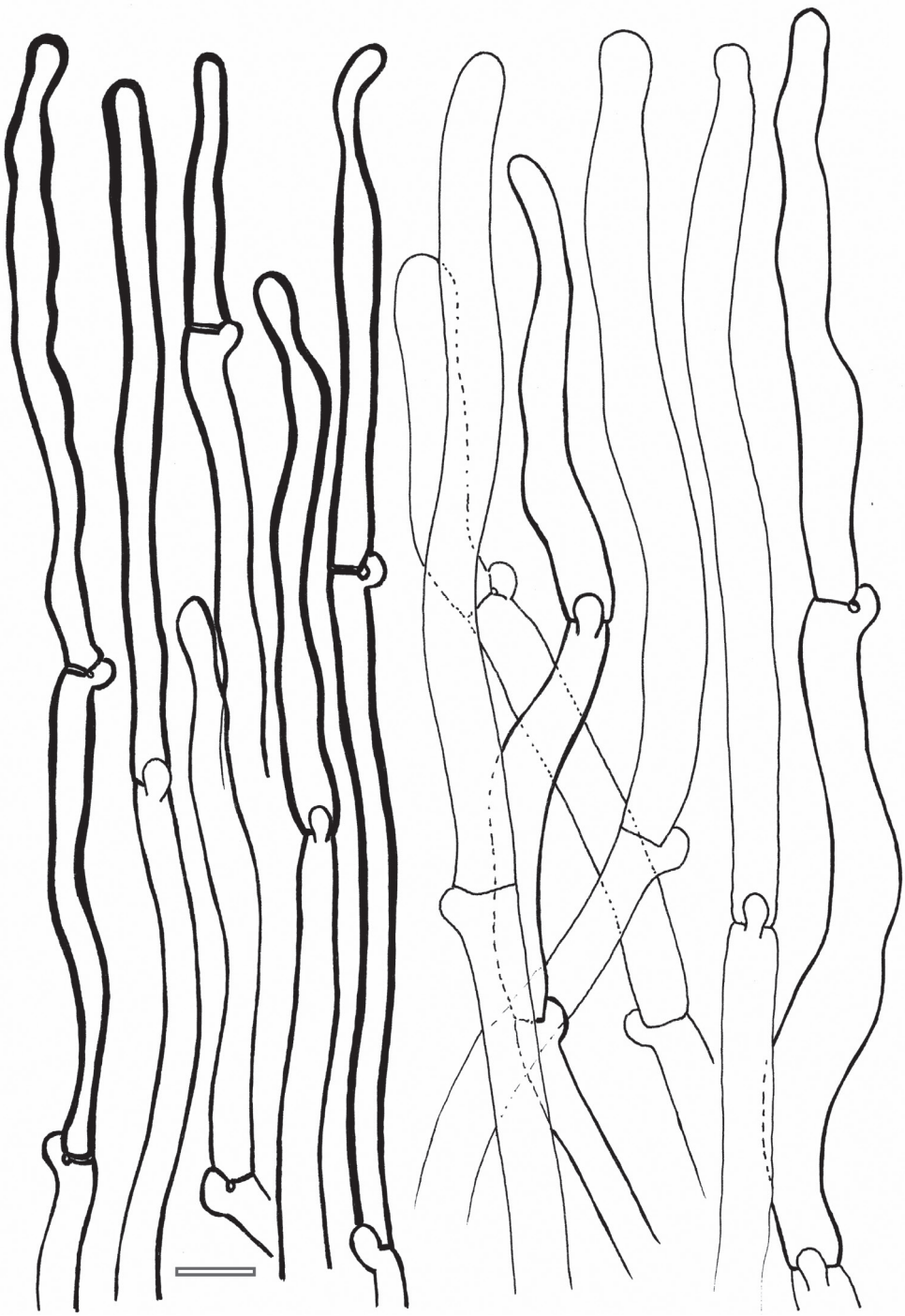

**Figure 7.** *Cantharellus anzutake*, microscopic features. Hyphal extremities at the pileus surface, on the left near the pileus center, on the right closer to the pileus margin. Scale bar: 10 µm. Drawings B. Buyck.

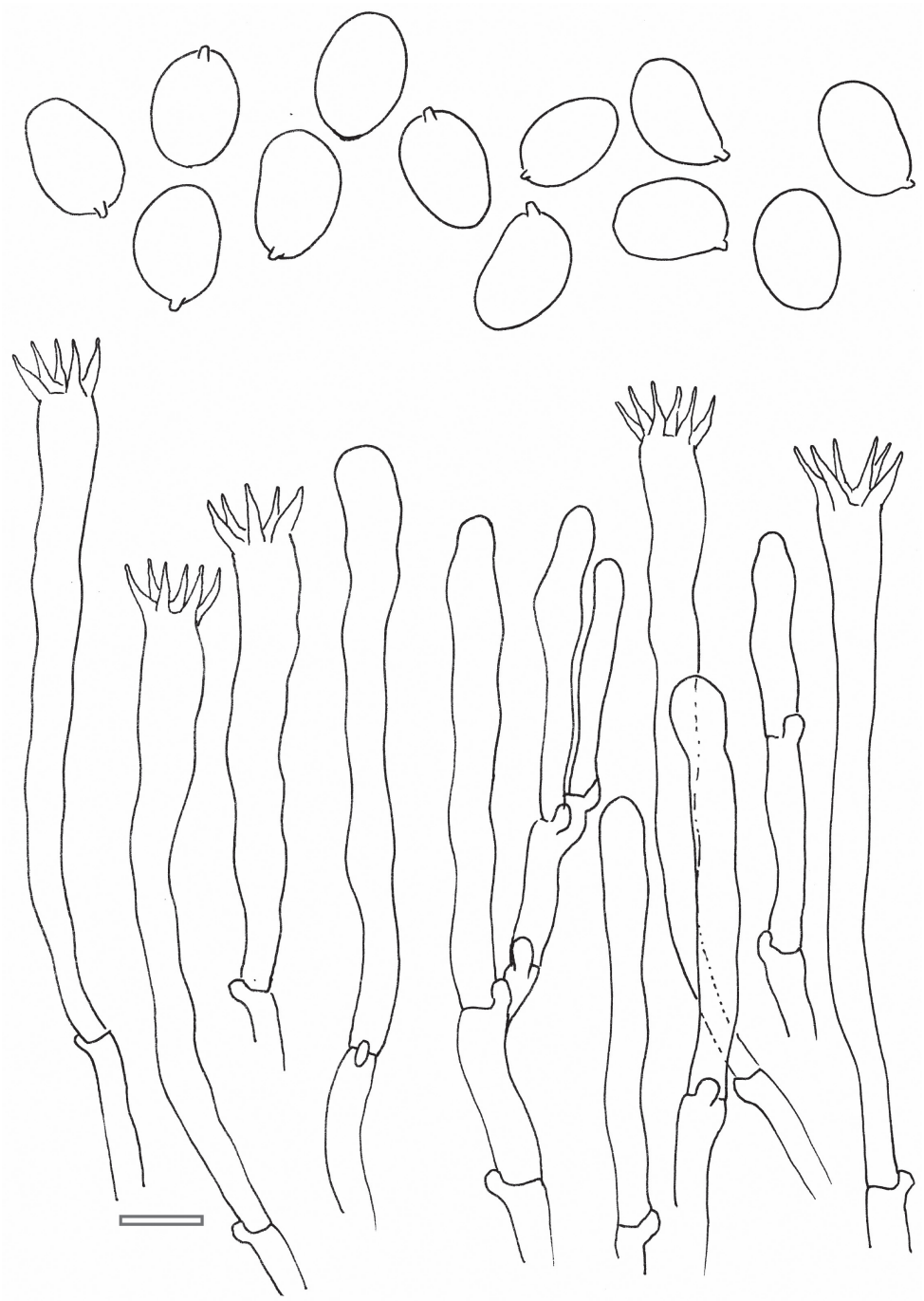

**Figure 8.** *Cantharellus anzutake*. Microscopic features. Basidia, basidiola and spores. Scale bar: 10 µm, but only 5 µm for spores. Drawings B. Buyck.

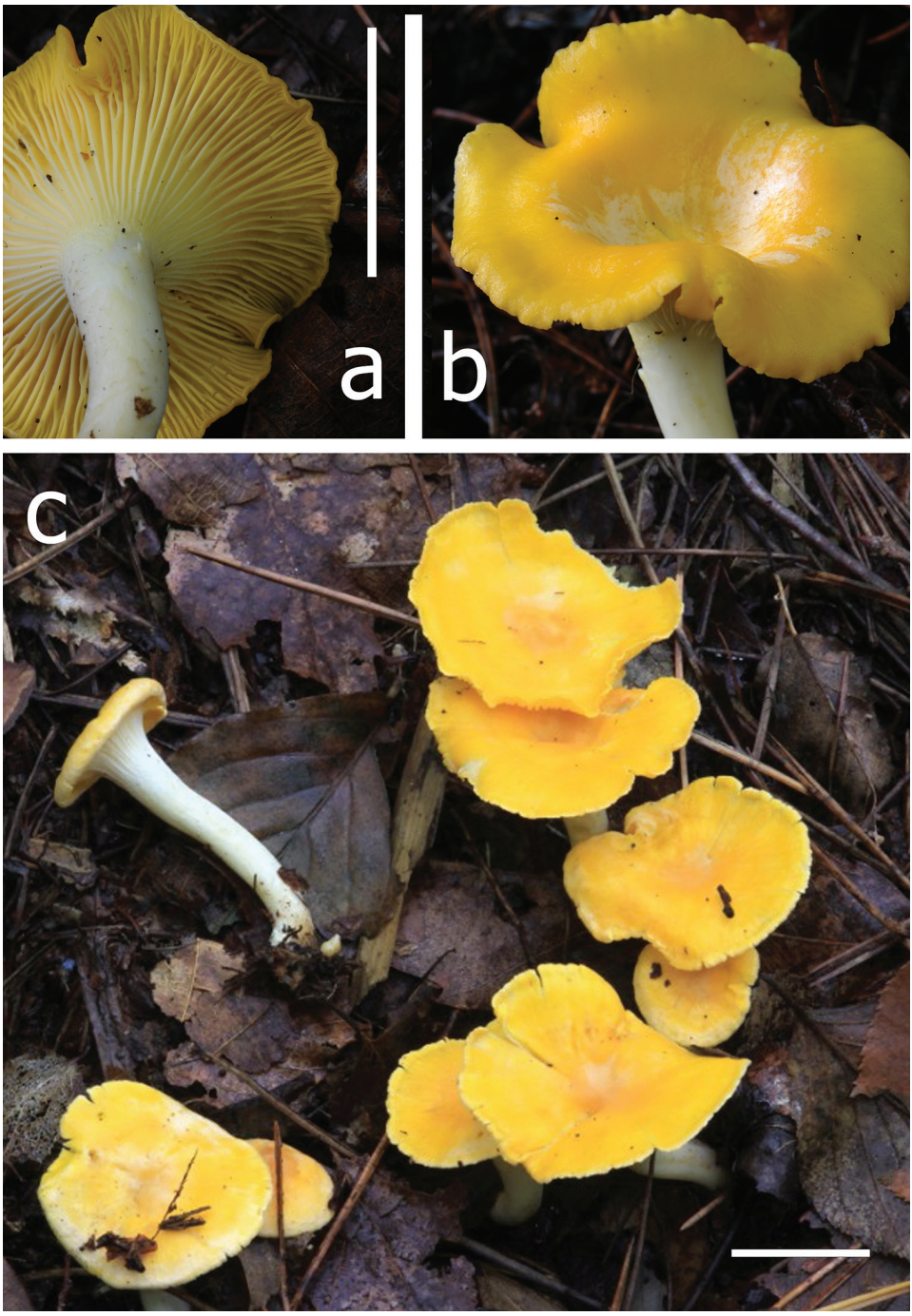


**Figure 9.** *Cantharellus anzutake* **a, b** Ka & Ryoo 3_Korea_1-2 [22/08/2012, Pyeongchang, Jungwangsan, 37°27'27.48"N, 128°29'04.35"E, 771 m asl, under *Pinus koraiensis* Siebold & Zucc.] **c** Antonín 16.140 (PC0142465). Note the very pale hymenophore in young specimens, remaining for a long time paler closer to the stipe when maturing. Scale bar: 20 mm.

with stout sterigmata. Subhymenium filamentous, composed of long and slender, cylindrical cells of similar diam. as the basidium base. Cystidia none. Pileipellis a loose tissue of intricately intertwining, sparsely septate, long and slender hyphal ends, near the pileus margin often aggregated in long tufts; hyphal ends composed of long, cylindrical, 5–8(–12) µm diam. cells, with refringent, thin- to slightly thickened walls, but in the pileus centre more frequently thick-walled; the terminal cell slender, toward the pileus margin (40–)60–130 µm long, obtuse rounded at the tip, cylindrical, hardly differentiated from subapical ones; in the pileus centre often somewhat irregularly constricted near the tip, but never very strongly so, and usually shorter, 30–100 µm, and on average somewhat narrower.

**Habitat.** On soil under *Pinus densiflora*, *Carpinus laxiflora* and *Quercus mongolica*.

**Specimens examined.** Jinan, Jeongcheon-myeon, Unjangsan Recreational Forest, 35°54'05.55"N, 127°24'53.89"E, alt. 400 m, 31 Aug 2016, V. Antonín, K.-H. Ka & S.-H. Kim, 1708 / VA 16.140 (BRNM 825751, PC 0142465). Ibid., VA 16.142 (BRNM 825752, PC 0142466).

**Remarks.** This species is a typical member of *Cantharellus* subg. *Cantharellus*, and belongs to a group that is often referred to as the 'golden chanterelles' or the *C. cibarius* Fr. complex, representing the commercially most important chanterelles on the international market. This species complex is reputedly very difficult to identify, in particular because of the very variable field aspect of the various species involved (Olariaga et al. 2015, 2016). Hence, positive identification frequently requires molecular sequence data. Our identification is here based on the high quality ITS sequence we obtained for VA 16.142 and which is identical to the one deposited for the *C. anzutake* holotype (GenBank LC085359, similarity 100% for 100% coverage); both these ITS differ from other yellow species of chanterelles described from Asia by a ca 100 bp deletion in the ITS1 region (Ogawa et al. 2018).

Because of the whitish hymenophore when young and the sometimes deep orange-yellow to cinnamon buff pileus surface, this species may be somewhat reminiscent of *C. albovenosus*. The latter species, however, has always a much brighter orange pileus and a more veined hymenophore that remains white, even with age, and it belongs in subgenus *Cinnabarini* (see Antonín et al. 2017). It is interesting to note that both Japanese and Korean specimens were collected near *Pinus densiflora* among possible host trees.

## Acknowledgements

V. Antonín is collaborating with South-Korean mycologists on various taxonomic projects since 2007. His collection trips to South Korea were supported by project FP 0801-2010-01 and FP0801-2018-01 of the National Institute of Forest Science in South Korea, and his laboratory studies were funded through the institutional support of long-term conceptual development of research institutions provided by the Ministry of Culture (ref. MK000094862).

## References

Abadi S, Azouri D, Pupko T, Mayrose I (2019) Model selection may not be a mandatory step for phylogeny reconstruction. Nature Communications 10: e934. https://doi.org/10.1038/s41467-019-08822-w

An DY, Liang ZQ, Jiang S, Su MS, Zeng NK (2017) *Cantharellus hainanensis*, a new species with a smooth hymenophore from tropical China. Mycoscience 58(6): 438–444. https://doi.org/10.1016/j.myc.2017.06.004

Antonín V, Hofstetter V, Ryoo R, Ka K-H, Buyck B (2017) New *Cantharellus* species from the Republic of Korea. Mycological Progress 16(8): 753–759. https://doi.org/10.1007/s11557-017-1312-2

Ariyawansa HA, Hyde KD, Jayasiri SC, Buyck B, Chethana, KWT, Dai DQ, Dai YC, Daranagama DA, Jayawardena RS, Lücking R, Ghobad-Nejhad M, Niskanen T, Thambugala KM, Voigt K, Zhao RL, Li GJ, Doilom M, Boonmee S, Yang ZL, Cai Q, Cui YY, Bahkali AH, Chen J, Cui BK, Chen JJ, Dayarathne MC, Dissanayake AJ, Ekanayaka AH, Hashimoto A, Hongsanan S, Jones EBG, Larsson E, Li WJ, Li QR, Liu JK, Luo ZL, Maharachchikumbura SSN, Mapook A, McKenzie EHC, Norphanphoun C, Konta S, Pang KL, Perera RH, Phookamsak R, Phukhamsakda C, Pinruan U, Randrianjohany E, Singtripop C, Tanaka K, Tian CM, Tibpromma S, Abdel-Wahab MA, Wanasinghe DN, Wijayawardene NN, Zhang JF, Zhang H, Abdel-Aziz FA, Wedin M, Westberg M, Ammirati JF, Bulgakov TS, Lima DX, Callaghan TM, Callac P, Chang CH, Coca LF, Dal-Forno M, Dollhofer V, Fliegerová K, Greiner K, Griffith GW, Ho HM, Hofstetter V, Jeewon R, Kang JC, Wen TC, Kirk PM, Kytövuori I, Lawrey JD, Xing J, Li H, Liu ZY, Liu XZ, Liimatainen K, Lumbsch HT, Matsumura M, Moncada B, Nuankaew S, Parnmen S, Santiago A, Sommai S, Song Y, Souza CAF, Souza-Motta CM, Su HY, Suetrong S, Wang Y, Wei SF, Yuan HS, Zhou LW, Réblová M, Fournier J, Camporesi E, Luangsa-ard JJ, Tasanathai K, Khonsanit A, Thanakitpipattana D, Somrithipol S, Diederich P, Millanes AM, Common RS, Stadler M, Yan JY, Li XH, Eberhardt U, Simonini G, Wen HA, Chen XH (2015) Fungal diversity notes 111–252: taxonomic and phylogenetic contributions to fungal taxa. Fungal Diversity 75: 27–274. https://doi.org/10.1007/s13225-015-0346-5

Buyck B, Antonín V, Chakraborty D, Baghela A, Das K, Hofstetter V (2018) *Cantharellus* sect. *Amethystini* in Asia. Mycological Progress 17: 917–924. https://doi.org/10.1007/s11557-018-1403-8

Buyck B, Kauff F, Eyssartier G, Couloux A, Hofstetter V (2014) A multilocus phylogeny for worldwide *Cantharellus* (Cantharellales, Agaricomycetidae). Fungal Diversity 64: 101–121. https://doi.org/10.1007/s13225-013-0272-3

Corner EJH (1966) A monograph of cantharelloid fungi. Annals of Botany Memoirs 2: 1–255.

Das K, Hofstetter V, Chakraborty D, Baghela A, Singh SK, Buyck B (2015) *Cantharellus sikkimensis* sp. nov. (Cantharellales, Agaricomycetes) from the Indian Himalayas. Phytotaxa 222(4): 267–275. https://doi.org/10.11646/phytotaxa.222.4.4

Eyssartier G, Stubbe D, Walleyn R, Verbeken A (2009) New records of *Cantharellus* species (Basidiomycota, Cantharellaceae) from Malaysian dipterocarp rainforest. Fungal Diversity 36: 57–67.

Guindon S, Gascuel O (2003) A simple, fast, and accurate algorithm to estimate large phylogenies by maximum likelihood. Systematic Biology 52: 696–704. https://doi.org/10.1080/10635150390235520

Kim Y-S (2004) The mushrooms of Korea. National Institute of Agricultural Science and Technology, Suwon, 467 pp.

Kim YP, Seok S-J, Kim WK, Won HY, Lee KH (2006) The mushrooms of Halla Mountain. Jeju Special Self-Governing Province Agricultural Research and Extension Service, 317 pp.

Kornerup A, Wanscher JH (1983) Methuen handbook of colour (3rd edn.). Eyre Methuen, London, 252 pp.

Kumari D, Upadhyay RC, Reddy MS (2011) *Cantharellus pseudoformosus*, a new species associated with *Cedrus deodara* from India. Mycoscience 52: 147–151. https://doi.org/10.1007/S10267-010-0080-5

Kumari D, Upadhyay RC, Reddy MS (2013) New records of *Cantharellus* species from the northwestern Himalayas of India. Mycology 4(4): 205–220. https://doi.org/10.1080/21501203.2013.872205

Lee T-S (2011) Rearrangement list of Korean recorded mushrooms. Josoop Publishing Co., Seoul, 87 pp.

Ogawa W, Endo N, Fukuda M, Yamada A (2018) Phylogenetic analyses of Japanese golden chanterelles and a new species description, *Cantharellus anzutake* sp. nov. Mycoscience 59(2): 153–165. https://doi.org/10.1016/j.myc.2017.08.014

Olariaga I, Buyck B, Esteve-Raventos F, Hofstetter V, Manjon JL, Moreno G, Salcedo I (2015) Assessing the taxonomic identity of white and orange specimens of *Cantharellus*: occasional colour variants or independent species? Cryptogamie Mycologie 36(3): 287–300. https://doi.org/10.7872/crym/v36.iss3.2015.287

Olariaga I, Moreno G, Manjoni J-L, Salcedo I, Rodriguez D, Hofstetter V, Buyck B (2016) *Cantharellus* (Cantharellales, Basidiomycota) revisited in Europe through a multigene phylogeny. Fungal Diversity 83(1): 263–292. https://doi.org/10.1007/s13225-016-0376-7

Park WH, Lee HD (1991) Wild fungi of Korea. Kyo-Hak Publishing Co., Seoul, 508 pp.

Shao SC, Buyck B, Hofstetter V, Tian XF, Geng YH, Yu FQ, Liu PG (2014) *Cantharellus hygrophorus*, a new species in subgenus *Afrocantharellus* from tropical southwestern China. Cryptogamie Mycologie 35(3): 281–289. https://doi.org/10.7872/crym.v35.iss3.2014.283

Shao SC, Buyck B, Tian XF, Liu PG, Geng YH (2016a) *Cantharellus phloginus*, a new pink-colored species from southwestern China. Mycoscience 57: 144–149. https://doi.org/10.1016/j.myc.2015.12.004

Shao SC, Liu PG, Tian XF, Buyck B, Geng YH (2016b) A new species of *Cantharellus* (Cantharellales) from subalpine forest in Shangri-la, Yunnan, China. Phytotaxa 252(4): 273–279. https://doi.org/10.11646/phytotaxa.252.4.3

Shao SC, Tian XF, Liu PG (2011) *Cantharellus* in southwestern China: a new species and a new record. Mycotaxon 116: 437–446. https://doi.org/10.5248/116.437

Suhara H, Kurogi S (2015) *Cantharellus cyphelloides* sp. nov., an unusual *Cantharellus* species from the evergreen broad-leaved forest of Japan. Mycological Progress 14: 1–7. https://doi.org/10.1007/s11557-015-1079-2

Tian XF, Buyck B, Shao SC, Liu PG, Fang Y (2012) *Cantharellus zanghii*, a new subalpine basidiomycete from southwestern China. Mycotaxon 120: 99–103. https://doi.org/10.5248/120.99

MycoKeys 76: 49–79 (2020)
doi: 10.3897/mycokeys.76.58406
https://mycokeys.pensoft.net

RESEARCH ARTICLE

A peer-reviewed open-access journal
MycoKeys
Launched to accelerate biodiversity research

# Cryphonectriaceae associated with rust-infected *Syzygium jambos* in Hawaii

Jolanda Roux[1], Gilbert Kamgan Nkuekam[1], Seonju Marincowitz[2], Nicolaas A. van der Merwe[2], Janice Uchida[3], Michael J. Wingfield[2], ShuaiFei Chen[2,4]

**1** *Department of Plant and Soil Sciences, Forestry and Agricultural Biotechnology Institute (FABI), University of Pretoria, Pretoria 0028, South Africa* **2** *Department of Biochemistry, Genetics and Microbiology, FABI, University of Pretoria, Pretoria 0028, South Africa* **3** *Department of Plant and Environmental Protection Sciences, Tropical Plant Pathology Program, College of Tropical Agriculture and Human Resources, University of Hawaii at Manoa, Honolulu, Hawaii 96822, USA* **4** *China Eucalypt Research Centre (CERC), Chinese Academy of Forestry (CAF), ZhanJiang, 524022, GuangDong Province, China*

Corresponding author: ShuaiFei Chen (shuaifei.chen@gmail.com)

Academic editor: D. Haelewaters | Received 6 September 2020 | Accepted 8 December 2020 | Published 31 December 2020

**Citation:** Roux J, Kamgan Nkuekam G, Marincowitz S, van der Merwe NA, Uchida J, Wingfield MJ, Chen SF (2020) Cryphonectriaceae associated with rust-infected *Syzygium jambos* in Hawaii. MycoKeys 76: 49–79. https://doi.org/10.3897/mycokeys.76.58406

## Abstract

*Syzygium jambos* (Myrtales, Myrtaceae) trees in Hawaii are severely affected by a rust disease caused by *Austropuccinia psidii* (Pucciniales, Sphaerophragmiaceae), but they are commonly co-infected with species of Cryphonectriaceae (Diaporthales). In this study, *S. jambos* and other trees in the Myrtales were examined on three Hawaiian Islands for the presence of Cryphonectriaceae. Bark samples with fruiting bodies were collected from infected trees and fungi were isolated directly from these structures. Pure cultures were produced and the fungi were identified using DNA sequence data for the internal transcribed spacer (ITS) region, part of the β-tubulin (*BT1*) gene and the transcription elongation factor-1α (*TEF1*) gene. Five species in three genera of Cryphonectriaceae were identified from Myrtaceae tree samples. These included *Chrysoporthe deuterocubensis*, *Microthia havanensis* and three previously-unknown taxa described here as *Celoporthe hauoliensis* sp. nov., *Cel. hawaiiensis* sp. nov. and *Cel. paradisiaca* sp. nov. Representative isolates of *Cel. hauoliensis*, *Cel. hawaiiensis*, *Cel. paradisiaca*, *Chr. deuterocubensis* and *Mic. havanensis* were used in artificial inoculation studies to consider their pathogenicity on *S. jambos*. *Celoporthe hawaiiensis*, *Cel. paradisiaca* and *Chr. deuterocubensis* produced lesions on young *S. jambos* trees in inoculation trials, suggesting that, together with *A. psidii*, they may contribute to the death of trees. Microsatellite markers were subsequently used to consider the diversity of *Chr. deuterocubensis* on the Islands and thus to gain

insights into its possible origin in Hawaii. Isolates of this important Myrtaceae and particularly *Eucalyptus* pathogen were found to be clonal. This provides evidence that *Chr. deuterocubensis* was introduced to the Hawaiian Islands as a single introduction, from a currently unknown source.

**Keywords**
*Austropuccinia psidii*, fungi, genetic diversity, Myrtales, pathogen introductions

## Introduction

Fungi in the Cryphonectriaceae (Diaporthales) include at least twenty-three genera of bark-, wood- and leaf-infecting fungi (Gryzenhout et al. 2009, 2010; Begoude et al. 2010; Vermeulen et al. 2011, 2013; Crous et al. 2012; Chen et al. 2013a, b, 2016, 2018; Crane and Burgess 2013; Beier et al. 2015; Ali et al. 2018; Ferreira et al. 2019; Jiang et al. 2020; Wang et al. 2020). They occur on trees and shrubs in various parts of the world and include saprophytes, facultative parasites and important pathogens of woody plants (Gryzenhout et al. 2009). Pathogens in the family reside mainly in the genera *Cryphonectria* and *Chrysoporthe* and include important agents of tree disease, both in natural forest ecosystems, as well as in intensively-managed plantations (Wingfield 2003; Gryzenhout et al. 2009; Wang et al. 2020). These fungi generally have yellow to orange or brown stromata and these structures turn purple in 3% potassium hydroxide (KOH) or yellow in lactic acid (Gryzenhout et al. 2006c, 2009; Jiang et al. 2020).

The Cryphonectriaceae infect trees and shrubs residing in more than 100 species in at least 26 families and 16 orders of plants worldwide (Gryzenhout et al. 2009; Jiang et al. 2020; Wang et al. 2020). The chestnut blight pathogen, *Cryphonectria parasitica* (Murrill) M.E. Barr is the best-known tree-killing pathogen in the family. It is native to Asia and outbreaks of the disease in North America and Europe have caused the virtual extinction of endemic populations of chestnut trees on these two continents (Anagnostakis 1987; Heiniger and Rigling 1994; Gryzenhout et al. 2009). Other important pathogens in the Cryphonectriaceae include: *Chrysoporthe cubensis* (Bruner) Gryzenh. & M.J. Wingf., which is native to South and Central America and causes a canker disease of *Eucalyptus* species in West Africa and South America (Alfenas et al. 1983; Gryzenhout et al. 2004, 2009; Roux and Apetorgbor 2010); *Chrysoporthe deuterocubensis* Gryzenh. & M.J. Wingf., native to Southeast Asia and causal agent of a canker disease of *Eucalyptus* species in Africa, Australia, China and Hawaii (Davison and Coates 1991; Roux et al. 2005; Nakabonge et al. 2006; Zhou et al. 2008; Chen et al. 2010; Van der Merwe et al. 2010; Wang et al. 2020); and *Chrysoporthe austroafricana* Gryzenh. & M.J. Wingf., endemic to Africa and causal agent of a canker disease of *Eucalyptus*, *Syzygium* and *Tibouchina* species in southern and eastern Africa (Wingfield et al. 1989; Myburg et al. 2002a; Gryzenhout et al. 2004; Roux et al. 2005; Nakabonge et al. 2006).

Hawaii, in the central Pacific Ocean, is comprised entirely of islands and is the northernmost island group in Polynesia (Little and Skolmen 1989). The vegetation

is multivariate including many forest types that cover more than 41% of the State's total land area (Anonymous 2003). Hawaii's forests broadly comprise native forest and plantations of non-native trees, interspersed with stands of non-native, invasive tree species. Native forests are dominated by *Metrosideros polymorpha* Gaudich. (Myrtaceae, Myrtales) and *Acacia koa* A. Gray (Fabaceae, Fabales) trees, whereas plantations of non-native trees include various conifers and many tree species (mostly *Eucalyptus*) that reside in the Myrtaceae (Anonymous 2003). Eight species of indigenous Myrtaceae and more than 200 non-native Myrtaceae have been recorded from the Islands (Loope 2010).

In April 2005, a rust disease caused by *Austropuccinia psidii* G. Winter (syn. *Puccinia psidii*, Sphaerophragmiaceae, Pucciniales), was detected on the Island of O'ahu (Uchida et al. 2006; Loope 2010). The pathogen spread rapidly and, consistent with its broad host range in the Myrtaceae (Coutinho et al. 1998; Glen et al. 2007; Carnegie et al. 2016), has been reported to cause disease on at least five native and fifteen non-native Hawaiian species. Of these, the non-native and invasive *Syzygium jambos* (rose apple) has been especially severely affected by the disease (Loope 2010). Instances of crown death of *S. jambos* are common and, in some cases, large areas of trees have died (Loope 2010).

During a casual inspection of rust-infected *S. jambos* in Hawaii by M.J. Wingfield during August 2011 (unpublished data), fruiting bodies of fungi resembling species in the Cryphonectriaceae were observed on the stems and branches of dying trees. This raised interest as very little was known regarding the diversity and distribution of the Cryphonectriaceae infecting Myrtaceae on the Hawaiian Islands. Two species are known to occur and these include, *Chr. deuterocubensis*, collected from cankers on *Eucalyptus* species on the Islands of Kauai and Hawaii (Gryzenhout et al. 2006a, 2009; Van der Merwe et al. 2010) and *Microthia havanensis* (Bruner) Gryzenh. & M.J. Wingf., first found on *Eucalyptus* species grown on the same Islands (Gryzenhout et al. 2006a).

The dramatic death of *S. jambos* in Hawaii could be caused solely by *A. psidii*, but the extent of the rapid die-back of branches and stems raised the question as to whether other pathogens, such as the Cryphonectriaceae, might be involved. The aim of this study was, thus, to identify species of Cryphonectriaceae on rust-infected *S. jambos*, as well as on some other species of Myrtaceae. Furthermore, pathogenicity tests were used to consider the possibility that species in the Cryphonectriaceae might contribute to the death of trees that had become infected and were consequently stressed by *A. psidii*. The genetic diversity of a collection of the most commonly isolated Cryphonectriaceae species was also characterised to gain insight into its possible origin in Hawaii.

## Materials and methods

### Collection of samples and fungal isolation

Surveys for Cryphonectriaceae were conducted in Hawaii during July 2012. Samples were collected mainly from non-native *S. jambos* trees infected by *A. psidii*, but also from various native and non-native Myrtaceae, on the Islands of Maui, O'ahu and

Hawaii. Samples were collected using an unstructured approach where the areas sampled were determined by the time available for collections to be made on the three selected Islands. On each of the Islands, two to three sites, where rust-infected trees had previously been found, were selected and surveyed during the course of a single day. As much as possible of each Island was also covered by driving along main roads and sampling at regular intervals where *S. jambos* plants were observed.

The presence on samples of fruiting structures (ascostromata, conidiomata), typical of the Cryphonectriaceae, was ascertained using a 10× magnification hand lens. Pieces of bark bearing these fruiting structures were excised from infected stems and branches and placed in separate brown paper bags for each tree sampled. Samples from each Island were labelled and placed in plastic bags to prevent desiccation and to promote sporulation of the fungi. Isolations and purification of the Cryphonectriaceae from the wood samples followed the technique described by Chen et al. (2011). All isolates used in this study were deposited in the culture collection (CMW) of the Forestry and Agricultural Biotechnology Institute (FABI, www.fabinet.up.ac.za), University of Pretoria, Pretoria, South Africa. Representative isolates, including ex-type cultures, were deposited in the culture collection (CBS) of the Westerdijk Fungal Biodiversity Institute, Utrecht, The Netherlands. Dried specimens of cultures were deposited in the National Collection of Fungi (PREM), Roodeplaat, Pretoria, South Africa.

## DNA extraction, PCR amplification and sequencing

DNA was extracted from all isolates using PrepMan Ultra Sample Preparation Reagent kits (Applied Biosystems, California, USA) following the manufacturer's instructions. An Eppendorf Mastercycler (Merck, Germany) was used for PCR amplification of the nuclear rDNA region encompassing the internal transcribed spacer regions (ITS1, ITS2) and 5.8S gene of the ribosomal RNA (ITS) operon, part of the β-tubulin gene (*BT1*) and the transcription elongation factor-1α gene (*TEF1*). The ITS was amplified using primers ITS1 and ITS4 (White et al. 1990), the *BT1* using primers βt1a and βt1b (Glass and Donaldson 1995) and *TEF1* using primers EF728F and EF986R (Carbone and Kohn 1999). The PCR reaction mixtures and thermal cycling conditions were the same as described previously for the ITS, *BT1* (Chen et al. 2011, 2013a) and *TEF1* gene regions (Vermeulen et al. 2013).

A 5 µl aliquot of the PCR products was pre-stained with GelRed™ Nucleic Acid Gel stain (Biotium, Hayward, USA), separated on 1% agarose gels and visualised under UV light. PCR products were purified using Sephadex G-50 Gel (Sigma-Aldrich), following the manufacturer's instructions. The concentrations of the purified PCR products were determined using a Nanodrop ND-1000 Spectrophotometer (Nanodrop Technologies, Rockland, USA). Sequencing reactions were performed using the Big Dye cycle sequencing kit with Amplitaq DNA polymerase FS (Perkin-Elmer, Warrington, UK), following the manufacturer's protocols, on an ABI PRISM 3100 Genetic Analyzer (Applied Biosystems). Protocols for sequencing PCR amplicons were the same as those described by Chen et al. (2011) and both DNA strands were sequenced for each gene region. Sequences of both DNA strands for each isolate were examined

visually and combined using the programme Sequence Navigator v. 1.01 (ABI PRISM, Perkin Elmer). The ITS and *BT1* gene regions were sequenced for all isolates used in this study. The *TEF1* gene region was sequenced for selected isolates in genera for which this region was required for species-level identification.

## Phylogenetic analyses

A preliminary identification of the isolates was obtained by performing a similarity search (standard nucleotide BLAST) against the GenBank database (http://www.ncbi.nlm.nih.gov) using the ITS and *BT1* sequences. The BLAST results showed that the isolates obtained in the current study grouped in the genera *Celoporthe*, *Chrysoporthe* and *Microthia*.

For analyses of the ITS and *BT1* sequences of isolates from Hawaii, the datasets of Wang et al. (2020) were used as templates. Sequences of the ITS and *BT1* gene regions were analysed separately and in combination. A partition homogeneity test (PHT), as implemented in PAUP (Phylogenetic Analysis Using Parsimony) v. 4.0b10 (Swofford 2003), was used to determine whether there was conflict between the datasets, prior to performing combined analyses in PAUP (Farris et al. 1995; Huelsenbeck et al. 1996). Two isolates of *Diaporthe ambigua* (CMW5288 and CMW5587), residing in the Diaporthaceae (Diaporthales), were used as outgroups.

For isolates that grouped in *Celoporthe*, based on ITS and *BT1* gene sequences, *TEF1* sequences were required to obtain accurate species-level identifications (Chen et al. 2011; Vermeulen et al. 2013). The ITS, *BT1* and *TEF1* gene regions were analysed separately and in combination. This made it possible to determine the phylogenetic relationships amongst the isolates from Hawaii and all 10 previously described *Celoporthe* species (Nakabonge et al. 2006; Chen et al. 2011; Vermeulen et al. 2013; Ali et al. 2018; Wang et al. 2018). A PHT was used to determine if conflict existed amongst the ITS, *BT1* and *TEF1* datasets (Farris et al. 1995; Huelsenbeck et al. 1996). Two isolates of *Holocryphia capensis* (CMW37329 and CMW37887) were used as outgroups.

The sequences for each of the single gene datasets, as well as for a combined dataset consisting of two or three gene regions, were aligned using MAFFT online v. 7 (http://mafft.cbrc.jp/alignment/server/) (Katoh and Standley 2013) and applying the iterative refinement method (FFT-NS-i setting). The alignments were edited manually with MEGA4 (Tamura et al. 2007). For each dataset, Maximum Parsimony (MP) and Maximum Likelihood (ML) analyses were performed.

PAUP v. 4.0 b10 (Swofford 2003) was used for MP analyses, with gaps treated as the fifth character. Uninformative characters were excluded and informative characters were unordered and of equal weight with 1000 random addition replicates. The most parsimonious trees were obtained using the heuristic search function with stepwise addition, tree bisection and reconstruction branch swapping. Maxtrees were set to 5000 and zero-length branches were collapsed. A bootstrap analysis (50% majority rule, 1000 replicates) was undertaken to determine statistical support for the internal nodes in the trees. Tree length (TL), consistency index (CI), retention index (RI) and homoplasy index (HI) were used to assess the trees (Hillis and Huelsenbeck 1992).

PhyML v. 3.1 was used for the ML analyses for each dataset (Guindon and Gascuel 2003). The best nucleotide substitution model for each dataset was determined using the software package jModeltest v. 1.2.5 (Posada 2008). In PhyML, the maximum number of retained trees was set to 1000 and nodal support was determined by non-parametric bootstrapping with 1000 replicates. The phylogenetic trees for both MP and ML analyses were viewed in MEGA4 and edited in Microsoft Office PowerPoint version 2013.

## Morphology

Isolates of the Cryphonectriaceae were grown at 25 °C on 2% malt extract agar (MEA: 20 g/l malt extract and 15 g/l agar, Biolab, Midrand, South Africa and 1000 ml sterile deionised water) containing 0.05 g/l of the antibiotic streptomycin sulphate (Sigma-Aldrich, Steinheim, Germany). Where no sporulation was obtained on agar media, six isolates, representing the putative new species, were inoculated on water agar medium on to which ~ 5 cm long sterilised *Eucalyptus* stem sections had been placed. These were kept at room temperature (~ 25 °C) in the dark until fruiting structures were observed. For each new taxon, micro-morphological structures were studied using Nikon microscopes (Eclipse N*i*, SMZ18, Tokyo, Japan) and a mounted Nikon DS-Ri2 camera. The structures were initially mounted in water, later being replaced with 85% lactic acid on glass microscope slides. In order to study the morphology of fruiting structures and stromatic tissues, pieces of bark, bearing fungal fruiting structures, were mounted on discs in Leica Tissue Freezing Medium and dissected to 12–16 µm thickness using a Leica CM1520 cryostat (Wetzler, Germany). The cut sections were mounted in 85% lactic acid for observation. Whenever available, up to 50 measurements of characteristic features were made for isolates chosen to represent the types of putative new species. Measurements were recorded as minimum-maximum, except for spore dimensions for which supplementary information (mean ± standard deviation) was added.

Growth in culture was examined for two isolates of each putative new species identified. The protocols used to assess growth in culture were the same as those described by Chen et al. (2011). The growth rate at optimum temperature was repeated twice for ex-holotype isolates and the average was presented.

## Pathogenicity tests

*Syzygium jambos* seeds were collected from a garden in Pretoria, South Africa and germinated to produce seedlings for artificial inoculation studies under quarantine greenhouse conditions. These seedlings were grown for one year, until their stem diameters had reached at least 0.5 cm. Ten seedlings (~ 0.5–1 cm diam. × 30 cm high), were inoculated with each test strain and ten seedlings of the same size were inoculated with a sterile agar disc to serve as controls. Inoculations were made using the same technique as that described by Chen et al. (2011). Four weeks (28 days) after inoculation, the lengths of the lesions in the cambium on each plant were measured. The JMP version 5.0 of SAS software (SAS Institute Inc. 2002) was used for statistical analysis of the

lesion length data. One way ANOVA was used to test statistical differences between the means of the lesion lengths. Re-isolations were made from the lesions to confirm that they had resulted from the effects of the inoculated fungi.

### Genetic diversity of *Chr. deuterocubensis* isolates

The genetic diversity of the most commonly encountered and globally important species in the Cryphonectriaceae from Myrtales on the Hawaiian Islands was analysed using microsatellite markers. DNA was extracted from all isolates of freshly-prepared cultures using PrepMan Ultra Sample Preparation Reagent (Applied Biosystems, California, USA), following the manufacturer's instructions. A set of ten microsatellite markers (Suppl. material 1: Table S1), that had been developed and used in previous studies (Van der Merwe et al. 2003, 2010), was tested on ten randomly-selected isolates. The PCR reaction mixes and thermal cycling were the same as those described by Van der Merwe et al. (2003, 2010). PCR aliquots of 5 µl were pre-stained with GelRed Nucleic Acid Gel stain (Biotium, Hayward, USA) and amplicons were separated on 1% (w/v) agarose gels and visualised under UV light to confirm successful amplification. Primer pairs that did not amplify the target loci successfully after several repetitions were discarded. Those that were successful were used to amplify target loci from all the isolates of the available population.

PCR products for each isolate were multiplexed for GeneScan analysis. The composition of each sample mix was the same as that described by Kamgan Nkuekam et al. (2009). Sample mixes were separated on a 36-cm capillary column with POPTM4 polymer on an ABI Prism 3500 sequencer (Perkin-Elmer, Warrington, UK). Allele sizes were determined by comparing the mobility of the PCR products with that of a LIZ 500 size standard (Applied Biosystems, Foster City, California). Microsatellite size data were analysed using the software GeneMapper version 3.0 (Applied Biosystems, Foster City, California).

The allele size for each of the seven loci was scored for each isolate from the collection. These data were used to generate a multilocus haplotype profile for each isolate. Isolates that had identical alleles for each of the seven loci were treated as clones. The frequency of each allele within the collection was calculated by taking the number of times the allele was present in the population and dividing it by the population sample size. This was then used to calculate gene diversity using the formula $H = 1 - \sum_k x_k^2$ (Nei 1973), where $x_k$ is the frequency of the $k^{th}$ allele.

## Results

### Collection of samples and fungal isolation

A total of 139 Cryphonectriaceae isolates were obtained from 106 trees sampled on three Hawaiian Islands (Table 1). Trees, from which the fungi were obtained, included

**Table 1.** List of Cryphonectriaceae isolates collected during surveys in Hawaii and sequenced in the study.

| Species | Island | Hosts | Number of Trees | Number of Strains |
|---|---|---|---|---|
| *Chrysoporthe deuterocubensis* | O'ahu | *Syzygium jambos* | 18 | 19 |
| " | " | *Syzygium cumini* | 3 | 3 |
| " | " | *Syzygium* sp. | 11 | 11 |
| " | " | *Psidium cattleianum* | 9 | 12 |
| " | Hawaii | *S. jambos* | 28 | 38 |
| " | " | *Syzygium* sp. | 1 | 1 |
| " | " | *Metrosideros polymorpha* | 1 | 1 |
| " | Maui | *S. jambos* | 7 | 8 |
| *Microthia havanensis* | O'ahu | *P. cattleianum* | 5 | 7 |
| " | " | *S. cumini* | 1 | 1 |
| " | Hawaii | *P. cattleianum* | 1 | 1 |
| " | " | *S. jambos* | 1 | 1 |
| *Celoporthe hauoliensis* | Maui | *S. jambos* | 4 | 8 |
| " | Hawaii | *S. jambos* | 2 | 4 |
| " | " | *P. cattleianum* | 1 | 2 |
| *Cel. hawaiiensis* | O'ahu | *P. cattleianum* | 4 | 6 |
| " | " | *S. jambos* | 3 | 4 |
| " | " | *Syzygium* sp. | 1 | 1 |
| *Cel. paradisiaca* | O'ahu | *P. cattleianum* | 1 | 4 |
| " | " | *S. jambos* | 2 | 3 |
| " | " | *Syzygium* sp. | 1 | 3 |
| " | Hawaii | *S. jambos* | 1 | 1 |

a single specimen of the native species, Ohia (*Metrosideros polymorpha*) and multiple specimens of four non-native Myrtaceae hosts, including an unknown *Metrosideros* sp., *Psidium cattleianum*, *S. cumini* and *S. jambos*. The majority of trees sampled were those of *S. jambos* (66 trees), since this was the main tree of focus in the study and it also displayed the most evident examples of rust infection and death at the time of the survey. Samples were obtained from dead sapling trees (~ 0.5 cm or more diameter) or from older dying/dead trees and cankers on living trees. In the case of *M. polymorpha*, a species of Cryphonectriaceae was obtained from the surface of a single cut stump. On older trees, signs and symptoms of the Cryphonectriaceae could be found on dead branches and stem cankers, including on trees with no obvious infection by the myrtle rust pathogen.

## Phylogenetic analyses

For the isolates selected for sequencing, the PCR fragments were approximately 550, 450 and 260 bp for the ITS, *BT1* and *TEF1* regions, respectively. All sequences obtained in this study were deposited in GenBank (Table 2). The alignments of each of the datasets were deposited in TreeBASE (http://treebase.org, study ID: S19035). The number of taxa and characters in each of the datasets and a summary of the most important parameters applied in the Maximum Parsimony (MP) and Maximum Likelihood (ML) analyses are presented in Suppl. material 2: Table S2.

For the ITS and *BT1* datasets, the PHT generated a value of P = 0.001, indicating that the accuracy of the combined data had not suffered relative to the individual partitions (Cunningham 1997). Sequences of the two regions were combined for analyses. For each of the ITS, *BT1* and ITS+*BT1* datasets, the ML and MP analyses generated

**Table 2.** List of isolates and their GenBank accession numbers used for DNA sequence comparisons.

| Identity | Isolate No.[1,2] | Host | Location | Collector | GenBank accession no. | | | Reference |
|---|---|---|---|---|---|---|---|---|
| | | | | | ITS | *BT1* | *TEF1* | |
| *Amphilogia gyrosa* | CMW10469T | *Elaeocarpus dentatus* | New Zealand | G.J. Samuels | AF452111 | AF525707 | N/A[3] | Gryzenhout et al. (2005a, 2006c) |
| | CMW10470 | *Ela. dentatus* | New Zealand | G.J. Samuels | AF452112 | AF525708 | N/A | Gryzenhout et al. (2005a, 2006c) |
| *Aurantioporthe corni* | CMW10526 | *Cornus alternifolia* | USA | S. Redlin | DQ120762 | DQ120769 | N/A | Gryzenhout et al. (2006c) |
| | MES1001 | N/A | USA | W. Cullina | KF495039 | KF495069 | N/A | Beier et al. (2015) |
| | CTS1001 | N/A | USA | K. Kitka | KF495033 | KF495063 | N/A | Beier et al. (2015) |
| *Aurantiosacculus acutatus* | CBS132181T | *Eucalyptus viminalis* | Australia | B.A. Summerell & P. Summerell | JQ685514 | N/A | N/A | Crous et al. (2012) |
| *Aurantiosacculus eucalyptorum* | CBS130826T | *Euc. globulus* | Australia | C. Mohammed & M. Glen | JQ685515 | N/A | N/A | Crous et al. (2012) |
| *Aurapex penicillata* | CMW10030T | *Miconia theaezans* | Colombia | C.A. Rodas | AY214311 | AY214239 | N/A | Gryzenhout et al. (2006b, 2009) |
| | CMW10035 | *Mic. theaezans* | Colombia | C.A. Rodas | AY214313 | AY214241 | N/A | Gryzenhout et al. (2006b, 2009) |
| *Aurifilum marmelostoma* | CMW28285T | *Terminalia mantaly* | Cameroon | D. Begoude & J. Roux | FJ882855 | FJ900585 | N/A | Begoude et al. (2010), Vermeulen et al. (2011) |
| | CMW28288 | *Ter. ivorensis* | Cameroon | D. Begoude & J. Roux | FJ882856 | FJ900586 | N/A | Begoude et al. (2010), Vermeulen et al. (2011) |
| *Aurifilum terminali* | CSF10757T | *Ter. neotaliala* | China | S.F. Chen & W. Wang | MN199837 | MN258775 | MN258780 | Wang et al. (2020) |
| | CSF10762 | *Ter. neotaliala* | China | S.F. Chen & W. Wang | MN199838 | MN258776 | MN258781 | Wang et al. (2020) |
| *Capillaureum caryovora* | CBL02T | *Caryocar brasiliense* | Brazil | M.E. Soares de Oliveira &M.A. Ferreira | MG192094 | MG211827 | N/A | Ferreira et al. (2019) |
| | CBL06 | *Car. brasiliense* | Brazil | M.E. Soares de Oliveira &M.A. Ferreira | MG192096 | MG211829 | N/A | Ferreira et al. (2019) |
| *Celoporthe borbonica* | CMW44128T | *Tibouchina grandiflora* | La Réunion | M.J. Wingfield | MG585741 | MG585725 | N/A | Ali et al. (2018) |
| | CMW44139 | *Tib. grandiflora* | La Réunion | M.J. Wingfield | MG585742 | MG585726 | N/A | Ali et al. (2018) |
| *Celoporthe cerciana* | CERC9128T | *Eucalyptus* hybrid tree 4 | China, GuangDong | S.F. Chen | MH084352 | MH084382 | MH084442 | Wang et al. (2018) |
| | CERC9125 | *Eucalyptus* hybrid tree 1 | China, GuangDong | S.F. Chen | MH084349 | MH084379 | MH084439 | Wang et al. (2018) |
| *Celoporthe dispersa* | CMW9976T | *S. cordatum* | South Africa | M. Gryzenhout | DQ267130 | DQ267136 | HQ730840 | Nakabonge et al. (2006), Chen et al. (2011) |
| | CMW9978 | *S. cordatum* | South Africa | M. Gryzenhout | AY214316 | DQ267135 | HQ730841 | Nakabonge et al. (2006), Chen et al. (2011) |
| *Celoporthe eucalypti* | CMW26900 | *Eucalyptus* cloneEC48 | China | X.D. Zhou & S.F. Chen | HQ730836 | HQ730816 | HQ730849 | Chen et al. (2011) |
| | CMW26908T | *Eucalyptus* cloneEC48 | China | X.D. Zhou & S.F. Chen | HQ730837 | HQ730817 | HQ730850 | Chen et al. (2011) |
| *Celoporthe fontana* | CMW29375 | *S. guineense* | Zambia | M. Vermeulen & J. Roux | GU726940 | GU726952 | JQ824073 | Vermeulen et al. (2013) |
| | CMW29376T | *S. guineense* | Zambia | M. Vermeulen & J Roux | GU726941 | GU726953 | JQ824074 | Vermeulen et al. (2013) |
| *Celoporthe guangdongensis* | CMW12750T | *Eucalyptus* sp. | China | T.I. Burgess | HQ730830 | HQ730810 | HQ730843 | Chen et al. (2011) |
| *Celoporthe hauoliensis* | **CMW38373**[5] | *S. jambos* | Hawaii | J. Roux | KJ027503 | KJ027479 | KJ027488 | This study |
| | **CMW38389**T[5] | *P. cattleianum* | Hawaii | J. Roux | KJ027502 | KJ027478 | KJ027487 | This study |
| | **CMW38546** | *Syzygium* sp. | Hawaii | J. Roux | KJ027504 | KJ027480 | KJ027489 | This study |
| *Celoporthe hawaiiensis* | **CMW38553**[5] | *S. jambos* | Hawaii | J. Roux | KJ027500 | KJ027476 | KJ027485 | This study |
| | **CMW38582** | *S. jambos* | Hawaii | J. Roux | KJ027501 | KJ027477 | KJ027486 | This study |
| | **CMW38610**T[5] | *S. jambos* | Hawaii | J. Roux | KJ027499 | KJ027475 | KJ027484 | This study |
| *Celoporthe indonesiensis* | CMW10781T | *S. aromaticum* | Indonesia | M.J. Wingfield | AY084009 | AY084033 | HQ730842 | Myburg et al. (2003), Chen et al. (2011) |
| *Celoporthe paradisiaca* | **CWM38360**T[4,5] | *Psidium cattleianum* | Hawaii | J. Roux | KJ027498 | KJ027474 | KJ027483 | This study |
| | **CMW38368** | *Syzygium jambos* | Hawaii | J. Roux | KJ027496 | KJ027472 | KJ027481 | This study |
| | **CMW38384** | *S. jambos* | Hawaii | J. Roux | KJ027497 | KJ027473 | KJ027482 | This study |

| Identity | Isolate No.[1,2] | Host | Location | Collector | GenBank accession no. | | | Reference |
|---|---|---|---|---|---|---|---|---|
| | | | | | ITS | *BT1* | *TEF1* | |
| *Celoporthe syzygii* | CMW34023T | *S. cumini* | China | S.F. Chen | HQ730831 | HQ730811 | HQ730844 | Chen et al. (2011) |
| | CMW24912 | *S. cumini* | China | M.J. Wingfield & X.D. Zhou | HQ730833 | HQ730813 | HQ730846 | Chen et al. (2011) |
| *Celoporthe tibouchineae* | CMW44126T | *Tib. grandiflora* | La Réunion | M.J. Wingfield | MG585747 | MG585731 | N/A | Ali et al. (2018) |
| | CMW44127 | *Tib. grandiflora* | La Réunion | M.J. Wingfield | MG585748 | MG585732 | N/A | Ali et al. (2018) |
| *Celoporthe woodiana* | CMW13936T | *Tib. granulosa* | South Africa | M. Gryzenhout | DQ267131 | DQ267137 | JQ824071 | Vermeulen et al. (2013) |
| | CMW13937 | *Tib. granulosa* | South Africa | M. Gryzenhout | DQ267132 | DQ267138 | JQ824072 | Vermeulen et al. (2013) |
| *Chrysomorbus lagerstroemiae* | CERC8780 | *Lagerstroemia speciosa* | China | J. Roux & S.F. Chen | KY929330 | KY929350 | N/A | Chen et al. (2018) |
| | CERC8810T | *L. speciosa* | China | S.F. Chen | KY929338 | KY929358 | N/A | Chen et al. (2018) |
| *Chrysoporthe austroafricana* | CMW62 | *Euc. grandis* | South Africa | M.J. Wingfield | AF292041 | AF273063 | N/A | Myburg et al. (2002b), Gryzenhout et al. (2006c) |
| | CMW9327 | *Tib. granulosa* | South Africa | J. Roux | AF273473 | AF273060 | N/A | Myburg et al. (2002a) |
| | CMW2113T | *Euc. grandis* | South Africa | M.J. Wingfield | AF046892 | AF273067 | N/A | Myburg et al. (1999, 2002b) |
| *Chrysoporthe cubensis* | CMW10453 | *Euc. saligna* | Democratic Republic of the Congo | N/A | AY063476 | AY063478 | N/A | Castlebury et al. (2002), Gryzenhout et al. (2004) |
| | CMW8758 | *Eucalyptus* sp. | Venezuela | M.J. Wingfield | AF046898 | AF273068 | N/A | Myburg et al. (2002b), Gryzenhout et al. (2006c) |
| | CMW10669 | *Eucalyptus* sp. | Republic of the Congo | J. Roux | AF535122 | AF535124 | N/A | Gryzenhout et al. (2004) |
| | CMW10639 | *Euc. grandis* | Colombia | C.A. Rodas | AY263421 | AY263419 | N/A | Gryzenhout et al. (2004) |
| *Chrysoporthe deuterocubensis* | CMW11290 | *Eucalyptus* sp. | Indonesia | M.J. Wingfield | AY214304 | AY214232 | N/A | Gryzenhout et al. (2004) |
| | CMW8651 | *S. aromaticum* | Indonesia | M.J. Wingfield | AY084002 | AY084026 | N/A | Myburg et al. (2003) |
| | **CMW38375**[5] | *P. cattleianum* | Hawaii | J. Roux | KJ027490 | KJ027466 | N/A | This study |
| | **CMW38549**[5] | *S. jambos* | Hawaii | J. Roux | KJ027491 | KJ027467 | N/A | This study |
| | **CMW38565** | *Metrosideros polymorpha* | Hawaii | J. Roux | KJ027492 | KJ027468 | N/A | This study |
| *Chrysoporthe doradensis* | CMW11287T | *Euc. grandis* | Ecuador | M.J. Wingfield | AY214289 | AY214217 | N/A | Gryzenhout et al. (2005b) |
| | CMW11286 | *Euc. grandis* | Ecuador | M.J. Wingfield | AY214290 | AY214218 | N/A | Gryzenhout et al. (2005b) |
| *Chrysoporthe hodgesiana* | CMW10625 | *Mic. theaezans* | Colombia | C.A. Rodas | AY956970 | AY956979 | N/A | Rodas et al. (2005) |
| | CMW9995 | *Tib. semidecandra* | Colombia | R. Arbelaez | AY956969 | AY956977 | N/A | Rodas et al. (2005) |
| | CMW10641T= CBS115854 | *Tib. semidecandra* | Colombia | R. Arbelaez | AY692322 | AY692326 | N/A | Gryzenhout et al. (2004) |
| *Chrysoporthe inopina* | CMW12727T | *Tib. lepidota* | Colombia | R. Arbelaez | DQ368777 | DQ368806 | N/A | Gryzenhout et al. (2006d) |
| | CMW12729 | *Tib. lepidota* | Colombia | R. Arbelaez | DQ368778 | DQ368808 | N/A | Gryzenhout et al. (2006d) |
| *Chrysoporthe syzygiicola* | CMW29940T= CBS124488 | *S. guineense* | Zambia | D. Chungu & J. Roux | FJ655005 | FJ805230 | N/A | Chungu et al. (2010) |
| | CMW29942= CBS124490 | *S. guineense* | Zambia | D. Chungu & J. Roux | FJ655007 | FJ805232 | N/A | Chungu et al. (2010) |

| Identity | Isolate No.[1,2] | Host | Location | Collector | GenBank accession no. | | | Reference |
|---|---|---|---|---|---|---|---|---|
| | | | | | ITS | *BT1* | *TEF1* | |
| *Chrysoporthe zambiensis* | CMW29928T= CBS124503 | *Euc. grandis* | Zambia | D. Chungu & J. Roux | FJ655002 | FJ858709 | N/A | Chungu et al. (2010) |
| | CMW29930= CBS124502 | *Euc. grandis* | Zambia | D. Chungu & J. Roux | FJ655004 | FJ858711 | N/A | Chungu et al. (2010) |
| *Corticimorbus sinomyrti* | CERC3629T | *Rhodomyrtus tomentosa* | China | S.F. Chen & G.Q. Li | KT167169 | KT167189 | N/A | Chen et al. (2016) |
| | CERC3631 | *Rho. tomentosa* | China | S.F. Chen & G.Q. Li | KT167170 | KT167190 | N/A | Chen et al. (2016) |
| *Cryphonectria parasitica* | CMW7048 | *Q. virginiana* | USA | R.J. Stipes | AF368330 | AF273076 | N/A | Venter et al. (2002), Gryzenhout et al. (2006c) |
| | CMW13749 | *Cas. mollisima* | Japan | N/A | AY697927 | AY697943 | N/A | Myburg et al. (2004) |
| *Cryphonectria quercus* | CFCC52138T | *Q. aliena* var. *acuteserrata* | China, ShaanXi | N. Jiang | MG866024 | MG896115 | N/A | Jiang et al. (2018) |
| | CFCC52139 | *Q. aliena* var. *acuteserrata* | China, ShaanXi | N. Jiang | MG866025 | MG896116 | N/A | Jiang et al. (2018) |
| *Cryphonectria radicalis* | CMW10455 | *Q. suber* | Italy | A. Biraghi | AF452113 | AF525705 | N/A | Gryzenhout et al. (2006c) |
| | CMW10477 | *Q. suber* | Italy | A. Biraghi | AF368328 | AF368347 | N/A | Venter et al. (2002), Gryzenhout et al. (2006c) |
| *Cryptometrion aestuescens* | CMW18790 | *Euc. grandis* | Indonesia | M.J. Wingfield | GQ369458 | GQ369455 | N/A | Gryzenhout et al. (2010), Vermeulen et al. (2011) |
| | CMW18793 | *Euc. grandis* | Indonesia | M.J. Wingfield | GQ369459 | GQ369456 | N/A | Gryzenhout et al. (2010), Vermeulen et al. (2011) |
| | CMW28535T= CBS124009 | *Euc. grandis* | North Sumatra, Indonesia | M.J. Wingfield | GQ369457 | GQ369454 | N/A | Gryzenhout et al. (2010) |
| *Diversimorbus metrosiderotis* | CMW37321 | *Metrosideros angustifolia* | South Africa | J. Roux | JQ862870 | JQ862911 | N/A | Chen et al. (2013b) |
| | CMW37322T | *Met. angustifolia* | South Africa | J. Roux | JQ862871 | JQ862912 | N/A | Chen et al. (2013b) |
| *Endothia gyrosa* | CMW2091 | *Q. palustris* | USA | R.J. Stipes | AF368325 | AF368337 | N/A | Venter et al. (2002), Gryzenhout et al. (2006c) |
| | CMW10442 | *Q. palustris* | USA | R.J. Stipes | AF368326 | AF368339 | N/A | Venter et al. (2002), Gryzenhout et al. (2006c) |
| *Holocryphia capensis* | CMW37887T | *Met. angustifolia* | South Africa | J. Roux, S.F. Chen & F. Roets | JQ862854 | JQ862895 | JQ863051 | Chen et al. (2013b) |
| | CMW37329 | *Met. angustifolia* | South Africa | J. Roux & S.F. Chen | JQ862859 | JQ862900 | JQ863056 | Chen et al. (2013b) |
| *Holocryphia eucalypti* | CMW7033T | *Euc. grandis* | South Africa | M. Venter | JQ862837 | JQ862878 | JQ863034 | Chen et al. (2013b) |
| | CMW7035 | *Euc. saligna* | South Africa | M. Venter | JQ862838 | JQ862879 | JQ863035 | Chen et al. (2013b) |
| *Holocryphia gleniana* | CMW37334T | *Met. angustifolia* | South Africa | J. Roux & S.F. Chen | JQ862834 | JQ862875 | JQ863031 | Chen et al. (2013b) |
| | CMW37335 | *Met. angustifolia* | South Africa | J. Roux & S.F. Chen | JQ862835 | JQ862876 | JQ863032 | Chen et al. (2013b) |
| *Holocryphia mzansi* | CMW37337T | *Met. angustifolia* | South Africa | J. Roux & S.F. Chen | JQ862841 | JQ862882 | JQ863038 | Chen et al. (2013b) |
| | CMW37338 | *Met. angustifolia* | South Africa | J. Roux & S.F. Chen | JQ862842 | JQ862883 | JQ863039 | Chen et al. (2013b) |
| *Holocryphia* sp. | CMW6246 | *Tib. granulosa* | Australia | M.J. Wingfield | JQ862845 | JQ862886 | JQ863042 | Chen et al. (2013b) |
| | CMW10015 | *Euc. fastigata* | New Zealand | R.J. van Boven | JQ862849 | JQ862890 | JQ863046 | Chen et al. (2013b) |
| *Immersiporthe knoxdaviesiana* | CMW37314T | *Rapanea melanophloeos* | South Africa | M.J. Wingfield & J. Roux | JQ862765 | JQ862785 | N/A | Chen et al. (2013a) |
| | CMW37315 | *Rap. melanophloeos* | South Africa | M.J. Wingfield & J. Roux | JQ862766 | JQ862786 | N/A | Chen et al. (2013a) |
| *Latruncella aurorae* | CMW28274 | *Galpinia transvaalica* | Swaziland | J. Roux | GU726946 | GU726958 | N/A | Vermeulen et al. (2011) |
| | CMW28276T | *G. transvaalica* | Swaziland | J. Roux | GU726947 | GU726959 | N/A | Vermeulen et al. (2011), Chen et al. (2011) |
| | CMW28275 | *G. transvaalica* | Swaziland | J. Roux | HQ171209 | HQ171207 | N/A | Vermeulen et al. (2011) |

| Identity | Isolate No.[1,2] | Host | Location | Collector | GenBank accession no. | | | Reference |
|---|---|---|---|---|---|---|---|---|
| | | | | | ITS | *BT1* | *TEF1* | |
| *Luteocirrhus shearii* | CBS130775 | *Banksia baxteri* | Australia | C. Crane | KC197024 | KC197015 | N/A | Crane and Burgess (2013) |
| | CBS130776T | *B. baxteri* | Australia | C. Crane | KC197021 | KC197012 | N/A | Crane and Burgess (2013) |
| *Microthia havanensis* | CMW11301 | *Myr. faya* | Azores | C.S. Hodges & D.E. Gardner | AY214323 | AY214251 | N/A | Gryzenhout et al. (2006a) |
| *Microthia havanensis* | CMW14550 | *E. saligna* | Mexico | C.S. Hodges | DQ368735 | DQ368741 | N/A | Gryzenhout et al. (2006a) |
| | **CMW38563**[c] | *S. jambos* | Hawaii | J. Roux | KJ027493 | KJ027469 | N/A | This study |
| | **CMW38367** | *P. cattleianum* | Hawaii | J. Roux | KJ027495 | KJ027471 | N/A | This study |
| | **CMW38585**[c] | *S. jambos* | Hawaii | J. Roux | KJ027494 | KJ027470 | N/A | This study |
| *Myrtonectria myrtacearum* | CMW46433T | *Heteropyxis natalensis* | South Africa | D.B. Ali & J. Roux | MG585736 | MG585720 | N/A | Ali et al. (2018) |
| | CMW46435 | *S. cordatum* | South Africa | D.B. Ali & J. Roux | MG585737 | MG585721 | N/A | Ali et al. (2018) |
| *Parvosmorbus eucalypti* | CSF2061T | *E. urophylla* × *E. grandis* hybrid clone | China | S.F. Chen & G.Q. Li | MN258788 | MN258816 | MN258830 | Wang et al. (2020) |
| | CSF8777 | *E. urophylla* hybrid clone | China | J.Roux & S.F. Chen | MN258794 | MN258822 | MN258836 | Wang et al. (2020) |
| *Parvosmorbus guangdongensis* | CSF10460T | *E. urophylla* hybrid clone | China | S.F. Chen & W. Wang | MN258799 | MN258827 | MN258841 | Wang et al. (2020) |
| | CSF10738 | *E. grandis* hybrid clone | China | S.F. Chen & W. Wang | MN258800 | MN258828 | MN258842 | Wang et al. (2020) |
| *Rostraureum tropicale* | CMW9972 | *Terminalia ivorensis* | Ecuador | M.J. Wingfield | AY167436 | AY167426 | N/A | Gryzenhout et al. (2005c, 2006c) |
| | CMW10796T | *Ter. ivorensis* | Ecuador | M.J. Wingfield | AY167438 | AY167428 | N/A | Gryzenhout et al. (2005c) |
| | CMW9971 | *Ter. ivorensis* | Ecuador | M.J. Wingfield | AY167435 | AY167425 | N/A | Gryzenhout et al. (2005c) |
| *Ursicollum fallax* | CMW18119T | *Coccoloba uvifera* | USA | C.S. Hodges | DQ368755 | DQ368758 | N/A | Gryzenhout et al. (2006a, 2009) |
| | CMW18115 | *Coc. uvifera* | USA | C.S. Hodges | DQ368756 | DQ368760 | N/A | Gryzenhout et al. (2006a) |
| *Diaporthe ambigua* | CMW5587 | *Malus domestica* | South Africa | W.A. Smit | AF543818 | AF543820 | N/A | Gryzenhout et al. (2006a) |
| | CMW5288 | *M. domestica* | South Africa | W.A. Smit | AF543817 | AF543819 | N/A | Gryzenhout et al. (2006a) |

[1] Designation of isolates and culture collections: ATCC = American Type Culture Collection, Manassas, USA; CBL represent isolates in Ferreira et al. (2019); CBS = Westerdijk Fungal Biodiversity Institute, Utrecht, Netherlands; CERC = China Eucalypt Research Centre (CERC), Chinese Academy of Forestry (CAF), ZhanJiang, GuangDong, China; CFCC = China Forestry Culture Collection Center, Beijing, China; CMW = Tree Protection Co-operative Program, Forestry and Agricultural Biotechnology Institute, University of Pretoria, South Africa; CSF = Culture Collection from Southern Forests (CSF), China Eucalypt Research Centre, Chinese Academy of Forestry, ZhanJiang, GuangDong, China; MES, CTS represent isolates in Beier et al. (2015).

[2] 'T' following isolate number means isolates are ex-type or from samples that have been linked morphologically to type material of the species.

[3] N/A = not available.

[4] Isolates identified in this study are in bold font type.

[5] Isolates used for inoculations.

trees with generally consistent topologies and phylogenetic relationships amongst taxa. Based on the phylogenetic analyses of the ITS, *BT1* and combined datasets, the isolates obtained in this study were grouped in three Clusters, referred to as Clusters A–C (Fig. 1; ITS and *BT1* trees not presented). Isolates in Cluster A grouped in the genus *Chrysoporthe* and they all resided in the same phylogenetic clade as *Chrysoporthe deuterocubensis*. Isolates in Cluster B grouped in the genus *Microthia* and were phylogenetically closely related to *Microthia havanensis*. Isolates in Cluster C grouped with species of *Celoporthe*. They formed three distinct Clades (Clades a–c) within *Celoporthe* based on the ITS+*BT1* tree (Fig. 1).

In the ITS, *BT1* and *TEF1* datasets for *Celoporthe* isolates, the PHT generated a value of P = 0.001, showing that the accuracy of the combined data were unaffected relative to the individual partitions (Cunningham 1997) and the three gene regions were thus combined in the analyses. Other than the ITS tree (Fig. 2A), Hawaiian isolates formed distinct lineages (Clades a–c) that differentiated them from other *Celoporthe* species (Fig. 2B–D). In the combined analyses of ITS, *BT1* and *TEF1* gene sequences, isolates in each of Clades a, b and c formed independent lineages, supported by high bootstrap values (Clade a: ML/MP = 98%/98%; Clade b: ML/MP = 88%/79%; Clade c: ML/MP = 99%/100%) (Fig. 2D). These three clades were consequently recognised as representing three undescribed species. Isolates in Clades a and b were most closely related to *Celoporthe guangdongensis* and those in Clade c were all most closely related to *Cel. eucalypti* and *Cel. cerciana* (Fig. 2D).

## Morphology

Fruiting bodies developed for all six isolates grown on *Eucalyptus* stem sections on water agar after two months of incubation at room temperature. Other than some minor differences, all fungal isolates, obtained in this study, were morphologically similar. This was consistent with the fact that fungi in the Cryphonectriaceae are mostly indistinguishable on artificial media (Gryzenhout et al. 2009).

Colonies on 2% MEA were fluffy and white when young, turning yellow or greenish-grey to greenish when old. The optimal growth temperatures for novel species was 30 °C, at which colonies reached 59–80 mm within 4 days.

## Taxonomy

Based on phylogenetic analyses of sequence data for the three gene regions, three previously unknown Cryphonectriaceae species are recognised from non-native Myrtaceae on the Hawaiian Islands. The three fungi reside in the genus *Celoporthe* and are distinct from described *Celoporthe* species, based on sequence data. Since limited numbers of fruiting bodies were available from the originally-collected plant material for these three species and mostly conidia were obtained under laboratory conditions, they are defined primarily based on multiple gene DNA sequence data. Morphological descriptions are provided for colonies on MEA and fruiting structures produced on *Eucalyptus* stem sections.


**Figure 1.** Phylogenetic trees based on Maximum Likelihood (ML) analyses of a combined DNA sequence dataset of ITS and *BT1* regions for various genera in the Diaporthales. Bootstrap values ≥ 70% for ML and MP (maximum parsimony) analyses are presented at branches as follows: ML/MP. Bootstrap values lower than 70% are marked with * and absent analysis values are marked with –. Isolates collected in this study are in boldface and blue. *Diaporthe ambigua* (CMW5287 and CMW5588) (Diaporthaceae) was used as the outgroup taxon.

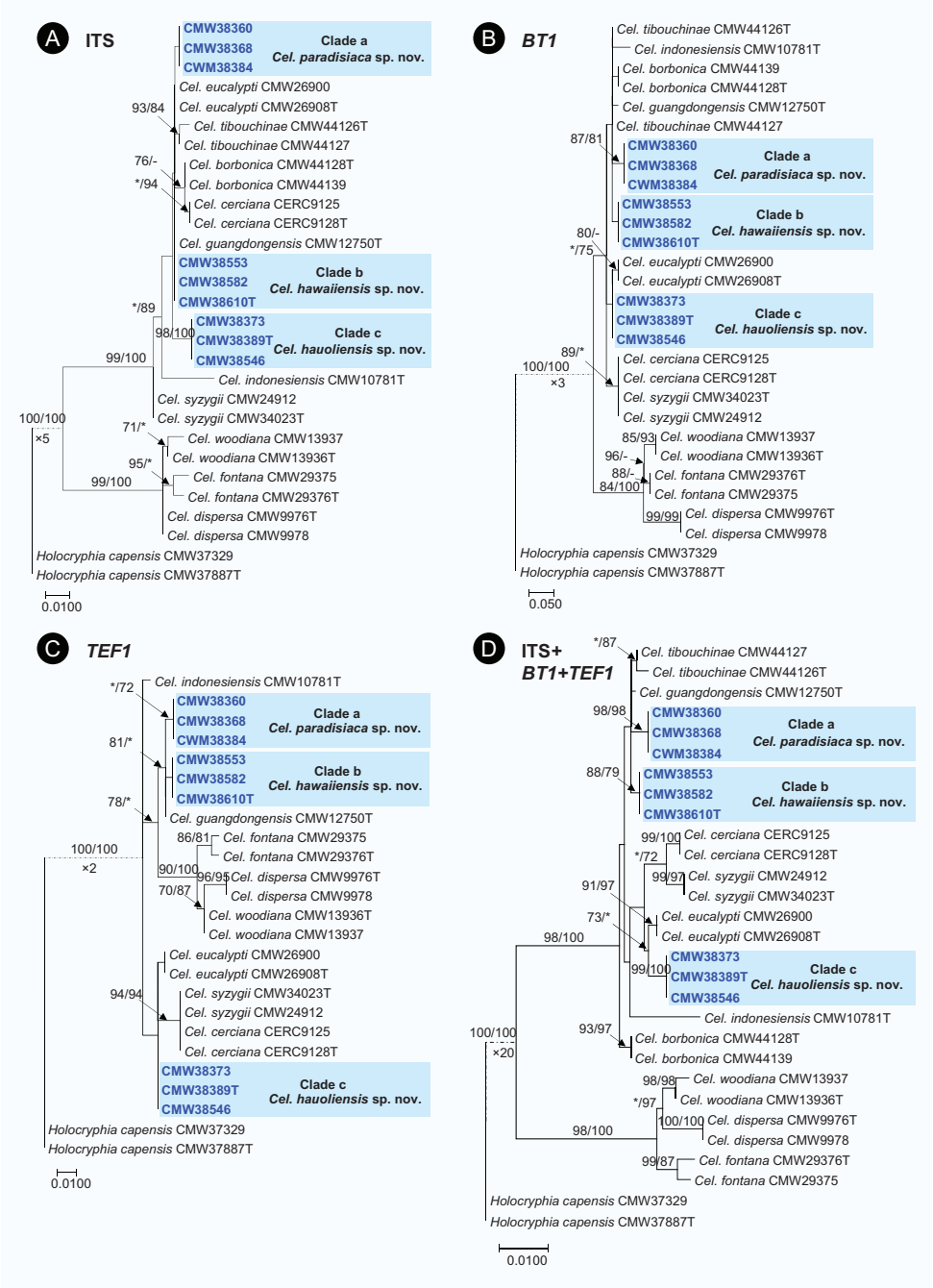


**Figure 2.** Phylogenetic trees, based on Maximum Likelihood (ML) analyses for species in *Celoporthe* **A** ITS region **B** *BT1* gene region **C** *TEF1* gene region **D** combined ITS, *BT1* and *TEF1* regions. Bootstrap values ≥ 70% for ML and MP (maximum parsimony) analyses are presented at branches as follows: ML/MP. Bootstrap values lower than 70% are marked with * and absent analysis values are marked with –. Isolates collected in this study are in boldface and blue. *Holocryphia capensis* (CMW37329 and CMW37887) was used as the outgroup taxon.

***Celoporthe hauoliensis*** **Kamgan, Jol. Roux & Marinc., sp. nov.**
MycoBank No: 808579
Fig. 3

**Etymology.** The species name refers to the Hawaiian word for happy, "Hau'oli", describing the collector's joy in visiting and discovering Cryphonectriaceae on the Islands.

**Types.** ***Holotype*****:** USA, Hawaii, O'ahu Island, Pu'u PiaManoa, isolated from bark of *Psidium cattleianum*, 23 July 2012, *J. Roux* (PREM 61309; Ex-type culture CMW38389 = CBS 140640); GenBank accession numbers KJ027502 (ITS), KJ027478 (*BT1*), KJ027487 (*TEF1*). ***Paratypes*****:** Hawaii, O'ahu Island, Waimea Valley Botanical Gardens, isolated from bark of *Syzygium* sp., 23 July 2012, *J. Roux* (PREM 61310; living culture CMW38546 = CBS 140641). Hawaii, O'ahu Island, Waimea Valley Botanical Garden, isolated from bark of *Syzygium jambos*, July 2012, *J. Roux* (CMW38373).

**Sexual morph.** Not observed.

**Asexual morph.** Formed after two months on *Eucalyptus* stem sections placed on water agar. *Conidiomata* superficial or with base embedded, pulvinate or conical with or without necks, often covered with pigmented hyphae, uni- or multilocular, convoluted, 287–722 µm long, 332–808 µm wide. *Conidiomatal walls* outer- and inter-locular

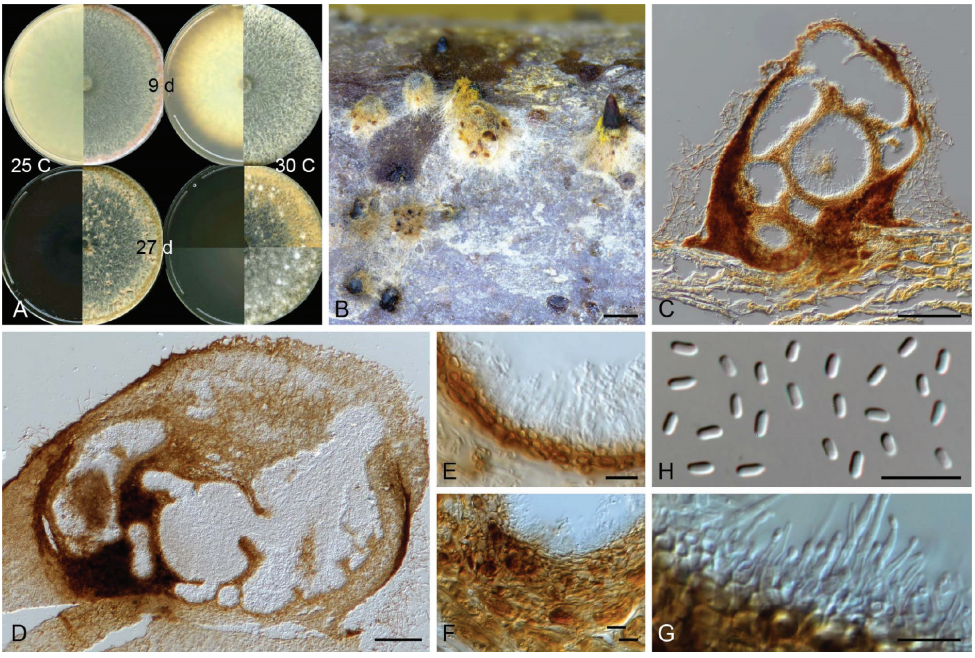


**Figure 3.** Micrographs of *Celoporthe hauoliensis* sp. nov. (holotype: PREM 61309; ex-holotype CBS 140640 = CMW38389) **A** culture morphology on 2% MEA at 25 °C and 30 °C at 9 and 27 days **B** conidiomata produced on *Eucalyptus* stem sections on water agar **C, D** vertical section of conidioma **E** inner fertile wall of conidioma **F** conidiomatal wall **G** conidiogenous cells **H** conidia. Scale bars: 1 mm (**B**); 100 µm (**C, D**); 10 µm (**E–H**).

stratum prosenchymatous; inner fertile stratum pseudoparenchymatous, composed of a few layers of brown, flattened, thick-walled cells, 8–26 µm thick. *Paraphyses* present, scarcely observed, 14–26 µm long. *Conidiophores* formed along inner layer of locule, simple or branched, often reduced to conidiogenous cells, 5–21 µm long. *Conidiogenous cells* enteroblastic, lageniform, tapering towards apex, 3–9 × 1–2.5 µm. *Conidia* hyaline, oblong, straight, occasionally curved, aseptate, 3–4 × 1–1.5 (3.09 ± 0.30 × 1.31 ± 0.08) µm.

**Culture characteristics.** Colonies on 2% MEA, when young showing circular growth with smooth margins, above white with tint of yellow (30 °C) or orange (25 °C) towards the edge of Petri dish, reverse yellow, except for at 30 °C becoming brown towards the edge; with age above becoming brown, except for 30 °C at which each colony showing variable yellow with white mycelial clumps, reverse dark brown at all temperatures; optimal growth at 30 °C (9.4 mm/d), followed by 25 °C (7.9 mm/d) and 20 °C (4.8 mm/d), minimal growth at 35 °C (0.2 mm/d), no growth at 5 °C; mycelia fluffy, density sparce in centre becoming thicker towards the edge.

**Habitat.** On/in bark of *Psidium cattleianum* and *Syzygium jambos*

**Distribution.** Hawaii, USA

**Notes.** *Celoporthe hauoliensis* is morphologically similar to its phylogenetically closest relatives *Cel. eucalypti* and *Cel. cerciana*, but can be differentiated by DNA sequences. In the ITS, *BT1* and *TEF1* datasets, *Cel. hauoliensis* differs from *Cel. eucalypti* by 8, 4 and 4 base pairs and from *Cel. cerciana* by 11, 9 and 6 base pairs, respectively (Tables 3–5).

**Table 3.** Nucleotide differences observed in the ITS region between *Celoporthe hauoliensis*, *Cel. eucalypti* and *Cel. cerciana*.

| Species/Isolate No. | ITS[1] | | | | | | | | | | | | |
|---|---|---|---|---|---|---|---|---|---|---|---|---|---|
| | 8[2] | 61 | 75 | 76 | 80 | 112 | 161 | 162 | 186 | 187 | 193 | 194 | 467 |
| *Cel. hauoliensis* CMW383735 | T[3] | A | **G** | **C** | **C** | – | – | **C** | T | A | – | **C** | – |
| *Cel. hauoliensis CMW38389*[4] | T | A | **G** | **C** | **C** | – | – | **C** | T | A | – | **C** | – |
| *Cel. hauoliensis* CMW38546 | T | A | **G** | **C** | **C** | – | – | **C** | T | A | – | **C** | – |
| *Cel. eucalypti* CMW26900 | – | A | – | T | G | G | **A** | A | T | A | – | A | – |
| *Cel. eucalypti CMW26908* | – | A | – | T | G | G | **A** | A | T | A | – | A | – |
| *Cel. cerciana* CERC9125 | T | **G** | – | T | G | G | – | A | **A** | **C** | **A** | A | **T** |
| *Cel. cerciana CERC9128* | T | **G** | – | T | G | G | – | A | **A** | **C** | **A** | A | **T** |

[1] Polymorphic nucleotides occurring only in all isolates are shown, not alleles that partially occur in individuals per phylogenetic group. [2] Numerical positions of the nucleotides in the DNA sequence alignments are indicated. [3] Fixed polymorphisms for each group are in bold. [4] Ex-type isolates are indicated in italic.

**Table 4.** Nucleotide differences observed in the *BT1* gene region between *Celoporthe hauoliensis*, *Cel. eucalypti* and *Cel. cerciana*.

| Species/Isolate No. | *BT1*[1] | | | | | | | | | |
|---|---|---|---|---|---|---|---|---|---|---|
| | 105[2] | 127 | 130 | 131 | 132 | 182 | 183 | 188 | 191 | 201 |
| *Cel. hauoliensis* CMW383735 | G[3] | C | – | – | – | – | – | – | T | C |
| *Cel. hauoliensis CMW38389*[4] | G | C | – | – | – | – | – | – | T | C |
| *Cel. hauoliensis* CMW38546 | G | C | – | – | – | – | – | – | T | C |
| *Cel. eucalypti* CMW26900 | **A** | C | C | T | C | – | – | – | T | C |
| *Cel. eucalypti CMW26908* | **A** | C | C | T | C | – | – | – | T | C |
| *Cel. cerciana* CERC9125 | G | **T** | C | T | C | **C** | **C** | **C** | **C** | **A** |
| *Cel. cerciana CERC9128* | G | **T** | C | T | C | **C** | **C** | **C** | **C** | **A** |

[1] Polymorphic nucleotides occurring only in all isolates are shown, not alleles that partially occur in individuals per phylogenetic group. [2] Numerical positions of the nucleotides in the DNA sequence alignments are indicated. [3] Fixed polymorphisms for each group are in bold. [4] Ex-type isolates are indicated in italic.

**Table 5.** Nucleotide differences observed in the *TEF1* gene region between *Celoporthe hauoliensis*, *Cel. eucalypti* and *Cel. cerciana*.

| Species/Isolate No. | *TEF1* | | | | | | |
|---|---|---|---|---|---|---|---|
| | **23**[2] | **43** | **44** | **112** | **113** | **114** | **127** |
| *Cel. hauoliensis* CMW383735 | C[3] | G | C | – | – | – | T |
| *Cel. hauoliensis* CMW38389[4] | C | G | C | – | – | – | T |
| *Cel. hauoliensis* CMW38546 | C | G | C | – | – | – | T |
| *Cel. eucalypti* CMW26900 | **T** | G | C | T | T | T | T |
| *Cel. eucalypti* CMW26908 | **T** | G | C | T | T | T | T |
| *Cel. cerciana* CERC9125 | C | **T** | **T** | T | T | T | **C** |
| *Cel. cerciana* CERC9128 | C | **T** | **T** | T | T | T | **C** |

[1] Polymorphic nucleotides occurring only in all isolates are shown, not alleles that partially occur in individuals per phylogenetic group. [2] Numerical positions of the nucleotides in the DNA sequence alignments are indicated. [3] Fixed polymorphisms for each group are in bold. [4] Ex-type isolates are indicated in italic.

## *Celoporthe hawaiiensis* Kamgan, Jol. Roux & Marinc., sp. nov.

MycoBank No: 808578
Fig. 4

**Etymology.** The species name refers to the Hawaiian Islands where the holotype was collected.

**Types.** ***Holotype*:** USA, Hawaii, Maui Island, Hana Road, 20 miles from Kahului, isolated from bark of *Syzygium jambos*, 30 July 2012, *J. Roux* (PREM61307; Ex-type culture CMW38610 = CBS140642); GenBank accession numbers KJ027499 (ITS), KJ027475 (*BT1*), KJ027484 (*TEF1*). ***Paratypes*:** Hawaii, Maui Island, Hana Road, 20 miles from Kahului, isolated from bark of *Syzygium jambos*, 30 July 2012, *J. Roux* (PREM 61308; living culture CMW38582 = CBS140643). Hawaii, Big Island, Rainbow Falls, Hilo, isolated from bark of *Syzygium jambos*, 26 July 2012, *J. Roux* (CMW38553).

**Sexual morph.** Not observed.

**Asexual morph.** Formed after two months on *Eucalyptus* stem sections placed on water agar. *Conidiomata* superficial or with base embedded, single or gregarious, uni- or multilocular, convoluted, base often covered with brown hyphal mass, dark brown to black, pulvinate to conical with or without necks, 450–1814 µm long, 329–1069 µm wide; necks attenuating towards apex, tip of neck paler than body. *Conidiomatal wall* outer-and inter-locular stratum prosenchymatous; inner fertile stratum pseudoparenchymatous, 5–19 µm thick. *Paraphyses* present, cylindrical, tapering towards apex, scarce, 16–29 µm long. *Conidiophores* formed along inner layer of locule, simple or branched, occasionally reduced to conidiogenous cell, 10–26 µm long. *Conidiogenous cells* enteroblastic, lageniform, tapering towards apex, 4–12 × 1–2 µm. *Conidia* hyaline, oblong, aseptate, exuding in yellow droplets or tendril, 2.5–4 × 1–1.5 (3.17 ± 0.27 × 1.27 ± 0.08) µm.

**Culture characteristics.** Colonies on 2% MEA, when young showing circular growth with smooth margins, above white with yellow tint towards edge (25 °C), reverse pale brown, becoming darker in centre at 25 °C and 30 °C; with age above

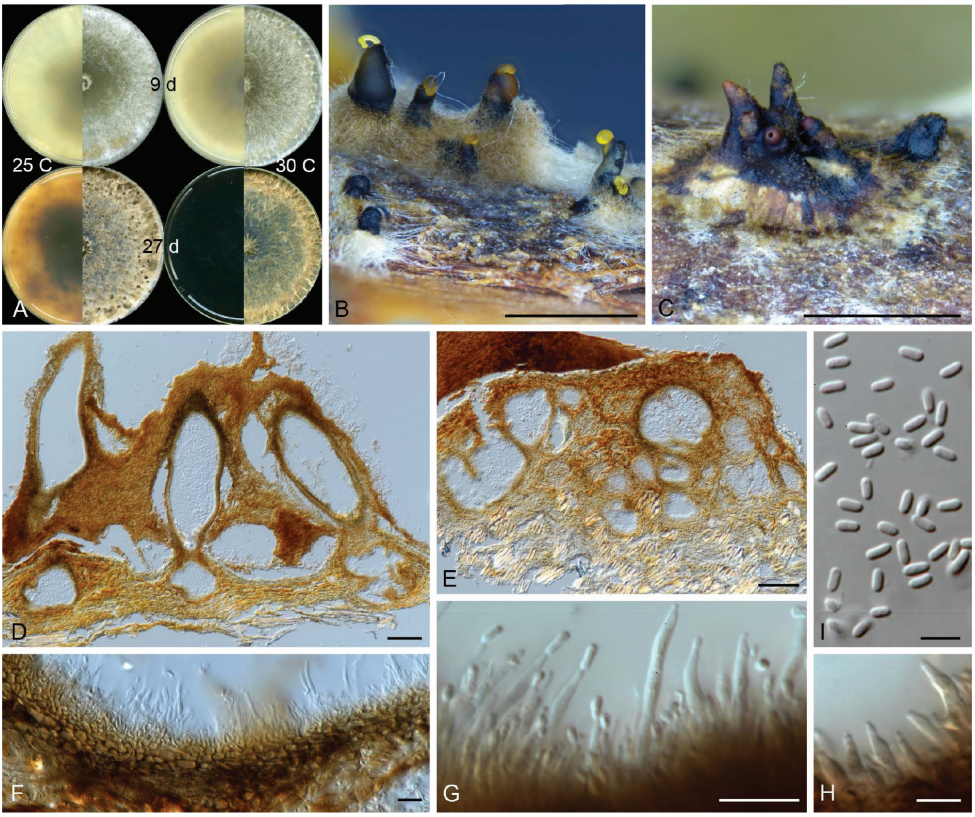


**Figure 4.** Micrographs of *Celoporthe hawaiiensis* sp. nov. (holotype: PREM 61307, ex-holotype CBS 140642 = CMW38610) **A** culture morphology on 2% MEA at 25 °C and 30 °C at 9 and 27 days **B, C** conidiomata produced on *Eucalyptus* stem sections on water agar **D, E** vertical section of conidioma **F** conidiomatal wall **G, H** conidiogenous cells **I** conidia. Scale bars: 1 mm (**B, C**); 100 µm (**D, E**); 10 µm (**F, G**); 5 µm (**H, I**).

becoming darker yellow to brown, reverse dark brown, except at 20 °C, 25 °C having yellow with dark brown patches; optimal growth at 30 °C (6.6 mm/d), followed by 25 °C (6.0 mm/d) and 20 °C (4.1 mm/d), minimal growth at 35 °C (0.1 mm/d), growth at 5 °C restricted to mycelial plug; mycelia fluffy, density sparse in centre becoming thicker towards the edge.

**Habitat.** On/in bark of *Psidium cattleianum*, *Syzygium jambos* and *Syzygium* sp. indet.

**Distribution.** Hawaii, USA

**Notes.** *Celoporthe hawaiiensis* is morphologically similar to *Cel. guangdongensis* and *Cel. paradisiaca*, its phylogenetic closest relatives, but can be differentiated by DNA sequences. In the ITS, *BT1* and *TEF1* datasets, *Cel. hawaiiensis* differs from *Cel. guangdongensis* by 3, 3 and 1 base pairs and from *Cel. paradisiaca* by 6, 3 and 3 base pairs, respectively (Tables 6, 7).

**Table 6.** Nucleotide differences observed in the ITS region between *Celoporthe hawaiiensis*, *Cel. guangdongensis* and *Cel. paradisiaca*.

| Species/Isolate No. | ITS[1] | | | | | | | |
|---|---|---|---|---|---|---|---|---|
| | 56[2] | 57 | 59 | 98 | 160 | 161 | 193 | 467 |
| *Cel. paradisiaca CWM38360*[3] | **A**[4] | **G** | **A** | – | – | A | **A** | – |
| *Cel. paradisiaca* CMW38368 | **A** | **G** | **A** | – | – | A | **A** | – |
| *Cel. paradisiaca* CWM38384 | **A** | **G** | **A** | – | – | A | **A** | – |
| *Cel. hawaiiensis* CMW38553 | – | – | G | – | – | – | – | T |
| *Cel. hawaiiensis* CMW38582 | – | – | G | – | – | – | – | T |
| *Cel. hawaiiensis CMW38610*[3] | – | – | G | – | – | – | – | T |
| *Cel. guangdongensis CMW12750*[3] | – | – | G | **C** | **A** | A | – | T |

[1] Polymorphic nucleotides occurring only in all isolates are shown, not alleles that partially occur in individuals per phylogenetic group. [2] Numerical positions of the nucleotides in the DNA sequence alignments are indicated. [3] Ex-type isolates are indicated in italic. [4] Fixed polymorphisms for each group are in bold.

**Table 7.** Nucleotide differences observed in the *BT1* and *TEF1* gene regions between *Celoporthe hawaiiensis*, *Cel. guangdongensis* and *Cel. paradisiaca*.

| Species/Isolate No. | *BT1*[1] | | | | | *TEF*[1] | | |
|---|---|---|---|---|---|---|---|---|
| | 57[2] | 131 | 139 | 175 | 272 | 77 | 220 | 222 |
| *Cel. paradisiaca CWM38360*[3] | C[4] | T | **A** | C | **C** | C | – | **A** |
| *Cel. paradisiaca* CMW38368 | C | T | **A** | C | **C** | C | – | **A** |
| *Cel. paradisiaca* CWM38384 | C | T | **A** | C | **C** | C | – | **A** |
| *Cel. hawaiiensis* CMW38553 | C | **G** | G | C | G | **A** | A | C |
| *Cel. hawaiiensis* CMW38582 | C | **G** | G | C | G | **A** | A | C |
| *Cel. hawaiiensis CMW38610*[3] | C | **G** | G | C | G | **A** | A | C |
| *Cel. guangdongensis CMW12750*[3] | **T** | T | G | – | G | C | A | C |

[1] Polymorphic nucleotides occurring only in all isolates are shown, not alleles that partially occur in individuals per phylogenetic group. [2] Numerical positions of the nucleotides in the DNA sequence alignments are indicated. [3] Ex-type isolates are indicated in italic. [4] Fixed polymorphisms for each group are in bold.

## *Celoporthe paradisiaca* S.F. Chen & Marinc., sp. nov.

MycoBank No: 836918
Fig. 5

**Etymology.** The species name refers to the fact that Hawaii, where the holotype of this fungus was collected, is regarded as a paradise by travellers.

**Types.** ***Holotype*:** USA, Hawaii, O'ahu Island, Ho'omaluhia, isolated from bark of *Psidium cattleianum*, 24 July 2012, *J. Roux* (PREM 63205; Ex-type culture CMW38360 = CBS 147169); GenBank accession numbers KJ027498 (ITS), KJ027474 (*BT1*), KJ027483 (*TEF1*). ***Paratype*:** Hawaii, O'ahu Island, Waimea Valley Botanical Gardens, isolated from bark of *Syzygium jambos*, 23 July 2012, *J. Roux* (PREM 63206; living culture CMW38368 = CBS 147170).

**Sexual morph.** Not observed.

**Asexual morph.** Produced after two months on *Eucalyptus* stem sections placed on water agar. *Conidiomata* superficial or with base embedded, singular or gregarious, pulvinate or conical with or without necks, often covered with mycelia, unilocular or multilocular, convoluted, 354–841 µm long, 185–654 µm wide. *Conidiomatal wall* outer or inter-locular stratum prosenchymatous; inner fertile layers pseudoparenchymatous, composed of several layers of flattened, thick-walled, pigmented cells, 8–19 µm

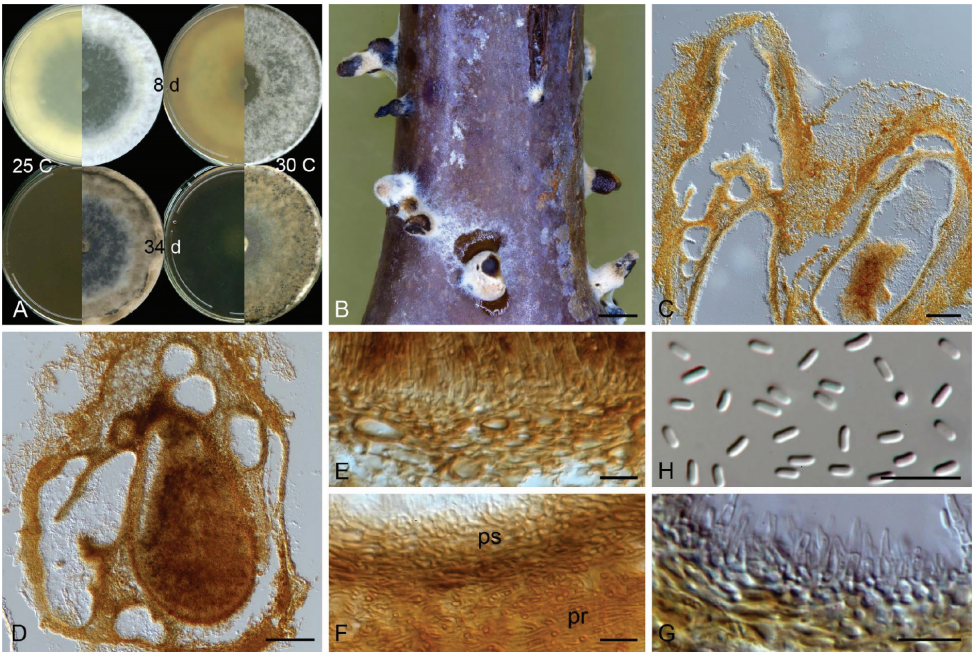


**Figure 5.** Micrographs of *Celoporthe paradisiaca* sp. nov. (holotype: PREM 63205, ex-holotype CBS 147169 = CMW38360) **A** culture morphology on 2% MEA at 25 °C and 30 °C at 8 and 34 days **B** conidiomata produced on *Eucalytpus* stem sections on water agar **C, D** vertical section of conidioma **E** inner wall of conidioma **F** conidiomatal walls (ps, pseudoparenchymatous inner wall; pr, prosenchymatous outer or interlocular wall) **G** conidiogenous cells **H** conidia. Scale bars: 1 mm (**B**); 100 µm (**C, D**); 10 µm (**E–H**).

thick. *Paraphyses* present, rarely observed. *Conidiophores* produced along inner layer of locule, simple or scarcely branched from basal cell, 8–11 µm long. *Conidiogenous cells* enteroblastic, lageniform, tapering towards apex, 5–11 × 1–2 µm. *Conidia* hyaline, oblong, straight or occasionally curved, 3–4 × 1–1.5 (3.2 ± 0.3 × 1.2 ± 0.07) µm.

**Culture characteristics.** Colonies on 2% MEA, when young, showing circular growth with smooth edges, above white, reverse pale to dark brown (30 °C) and yellow (25 °C); with age, above becoming brown and reverse dark yellow; optimal growth at 30 °C (7.7 mm/d), followed by 25 °C (7.0 mm/d) and 20 °C (4.6 mm/d), minimal growth at 35 °C (0.1 mm/d), no growth at 5 °C; mycelia fluffy, density-sparse in centre, becoming thicker towards the edge, aerial hyphae more abundant at 25 °C than at 30 °C when young.

**Habitat.** On/in bark of *Psidium cattleianum* and *Syzygium jambos*

**Distribution.** Hawaii, USA

**Notes.** *Celoporthe paradisiaca* is morphologically similar to its phylogenetically closest relatives, *Cel. hawaiiensis* and *Cel. guangdongensis*, but can be differentiated from them by DNA sequences. In the ITS, *BT1* and *TEF1* datasets, *Cel. paradisiaca* differs from *Cel. hawaiiensis* by 6, 3 and 3 base pairs and from *Cel. guangdongensis* by 7, 4 and 2 base pairs, respectively (Tables 6, 7).

## Pathogenicity tests

Inoculation with two isolates each of *Chr. deuterocubensis* (CMW38375, CMW38549), *Mic. havanensis* (CMW38563, CMW38585), *Cel. hawaiiensis* (CMW38553, CMW38610), *Cel. hauoliensis* (CMW38373, CMW38389) and *Cel. paradisiaca* (CMW38360, CMW38384) resulted in lesions on the cambium of one-year-old *S. jambos* trees. There were no significant differences between the means for *Cel. hauoliensis* and *Mic. havanensis* when compared to the negative control (Fig. 6). There were significant differences in the means for *Chr. deuterocubensis* and *Cel. hawaiiensis* when compared with one another, as well as with the negative control. A strain (CMW38610) of *Cel. hawaiiensis* was the most pathogenic (Mean = 23.4 mm) of all the fungi tested and it resulted in a mean lesion length that was statistically different when compared to the means for other test strains and the negative control (Fig. 6). The inoculated fungi were re-isolated from the treated plants and not from the controls, thus fulfilling the requirements of Koch's Postulates.

## Genetic Diversity of *Chr. deuterocubensis* isolates

*Chrysoporthe deuterocubensis* was the most commonly isolated fungus from Myrtales in this study (Table 1). Due to its known importance as a plantation tree pathogen, isolates obtained were subjected to a genetic diversity test using previously-developed microsatellite markers for this fungus. Seven of the 10 microsatellite primers amplified the desired target loci in 93 isolates obtained from four tree species on three Islands of Hawaii

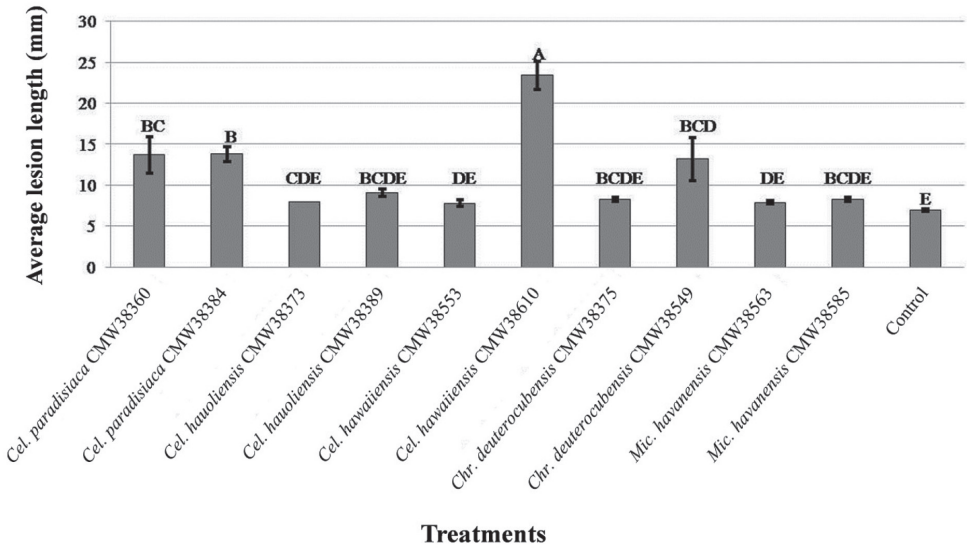


**Figure 6.** Vertical bar chart showing results of inoculation trial (xylem lesion) with Cryphonectriaceae isolates from Hawaii on *S. jambos* trees. Means with similar letters are not statistically significant, while those with different letters are statistically significant (significance level = 0.05).

(Table 1). Allele sizes at each locus were estimated and these were within the size ranges for each marker (Van der Merwe et al. 2003). A total of seven alleles (one allele at each locus) and one haplotype were identified in the collection. The gene diversity was zero and the *Chr. deuterocubensis* collection from Hawaii was determined as 100% clonal.

## Discussion

Five species of Cryphonectriaceae, residing in the genera *Celoporthe*, *Chrysoporthe* and *Microthia*, were identified from native and non-native Myrtaceae from three of the Hawaiian Islands (USA). Of these, only *Chr. deuterocubensis* and *Mic. havanensis* have previously been found in Hawaii (Gryzenhout et al. 2006a, 2009; Van der Merwe et al. 2010). In addition, three new species of *Celoporthe* were discovered and described.

*Chrysoporthe deuterocubensis* is known to occur in Hawaii where it has been previously recorded as a pathogen of *Eucalyptus* trees from the Islands of Kauai and Hawaii (Hodges et al. 1979; Gryzenhout et al. 2009; M.J. Wingfield, unpubl.). This fungus, originally known as *Chr. cubensis* and later recognised as distinct from that species (Van der Merwe et al. 2010), is well-known from many south-eastern Asian countries where it is believed to have originated (Zhou et al. 2008; Gryzenhout et al. 2009; Chen et al. 2010; Van der Merwe et al. 2010; Wang et al. 2020). It exclusively infects trees in the Myrtaceae and is an important pathogen of *Eucalyptus* outside the native range of this tree (Gryzenhout et al. 2009; Van der Merwe et al. 2010).

The occurrence of *Chr. deuterocubensis* on native Ohia (*M. polymorpha*) in Hawaii could be of concern given its importance as a tree pathogen. This prompted us to investigate the population diversity of the fungus in Hawaii and, thus, to gain insights into its possible origin and movement in the region. The seven microsatellite markers, used to study the population diversity of *Chr. Deuterocubensis*, amplified target loci in ninety-three isolates of the fungus. The trees from which isolates were obtained represented three genera and four different species. The single isolate of the fungus from native *M. polymorpha* was also included. All isolates, irrespective of the host or island on which they were collected, represented a single genotype of *Chr. deuterocubensis* and further comparisons were not justified. Overall, the results of this study provide convincing evidence that *Chr. deuterocubensis* has been introduced into Hawaii.

The occurrence of a single clone of *Chr. deuterocubensis* in Hawaii is consistent with that of an introduced pathogen that would be expected to have low gene diversity. This is in contrast to native pathogens that are typically genetically diverse in their areas of origin (Gordon et al. 1996; McDonald 1997). The area of origin of *Chr. deuterocubensis* in Hawaii is unknown, but it is most likely some part of Asia where the pathogen is found on native, as well as non-native, Myrtales (Van der Merwe et al. 2010). The discovery of only a single genotype of *Chr. deuterocubensis* in Hawaii was surprising and unexpected. This is especially because the isolates were collected from a wide range of different trees spanning three genera and four species and occurring on three different Islands.

*Chrysoporthe deuterocubensis* has been known on *Eucalyptus* in Kauai (as *Cryphonectria cubensis*) for many years (Hodges et al. 1979; Gryzenhout et al. 2004) and this could be the area where it was first introduced. The pathogen also occurs on highly sought-after ornamental trees/shrubs, such as *Tibouchina* species (Myrtales: Melastomataceae) (Myburg et al. 2003; Gryzenhout et al. 2009) and it is believed to have been moved on cuttings of this tree (Myburg et al. 2003; Gryzenhout et al. 2009). *Tibouchina* is commonly grown in Hawaii and these trees could also represent a source of a first introduction. This would be in contrast to other Myrtales, such as *Eucalyptus* spp., that are more commonly moved as seed.

*Chrysoporthe deuterocubensis* is an aggressive and important pathogen of trees in the Myrtales. It is clearly widespread in Hawaii and it has most likely been present in the state for many years. It appears that the population of the pathogen has increased substantially where it infects *S. jambos*, apparently being pre-disposed to the development of the canker pathogen by rust caused by *A. psidii*. Once large populations of a pathogen, such as *Chr. Deuterocubensis*, develop in an area, the chance of their moving to new environments is heightened by what has been termed a "bridgehead effect" and for which there are numerous examples in *Eucalyptus* forestry (Wingfield et al. 2013, 2015).

*Microthia havanens*, found in this study on *P. cattleianum*, *S. jambos* and *S. cumini*, was first described as a saprobe on *Eucalyptus* trees and other trees such as Mango [*Mangifera indica* L. (Anacardiacae, Sapindales)], avocado [*Persea americana* Mill. (Lauraceae, Laurales)] and Jobo trees [*Spondias mombin* L. (Anacardiaceae, Sapindales)] in Cuba (Bruner 1916). Other hosts and areas of occurrence for this fungus include *Eucalyptus* in Mexico and Hawaii, *Myrica faya* Ait (Myricaceae, Fagales) trees in Madeira and the Azores (Gryzenhout et al. 2006a) and *Eucalyptus grandis* Hill: Maiden trees in Florida (USA) (Barnard et al. 1987). *Microthia havanensis* is considered a weakly pathogenic bark-infecting fungus. This was also confirmed in our pathogenicity studies on *S. jambos*, where the two isolates tested produced lesions that did not differ significantly from the controls.

Three new species of *Celoporthe* were found in this study, with thirteen species now recognised in the genus. These include ten species, *Cel. borbonica*, *Cel. cerciana*, *Cel. eucalypti*, *Cel. guangdongensis*, *Cel. hauoliensis*, *Cel. hawaiiensis*, *Cel. indonesiensis*, *Cel. paradisiaca*, *Cel. syzygii* and *Cel. tibouchinae* in the Asian clade (Chen et al. 2011; Ali et al. 2018; Wang et al. 2018) and three species, *Cel. dispersa*, *Cel. fontana* and *Cel. woodiana* in the African clade of this genus (Nakabonge et al. 2006; Vermeulen et al. 2013). The present study expands the species diversity and geographic range of *Celoporthe*.

Preliminary pathogenicity trials on *S. jambos* showed that some of the isolates of *Chrysoporthe* and *Celoporthe*, tested under greenhouse conditions, can result in significant lesions on inoculated plants within a short period of time. Both isolates of *Cel. paradisiaca* caused distinct lesions, while one isolate each of *Cel. hawaiiensis* and *Chr. deuterocubensis* resulted in lesions that were significantly larger than those of the controls. One of the *Cel. hawaiiensis* isolates was the most aggressive fungus tested and surprisingly more so than the well-recognised pathogen *Chr. deuterocubensis*. This fungus clearly deserves further study.

*Austropuccinia psidii* infects mostly young, actively growing leaves and shoots, as well as fruits and sepals (Coutinho et al. 1998; Alfenas et al. 2004; Glen et al. 2017). Infections of leaves and meristems are severe on susceptible seedlings, cuttings, young trees and coppice, causing plants to be stunted and multibranched, inhibiting normal growth and development and sometimes causing death to young seedlings (Booth et al. 2000; Rayachhetry et al. 2001). This is in contrast to species of the Cryphonectriaceae that infect the bark of trees and shrubs (Gryzenthout et al. 2009). *Chrysoporthe* species, for example, infect the bark and cambium of trees, giving rise to rapidly-expanding cankers on the stems (Gryzenhout et al. 2009). These cankers often girdle the stems, killing the cambium and leading to rapid tree death (Hodges et al. 1976; Wingfield et al. 1989; Gryzenhout et al. 2009).

In the surveys conducted in this study, samples with symptoms of the Cryphonectriaceae were obtained from various parts of trees, including dead branches, stem cankers and also on trees with no obvious infection by the myrtle rust pathogen, *A. psidii*. We believe that the rapid die-back of *S. jambos* trees and other non-native myrtles in Hawaii is, at least in part, due to infection by one or more Cryphonectriaceae species that apparently proliferate in tissue stressed by the Myrtle rust fungus.

## Acknowledgements

We thank the National Research Foundation of South Africa (NRF), The Centre of Excellence in Tree Health Biotechnology (CoE-CTHB), the National Key R&D Program of China (China–South Africa Forestry Joint Research Centre Project; project No. 2018YFE0120900) for providing funding and the facility to conduct this study. We are also most grateful to Chris Kadooka and JB Friday, University of Hawaii and Lloyd Loope of the US Geological Survey, Makawao, Hawaii for invaluable advice and local support of the survey carried out in Hawaii. This work is based on the research supported by the National Research Foundation of South Africa, Grant specific unique reference number (UID83924). The grant holders acknowledge that opinions, findings and conclusions or recommendations expressed in any publication generated by NRF supported research are that of the authors and that the NRF accepts no liability whatsoever in this regard.

## References

Alfenas AC, Jeng R, Hubbes M (1983) Virulence of *Cryphonectria cubensis* on *Eucalyptus* species differing in resistance. European Journal of Forest Pathology 13: 197–205. https://doi.org/10.1111/j.1439-0329.1983.tb00118.x

Alfenas AC, Zauza EAV, Mafia RG, Assis TF (2004) Clonagem e DoencasdoEucalipto. Editora UFV: Universidade Federal doViçosa, Brazil.

Ali DB, Marincowitz S, Wingfield MJ, Roux J, Crous PW, McTaggart AR (2018) Novel Cryphonectriaceae from La Réunion and South Africa, and their pathogenicity on *Eucalyptus*. Mycological Progress 17: 953–966. https://doi.org/10.1007/s11557-018-1408-3

Anagnostakis SL (1987) Chestnut blight: the classical problem of an introduced pathogen. Mycologia 79: 23–37. https://doi.org/10.1080/00275514.1987.12025367

Anonymous (2003) Annual report to the twenty-second legislature regular session of 2003 relating to the forest stewardship program. The State of Hawaii, Department of Land and Natural Resources, Division of Forestry and Wildlife. Honolulu, Hawaii, 31 pp.

Barnard EL, Geary T, English JT, Gilly SP (1987) Basal cankers and coppice failure of *Eucalyptus grandis* in Florida. Plant Disease 71: 358–361. https://doi.org/10.1094/PD-71-0358

Begoude BAD, Gryzenhout M, Wingfield MJ, Roux J (2010) *Aurifilum*, a new fungal genus in the Cryphonectriaceae from *Terminalia*species in Cameroon. Antonie van Leeuwenhoek 98: 263–278. https://doi.org/10.1007/s10482-010-9467-8

Beier GL, Hokanson SC, Bates ST, Blanchette RA (2015) *Aurantioporthe corni* gen. et comb. nov., an endophyte and pathogen of *Cornus alternifolia*. Mycologia 107: 66–79. https://doi.org/10.3852/14-004

Booth TH, Old KM, Jovanovic T (2000) A preliminary assessment of high risk areas for *Puccinia psidii* (Eucalyptus rust) in the Neotropics and Australia. Agriculture Ecosystems & Environment 82: 295–301. https://doi.org/10.1016/S0167-8809(00)00233-4

Bruner SC (1916) A new species of *Endothia*. Mycologia 8: 239–242. https://doi.org/10.1080/00275514.1916.12018888

Carbone I, Kohn LM (1999) A method for designing primer sets for speciation studies in filamentous ascomycetes. Mycologia 91: 553–556. https://doi.org/10.1080/00275514.1999.12061051

Carnegie AJ, Kathuria A, Pegg GS, Entwistle P, Nagel M, Giblin FR (2016) Impact of the invasive rust *Puccinia psidii* (myrtle rust) on native Myrtaceae in natural ecosystems in Australia. Biological Invasions 18: 127–144. https://doi.org/10.1007/s10530-015-0996-y

Castlebury LA, Rossman AY, Jaklitsch WJ, Vasilyeva LN (2002) A preliminary overview of the Diaporthales based on large subunit nuclear ribosomal DNA sequences. Mycologia 94: 1017–1031. https://doi.org/10.1080/15572536.2003.11833157

Chen SF, Gryzenhout M, Roux J, Xie YJ, Wingfield MJ, Zhou XD (2010) Identification and pathogenicity of *Chrysoporthe cubensis* on *Eucalyptus* and *Syzygium* spp. in South China. Plant Disease 94: 1143–1150. https://doi.org/10.1094/PDIS-94-9-1143

Chen SF, Gryzenhout M, Roux J, Xie YJ, Wingfield MJ, Zhou XD (2011) Novel species of *Celoporthe* from *Eucalyptus* and *Syzygium* trees in China and Indonesia. Mycologia 103: 1384–1410. https://doi.org/10.3852/11-006

Chen SF, Wingfield MJ, Roets F, Roux J (2013a) A serious canker caused by *Immersiporthe knoxdaviesiana* gen. et sp. nov. (Cryphonectriaceae) on native *Rapanea melanophloeos* in South Africa. Plant Pathology 62: 667–678. https://doi.org/10.1111/j.1365-3059.2012.02671.x

Chen SF, Wingfield MJ, Roux J (2013b) *Diversimorbus metrosiderotis* gen. et sp. nov. and three new species of *Holocryphia* (Cryphonectriaceae) associated with cankers on native *Metrosideros angustifolia* trees in South Africa. Fungal Biology 117: 289–310. https://doi.org/10.1016/j.funbio.2013.02.005

Chen SF, Wingfield MJ, Li GQ, Liu FF (2016) *Corticimorbus sinomyrti* gen. et sp. nov. (Cryphonectriaceae) pathogenic to native *Rhodomyrtus tomentosa* (Myrtaceae) in South China. Plant Pathology 65: 1254–1266. https://doi.org/10.1111/ppa.12507

Chen SF, Liu QL, Li GQ, Wingfield MJ, Roux J (2018) A new genus of Cryphonectriaceae causes stem canker on *Lagerstroemia speciosa* in South China. Plant Pathology 67: 107–123. https://doi.org/10.1111/ppa.12723

Chungu D, Gryzenhout M, Muimba-Kankolongo A, Wingfield MJ, Roux J (2010) Taxonomy and pathogenicity of two novel *Chrysoporthe* species from *Eucalyptus grandis* and *Syzygium guineense* in Zambia. Mycological Progress 9: 379–393. https://doi.org/10.1007/s11557-009-0646-9

Coutinho TA, Wingfield MJ, Alfenas AC, Crous PW (1998) *Eucalyptus* rust: a disease with the potential for serious international implications. Plant Disease 82: 819–825. https://doi.org/10.1094/PDIS.1998.82.7.819

Crane C, Burgess TI (2013) *Luteocirrhus shearii* gen. sp. nov. (Diaporthales, Cryphonectriaceae) pathogenic to Proteaceae in the South Western Australian Floristic Region. IMA Fungus 4: 111–122. https://doi.org/10.5598/imafungus.2013.04.01.11

Crous PW, Summerell BA, Alfenas AC, Edwards J, Pascoe IG, Porter IJ, Groenewald JZ (2012) Genera of diaporthalean coelomycetes associated with leaf spots of tree hosts. Persoonia 28: 66–75. https://doi.org/10.3767/003158512X642030

Cunningham CW (1997) Can three incongruence tests predict when data should be combined. Molecular Biology and Evolution 14: 733–740. https://doi.org/10.1093/oxfordjournals.molbev.a025813

Davison EM, Coates DJ (1991) Identification of *Cryphonectria cubensis* and *Endothia gyrosa* from eucalypts in Western Australia using isozyme analysis. Australasian Plant Pathology 20: 157–160. https://doi.org/10.1071/APP9910157

Farris JS, Kallersjo M, Kluge AG, Bult C (1995) Testing significance of incongruence. Cladistics 10: 315–319. https://doi.org/10.1111/j.1096-0031.1994.tb00181.x

Ferreira MA, Soares de Oliveira ME, Silva GA, Mathioni SM, Mafia RG (2019) *Capillaureum caryovora* gen. sp. nov. (Cryphonectriaceae) pathogenic to pequi (*Caryocar brasiliense*) in Brazil. Mycological Progress 18: 385–403. https://doi.org/10.1007/s11557-018-01461-3

Glass NL, Donaldson GC (1995) Development of primer sets designed for use with the PCR to amplify conserved genes from filamentous Ascomycetes. Applied and Environmental Microbiology 61: 1323–1330. https://doi.org/10.1128/AEM.61.4.1323-1330.1995

Glen M, Alfenas AC, Zauza EAV, Wingfield MJ, Mohammed C (2007) *Puccinia psidii*: a threat to the Australian environment and economy – a review. Australasian Plant Pathology 36: 1–16. https://doi.org/10.1071/AP06088

Gordon TR, Storer AJ, Okamoto D (1996) Population structure of the pitch canker pathogen, *Fusarium subglutinans* f. sp. *pini*, in California. Mycological Research 100: 850–854. https://doi.org/10.1016/S0953-7562(96)80033-5

Gryzenhout M, Myburg H, Van der Merwe NA, Wingfield BD, Wingfield MJ (2004) *Chrysoporthe*, a new genus to accommodate *Cryphonectria cubensis*. Studies in Mycology 50: 119–142.

Gryzenhout M, Glen HF, Wingfield BD, Wingfield MJ (2005a) *Amphilogia* gen. nov. for Cryphonectria-like fungi from *Elaeocarpus* spp. in New Zealand and Sri Lanka. Taxon 54: 1009–1021. https://doi.org/10.2307/25065485

Gryzenhout M, Myburg H, Wingfield BD, Montenegro F, Wingfield MJ (2005b) *Chrysoporthe doradensis* sp. nov. pathogenic to *Eucalyptus* in Ecuador. Fungal Diversity 20: 39–57.

Gryzenhout M, Myburg H, Wingfield BD, Montenegro F, Wingfield MJ (2005c) *Rostraureum tropicale* gen. sp. nov. (Diaporthales) associated with dying *Terminalia ivorensis* in Ecuador. Mycological Research 109: 1029–1044. https://doi.org/10.1017/S0953756205003291

Gryzenhout M, Myburg H, Hodges CS, Wingfield BD, Wingfield MJ (2006a) *Microthia*, *Holocryphia* and *Ursicollum*, three new genera on *Eucalyptus* and *Coccoloba* for fungi previously known as *Cryphonectria*. Studies in Mycology 55: 35–52. https://doi.org/10.3114/sim.55.1.35

Gryzenhout M, Myburg H, Rodas CA, Wingfield BD, Wingfield MJ (2006b) *Aurapex penicillata* gen. sp. nov. from native *Miconia theaezans* and *Tibouchina* spp. in Colombia. Mycologia 98: 105–115. https://doi.org/10.3852/mycologia.98.1.105

Gryzenhout M, Myburg H, Wingfield BD, Wingfield MJ (2006c) Cryphonectriaceae (Diaporthales), a new family including *Cryphonectria*, *Chrysoporthe*, *Endothia* and allied genera. Mycologia 98: 239–249. https://doi.org/10.3852/mycologia.98.2.239

Gryzenhout M, Rodas CA, Menas Portales J, Clegg P, Wingfield BD, Wingfield MJ (2006d) Novel hosts of the Eucalyptus canker pathogen *Chrysoporthe cubensis* and a new *Chrysoporthe* species from Colombia. Mycological Research 110: 833–845. https://doi.org/10.1016/j.mycres.2006.02.010

Gryzenhout M, Wingfield BD, Wingfield MJ (2009) Taxonomy, phylogeny, and ecology of bark-inhabiting and tree pathogenic fungi in the Cryphonectriaceae. St Paul, MN, USA: APS Press.

Gryzenhout M, Tarigan M, Clegg PA, Wingfield MJ (2010) *Cryptometrion aestuescens* gen. sp. nov. (Cryphonectriaceae) pathogenic to *Eucalyptus* in Indonesia. Australasian Plant Pathology 39: 161–169. https://doi.org/10.1071/AP09077

Guindon S, Gascuel O (2003) A simple, fast, and accurate algorithm to estimate large phylogenies by maximum likelihood. Systematic Biology 52: 696–704. https://doi.org/10.1080/10635150390235520

Heiniger U, Rigling D (1994) Biological control of Chestnut blight in Europe. Annual Review of Phytopathology 32: 581–599. https://doi.org/10.1146/annurev.py.32.090194.003053

Hillis DM, Huelsenbeck JP (1992) Signal, noise, and reliability in molecular phylogenetic analyses. Journal of Heredity 83: 189–195. https://doi.org/10.1093/oxfordjournals.jhered.a111190

Hodges CS, Reis MS, Ferreira FA, Henfling JDM (1976) O cancro do eucalipto causado por *Diaporthe cubensis*. Fitopatologia Brasileira 1: 129–167.

Hodges CS, Geary TF, Cordell CE (1979) The occurrence of *Diaporthe cubensis* on *Eucalyptus* in Florida, Hawaii and Puerto Rico. Plant Disease Report 63: 216–220.

Huelsenbeck JP, Bull JJ, Cunningham CW (1996) Combining data in phylogenetic analysis. Trends in Ecology & Evolution 11: 152–158. https://doi.org/10.1016/0169-5347(96)10006-9

Jiang N, Fan XL, Yang Q, Du Z, Tian CM (2018) Two novel species of *Cryphonectria* from *Quercus* in China. Phytotaxa 347: 243–250. https://doi.org/10.11646/phytotaxa.347.3.5

Jiang N, Fan XL, Tian CM, Crous PW (2020) Re-evaluating Cryphonectriaceae and allied families in Diaporthales. Mycologia 112(2): 267–292. https://doi.org/10.1080/00275514.2019.1698925

Kamgan Nkuekam G, Barnes I, Wingfield MJ, Roux J (2009) Distribution and population diversity of *Ceratocystis pirilliformis* in South Africa. Mycologia 101: 17–25. https://doi.org/10.3852/07-171

Katoh K, Standley DM (2013) MAFFT multiple sequence alignment software version 7: improvements in performance and usability. Molecular Biology and Evolution 30: 772–780. https://doi.org/10.1093/molbev/mst010

Little Jr EL, Skolmen RG (1989) Common forest trees of Hawaii (Native and Introduced). Agricultural Handbook 679. USDA Forest Service, Washington.

Loope L (2010) A summary of information on the rust *Puccinia psidii* Winter (guava rust) with emphasis on means to prevent introduction of additional strains to Hawaii: U.S. Geological Survey Open-File Report 2010–1082. https://doi.org/10.3133/ofr20101082

McDonald BA (1997) The population genetics of fungi: tools and techniques. Phytopathology 87: 448–453. https://doi.org/10.1094/PHYTO.1997.87.4.448

Myburg H, Wingfield BD, Wingfield MJ (1999) Phylogeny of *Cryphonectria cubensis* and allied species inferred from DNA analysis. Mycologia 91: 243–250. https://doi.org/10.1080/00275514.1999.12061014

Myburg H, Gryzenhout M, Heath R, Roux J, Wingfield BD, Wingfield MJ (2002a) Cryphonectria canker on *Tibouchina* in South Africa. Mycological Research 106: 1299–1306. https://doi.org/10.1017/S095375620200669X

Myburg H, Gryzenhout M, Wingfield BD, Wingfield MJ (2002b) β-tubulin and histone H3 gene sequences distinguish *Cryphonectria cubensis* from South Africa, Asia and South America. Canadian Journal of Botany 80: 590–596. https://doi.org/10.1139/b02-039

Myburg H, Gryzenhout M, Wingfield BD, Wingfield MJ (2003) Conspecificity of *Endothia eugeniae* and *Cryphonectria cubensis*: A re-evaluation based on morphology and DNA sequence data. Mycoscience 44: 187–196. https://doi.org/10.1007/S10267-003-0101-8

Myburg H, Gryzenhout M, Wingfield BD, Milgroom MG, Shigeru K, Wingfield MJ (2004) DNA sequence data and morphology define *Cryphonectria* species in Europe, China, and Japan. Canadian Journal of Botany 82: 1730–1743. https://doi.org/10.1139/b04-135

Nakabonge G, Gryzenhout M, Roux J, Wingfield BD, Wingfield MJ (2006) *Celoporthe dispersa* gen. et sp. nov. from native Myrtales in South Africa. Studies in Mycology 55: 255–267. https://doi.org/10.3114/sim.55.1.255

Nei M (1973) Analysis of gene diversity in subdivided populations. Proceedings of the National Academy of Sciences of the United States of America 70: 3321–3323. https://doi.org/10.1073/pnas.70.12.3321

Posada D (2008) jModelTest: phylogenetic model averaging. Molecular Biology and Evolution 25: 1253–1256. https://doi.org/10.1093/molbev/msn083

Rayachhetry MB, Van TK, Center TD, Elliott ML (2001) Host range of *Puccinia psidii*, a potential biological control agent of *Melaleuca quinquenervia* in Florida. Biological Control 22: 38–45. https://doi.org/10.1006/bcon.2001.0949

Rodas CA, Gryzenhout M, Myburg H, Wingfield BD, Wingfield MJ (2005) Discovery of the Eucalyptus canker pathogen *Chrysoporthe cubensis* on native *Miconia* (Melastomataceae) in Colombia. Plant Pathology 54: 460–470. https://doi.org/10.1111/j.1365-3059.2005.01223.x

Roux J, Meke G, Kanyi B, Mwangi L, Mbaga A, Hunter GC, Nakabonge G, Heath RN, Wingfield MJ (2005) Diseases of plantation forestry tree species in eastern and southern Africa. South African Journal of Science 101: 409–413.

Roux J, Apetorgbor MM (2010) First report of *Chrysoporthe cubensis* from *Eucalyptus* in Ghana. Plant Pathology 59(4): 806–806. https://doi.org/10.1111/j.1365-3059.2009.02252.x

SAS (2002) JMP Software Version 5. SAS Institute Inc., Cary.

Swofford DL (2003) PAUP*. Phylogenetic Analysis Using Parsimony (*and other methods). Version 4.0b10. Sunderland, MA, USA: Sinauer Associates.

Tamura K, Dudley J, Nei M, Kumar S (2007) MEGA4: Molecular Evolutionary Genetics Analysis (MEGA) software version 4.0. Molecular Biological and Evolution 24: 1596–1599. https://doi.org/10.1093/molbev/msm092

Tommerup IC, Alfenas AC, Old KM (2003) Guava rust in Brazil – a threat to *Eucalyptus* and other Myrtaceae. New Zealand Journal of Forestry Science 33: 420–428.

Uchida J, Zhong S, Killgore E (2006) First report of a rust disease on Ohia caused by *Puccinia psidii* in Hawaii. Plant Disease 90(4): 524–524. https://doi.org/10.1094/PD-90-0524C

Van der Merwe NA, Wingfield BD, Wingfield MJ (2003) Primers for the amplification of sequence-characterized loci in *Cryphonectria cubensis* populations. Molecular Ecology Notes 3: 494–497. https://doi.org/10.1046/j.1471-8286.2003.00508.x

Van der Merwe NA, Gryzenhout M, Steenkamp ET, Wingfield BD, Wingfield MJ (2010) Multigene phylogenetic and population differentiation data confirm the existence of a cryptic species within *Chrysoporthe cubensis*. Fungal Biology 114: 966–979. https://doi.org/10.1016/j.funbio.2010.09.007

Venter M, Myburg H, Wingfield BD, Coutinho TA, Wingfield MJ (2002) A new species of *Cryphonectria* from South Africa and Australia, pathogenic on *Eucalyptus*. Sydowia 54: 98–117.

Vermeulen M, Gryzenhout M, Wingfield MJ, Roux J (2011) New records of Cryphonectriaceae from southern Africa including *Latruncellus aurorae* gen. sp. nov. Mycologia 103: 554–569. https://doi.org/10.3852/10-283

Vermeulen M, Gryzenhout M, Wingfield MJ, Roux J (2013) Species delineation in the tree pathogen genus *Celoporthe* (Cryphonectriaceae) in southern Africa. Mycologia 105: 297–311. https://doi.org/10.3852/12-206

Wang W, Liu QL, Li GQ, Chen SF (2018) Phylogeny and pathogenicity of *Celoporthe* species from plantation *Eucalyptus* in southern China. Plant Disease 102: 1915–1927. https://doi.org/10.1094/PDIS-12-17-2002-RE

Wang W, Li GQ, Liu QL, Chen SF (2020) Cryphonectriaceae on Myrtales in China: phylogeny, host range, and pathogenicity. Persoonia 45: 101–131. https://doi.org/10.3767/persoonia.2020.45.04

White TJ, Bruns T, Lee S, Taylor J (1990) Amplification and direct sequencing of fungal ribosomal RNA genes for phylogenetics. In: Innis MA, Gelfand DH, Sninsky JJ, White TJ (Eds) PCR Protocols: A sequencing guide to methods and applications. Academic Press, San Diego, 315–322. https://doi.org/10.1016/B978-0-12-372180-8.50042-1

Wingfield MJ, Swart WJ, Abear BJ (1989) First record of Cryphonectria canker of *Eucalyptus* in South Africa. Phytophylactica 21: 311–313.

Wingfield MJ (2003) Daniel McAlpine Memorial Lecture. Increasing threat of diseases to exotic plantation forests in the Southern Hemisphere: lessons from Cryphonectria canker. Australasian Plant Pathology 23: 133–139. https://doi.org/10.1071/AP03024

Wingfield MJ, Roux J, Slippers B, Hurley BP, Garnas J, Myburg AA, Wingfield BD (2013) Established and new technologies reduce increasing pest and pathogen threats to eucalypt plantations. Forest Ecology and Management 301: 35–42. https://doi.org/10.1016/j.foreco.2012.09.002

Wingfield MJ, Brockerhoff EG, Wingfield BD, Slippers B (2015) Planted forest health: The need for a global strategy. Science 349: 832–836. https://doi.org/10.1126/science.aac6674
Zhou X, Xie Y, Chen SF, Wingfield MJ (2008) Diseases of eucalypt plantations in China: challenges and opportunities. Fungal Diversity 32: 1–7.

## Supplementary material 1

**Table S1**
Authors: Jolanda Roux, Gilbert Kamgan Nkuekam, Seonju Marincowitz, Nicolaas A. van der Merwe, Janice Uchida, Michael J. Wingfield, ShuaiFei Chen
Data type: PCR-based microsatellite markers
Explanation note: List of PCR-based microsatellite markers used in this study.

Link: https://doi.org/10.3897/mycokeys.76.58406.suppl1

## Supplementary material 2

**Table S2**
Authors: Jolanda Roux, Gilbert Kamgan Nkuekam, Seonju Marincowitz, Nicolaas A. van der Merwe, Janice Uchida, Michael J. Wingfield, ShuaiFei Chen
Data type: datasets and statistics
Explanation note: Datasets used and the statistics resulting from the phylogenetic analyses.

Link: https://doi.org/10.3897/mycokeys.76.58406.suppl2

MycoKeys 76: 81–106 (2020)
doi: 10.3897/mycokeys.76.58465
https://mycokeys.pensoft.net

RESEARCH ARTICLE

A peer-reviewed open-access journal
MycoKeys
Launched to accelerate biodiversity research

# Morpho-phylogenetic evidence reveals new species in Rhytismataceae (Rhytismatales, Leotiomycetes, Ascomycota) from Guizhou Province, China

Jin-Feng Zhang[1,2,3], Jian-Kui Liu[2,4], Kevin D. Hyde[3,5,6], Anusha H. Ekanayaka[3,6], Zuo-Yi Liu[2]

**1** *Institute of Tea Research, Guizhou Academy of Agricultural Sciences, Guiyang 550006, China* **2** *Guizhou Key Laboratory of Agriculture Biotechnology, Guizhou Academy of Agricultural Sciences, Guiyang 550006, China* **3** *Center of Excellence in Fungal Research and School of Science, Mae Fah Luang University, Chiang Rai 57100, Thailand* **4** *School of Life Science and Technology, University of Electronic Science and Technology of China, Chengdu 611731, China* **5** *Innovative Institute of Plant Health, Zhongkai University of Agriculture and Engineering, Haizhu District, Guangzhou 510225, China* **6** *Key Laboratory for Plant Diversity and Biogeography of East Asia, Kunming Institute of Botany, Chinese Academy of Sciences, Kunming 650201, China*

Corresponding author: Zuo-Yi Liu (gzliuzuoyi@163.com)

Academic editor: R. Phookamsak | Received 8 September 2020 | Accepted 12 December 2020 | Published 31 December 2020

**Citation:** Zhang J-F, Liu J-K, Hyde KD, Ekanayaka AH, Liu Z-Y (2020) Morpho-phylogenetic evidence reveals new species in Rhytismataceae (Rhytismatales, Leotiomycetes, Ascomycota) from Guizhou Province, China. MycoKeys 76: 81–106. https://doi.org/10.3897/mycokeys.76.58465

## Abstract

Karst formations represent a unique eco-environment. Research in the microfungi inhabiting this area is limited. During an ongoing survey of ascomycetous microfungi from karst terrains in Guizhou Province, China, we discovered four new species, which are introduced here as *Hypoderma paralinderae*, *Terriera karsti*, *T. meitanensis* and *T. sigmoideospora* placed in Rhytismataceae, based on phylogenetic analyses and morphological characters. Molecular analyses, based on concatenated LSU-ITS-mtSSU sequence data, were used to infer phylogenetic affinities. Detail descriptions and comprehensive illustrations of these new taxa are provided and relationships with the allied species are discussed, based on comparative morphology and molecular data.

## Keywords

four new taxa, *Hypoderma*, karst formations, taxonomy, *Terriera*

## Introduction

Rhytismataceae (Rhytismatales) was established by Chevallier (1826), typified by *Rhytisma* with *R. acerinum* (Pers.) Fr. as the type species and belongs in Rhytismatales, Leotiomycetes, Ascomycota (Wijayawardene et al. 2020). Members of this family produce variously shaped apothecia that may be sessile, circular, navicular or hysteriform and that typically open by a longitudinal split or radial fissures. Asci are cylindrical, saccate to clavate. Ascospores are one-celled or multi-septate and vary from bacilliform to fusiform or filiform, with or without a sheath (Darker 1967; Ekanayaka et al. 2019). Species of Rhytismataceae occur on a wide range of hosts with a worldwide distribution (Cannon and Minter 1986; Johnston 1986; Hou and Piepenbring 2009; Hernández et al. 2014; Li et al. 2014; Tanney and Seifert 2017; Cai et al. 2020).

Darker (1967) proposed the generic delimitation for Rhytismataceae, based on ascoma and ascospore shapes, although this has been challenged in later studies (Cannon and Minter 1986; Johnston 1990, 2001; Hou et al. 2005). However, Darker (1967) and Cannon and Minter (1986) were followed due to lack of an alternative scheme. Molecular studies (Gernandt et al. 2001; Johnston and Park 2007; Lantz et al. 2011; Tian et al. 2013; Zhang et al. 2015) had revealed the phylogenetic relationships amongst members of Rhytismatales, but the available sequence data for this group remains limited and a phylogenetic classification of some members is unresolved. There are around 50 genera with 1000 species presently accepted in Rhytismataceae (Lumbsch and Huhndorf 2007; Wijayawardene et al. 2018; Index Fungorum 2020); however, a systematic genus-level taxonomic revision is needed to provide a clear, natural generic delimitation within this family and the relationship between Rhytismataceae and allied families within Rhytismatales needs to be resolved (Johnston et al. 2019).

Karst formations are generally characterised by sinking streams, caves, enclosed depressions, fluted rock outcrops and large springs (Ford and Williams 2007). Guizhou, as the eastern portion of the Yunnan-Guizhou Plateau, has the largest proportion of rocky desertification and karst landforms in China (Huang and Cai 2006). The flora in this area, comprising of 264 families with 1667 genera and 7505 vascular plants species, were inventoried from Guizhou Province (Liu et al. 2018). Therefore, it would be interesting to study the fungi in this area because of its unique ecological environment and rich plant resources. A series of studies have already been carried out and yielded several new species (Zhang et al. 2016, 2017a, b, 2018, 2019). The objectives of this study are to introduce four novel species of Rhytismataceae, based on phylogenetic and morphological evidence and elucidate their affinities with related species.

## Materials and methods

### Collection, examination, isolation and specimen deposition

Specimens were collected from Guizhou Province from 2016 to 2017 and examined in the laboratory with a Motic SMZ 168 stereomicroscope. Vertical sections of fruiting

bodies were made by hand and mounted in water for microscopy. Macro-morphological characters were captured using a stereomicroscope (Nikon SMZ800N) with a Cannon EOS 70D digital camera. Micro-morphological characters were observed by differential interference contrast (DIC) using a Nikon ECLIPSE 80*i* compound microscope and captured by a Cannon EOS 600D digital camera. Measurements were processed in a Tarosoft (R) Image Frame Work version 0.9.7 programme and photographic plates were edited in Adobe Photoshop CS6 (Adobe Systems Inc., USA).

The single spore isolation technique described in Chomnunti et al. (2014) was followed to obtain the pure cultures of these specimens. Single germinated ascospore was picked up and transferred to potato dextrose agar (PDA; 39 g/l distilled water, Difco potato dextrose) for recording growth rates and culture characteristics.

The holotypes are deposited at the Herbarium of Mae Fah Luang University (**MFLU**), Chiang Rai, Thailand or Guizhou Academy of Agricultural Sciences (**GZAAS**), Guizhou, China. Ex-type living culture is deposited at Guizhou Culture Collection (**GZCC**), Guiyang, China. Index Fungorum and Facesoffungi numbers are provided according to Jayasiri et al. (2015) and Index Fungorum (2020). New species were established, based on the recommendations from Jeewon and Hyde (2016).

## DNA extraction, PCR and phylogenetic analyses

Following the manufacturer's instructions, the total genomic DNA was extracted from cultures using a Biospin Fungus Genomic DNA Extraction Kit (BioFlux, Hangzhou, P. R. China) or extracted from the fruiting bodies using an E.Z.N.A. Forensic DNA kit (Omega Bio-Tek, Doraville, Georgia, USA).

Polymerase chain reactions (PCR) were performed in 25 µl reaction volumes, which contained 9.5 µl distilled-deionised-water, 12.5 µl of 2 × Power Taq PCR Master Mix (TIANGEN Co., China), 1 µl of DNA template and 1 µl of each forward and reverse primers. Three different loci were used in this study. The internal transcribed spacer (ITS) and 28S large subunit of the nuclear ribosomal DNA (LSU) regions were amplified by using the primers ITS4/ITS5 and LR0R/LR5, respectively (White et al. 1990; Gardes and Bruns 1993). The primers mrSSU1 and mrSSU3R were used for amplification of the mitochondrial small subunit (mtSSU) partial regions (Zoller et al. 1999). The PCR thermal cycle programme was performed according to White et al. (1990), Gardes and Bruns (1993) and Zoller et al. (1999). Amplicon size and concentration were assessed by gel electrophoresis with 1.2% agarose stained with ethidium bromide. PCR products were purified and sequenced at Sangon Biotechnology Co. Ltd (Shanghai, P. R. China).

For phylogenetic reconstruction, newly-generated sequences were initially subjected to BLAST search (BLASTn) in NCBI (https://www.ncbi.nlm.nih.gov) and additional related sequences were selected and downloaded from GenBank (https://www.ncbi.nlm.nih.gov/genbank/), based on BLASTn results and recent publications (Tian et al. 2013; Wang et al. 2013; Zhang et al. 2015; Johnston et al. 2019; Cai et al. 2020). The sequences used in this study for phylogenetic analysis are listed in Table 1. All of these sequences were aligned and manually improved with BioEdit v. 7.2 (Hall 1999)

**Table 1.** Taxa used in this study. Strains generated/sequenced in this study are given in bold.

| Taxa | Specimen/Strain No. | GenBank accession numbers | | |
|---|---|---|---|---|
| | | LSU | ITS | mtSSU |
| *Bifusella camelliae* | HOU 1094 | KF797447 | KF797435 | KF797458 |
| | HOU 701B | KF797448 | KF797436 | KF797459 |
| *Coccomyces anhuiensis* | BJTC 201610 | MK371314 | MK371313 | MK371315 |
| *Coccomyces dentatus* | AFTOL ID-147 | AY544657 | DQ491499 | AY544736 |
| *Colpoma ledi* | Lantz 379 (UPS) | HM140512 | – | HM143788 |
| *Colpoma quercinum* | Lantz 368 (UPS) | HM140513 | – | HM143789 |
| *Cryptomyces maximus* | Lantz and Minter 424 (UPS) | HM140514 | – | HM143790 |
| *Discocainia nervalis* | BITC 201405 | KJ513473 | KJ507206 | – |
| *Duplicariella phyllodoces* | Lantz 389 (UPS) | HM140516 | – | – |
| *Hypoderma berberidis* | HOU 892 | JX232420 | JX232414 | KF813010 |
| | HOU 942 | JX232421 | JX232415 | KF813009 |
| *Hypoderma campanulatum* | ICMP 17383 | HM140517 | – | HM143792 |
| *Hypoderma carinatum* | ICMP 18322 | HM140518 | – | HM143793 |
| *Hypoderma cordylines* | ICMP 17344 | HM140521 | JF683421 | HM143796 |
| | ICMP 17396 | HM140520 | – | HM143795 |
| *Hypoderma hederae* | Lantz and Minter 421 (UPS) | HM140522 | JF690770 | HM143797 |
| *Hypoderma liliense* | ICMP 18323 | HM140523 | MH921859 | HM143798 |
| | ICMP 18324 | HM140524 | – | HM143799 |
| *Hypoderma minteri* | BJTC 201203 | JX232418 | JX232416 | – |
| *Hypoderma obtectum* | ICMP 17365 | HM140525 | – | HM143800 |
| ***Hypoderma paralinderae*** | **GZAAS 19-1769** | **MN638878** | **MN638873** | **MN638868** |
| *Hypoderma rubi* | Hanson 2006-451 (UPS) | HM140519 | JF690769 | HM143794 |
| | ICMP 17339 | HM140526 | JF683419 | HM143801 |
| | ICMP 18325 | HM140527 | JF683418 | HM143802 |
| | Lantz 405 (UPS) | HM140530 | JF690772 | HM143805 |
| *Hypoderma sticheri* | ICMP 17353 | HM140529 | MK039702 | HM143804 |
| *Hypohelion anhuiense* | BITC 201311 | KF797443 | KF797431 | KF797455 |
| *Hypohelion scirpinum* | Lantz 394 (UPS) | HM140531 | – | HM143806 |
| *Lirula macrospora* | Hou et al. 13 (BJTC) | HQ902159 | HQ902152 | – |
| *Lirula yunnanensis* | BJTC 2012 | HQ902149 | HQ902156 | – |
| *Lophodermium arundinaceum* | Lantz 323 (UPS) | HM140535 | – | HM143811 |
| *Lophodermium culmigenum* | ICMP 18328 | HM140538 | – | HM143814 |
| *Marthamyces emarginatus* | ICMP 22854 | MK599203 | MH921869 | MK598751 |
| *Meloderma dracophylli* | ICMP 17343 | HM140561 | MH921871 | HM143833 |
| *Nematococcomyces oberwinkleri* | BJTC 201205 | KC312686 | – | KC312689 |
| *Nematococcomyces rhododendri* | HOU 469A | KC312687 | KU213975 | KC312691 |
| *Rhytisma huangshanense* | HOU 564 | FJ495192 | GQ253101 | – |
| *Rhytisma salicinum* | Lantz 370 (UPS) | HM140566 | – | – |
| *Sporomega degenerans* | Lantz 367 (UPS) | HM140567 | – | HM143839 |
| *Terriera camelliicola* | AAUF 66555 | KP878552 | – | KP878553 |
| *Terriera cladophila* | Lantz & Minter 423 (UPS) | HM140568 | – | HM143840 |
| *Terriera elliptica* | BJTC 201419 | KP878550 | KP878549 | KP878551 |
| *Terriera guihzouensis* | BITC 2020149 | MT549890 | MT534526 | – |
| | BITC 2020147 | – | MT534519 | MT549863 |
| | BITC 2020148 | – | MT534527 | MT549874 |
| | BITC 2020149 | MT549872 | MT534528 | MT549865 |
| | BITC 2020150 | – | MT534591 | MT549888 |
| *Terriera houjiazhuangensis* | BITC 2020145 | MT549889 | MT549882 | – |
| | BITC 2020146 | MT549864 | MT549879 | MT549884 |
| | BITC 2020192 | MT549869 | MT549883 | – |
| *Terriera ilicis* | BJTC 2020141 | MT549885 | MT549875 | MT549868 |
| | BJTC 2020193 | MT549873 | MT549861 | MT549886 |
| | BJTC 2020142 | MT549881 | MT549877 | MT549870 |
| ***Terriera karsti*** | **MFLU 18-2288** | **MN638881** | **MN638876** | **MN638871** |
| ***Terriera meitanensis*** | **MFLU 18-2299** | **MN638879** | **MN638874** | **MN638869** |
| ***Terriera meitanensis*** | **MFLU 18-2301** | **MN638880** | **MN638875** | **MN638870** |

| Taxa | Specimen/Strain No. | GenBank accession numbers | | |
|---|---|---|---|---|
| | | LSU | ITS | mtSSU |
| *Terriera minor* | ICMP 13973 | HM140570 | – | HM143842 |
| *Terriera pandanicola* | MFLU 16-1931 | MH260320 | MH275086 | MW334971 |
| ***Terriera sigmoideospora*** | **MFLU 18-2297** | **MN638882** | **MN638877** | **MN638872** |
| *Terriera thailandica* | MFLUCC 14-0818 | KX765301 | – | – |
| *Therrya abieticola* | HOU 447A | KP322580 | KP322574 | KP322587 |
| *Tryblidiopsis pinastri* | CBS 445.71 | MH871979 | JF793678 | AF431963 |
| *Tryblidiopsis sichuanensis* | BJTC 201211 | KC312683 | KC312676 | KC312692 |
| *Tryblidiopsis sinensis* | BJTC 201212 | KC312681 | KC312674 | KC312694 |

and then assembled as a dataset of LSU-ITS-mtSSU to infer the phylogenetic placement of newly identified taxa.

Phylogenetic analyses were performed using the algorithm of Maximum-Parsimony (MP) and Bayesian Inference (BI). MP analyses were run using PAUP v. 4.0b10 (Swofford 2002) with 1000 replications and inferred using the heuristic search option with 1000 random taxa. All characters were unordered and of equal weight and gaps were treated as missing data. Maxtrees was set as 1000, zero-length branches were collapsed and all equally parsimonious trees were saved. Clade stability was accessed using a bootstrap (BT) analysis with 1000 replicates, each with ten replicates of random stepwise addition of taxa (Hillis and Bull 1993).

BI analyses were carried out by using MrBayes v. 3.2 (Ronquist et al. 2012). The best-fit model (GTR+I+G for LSU, ITS and mtSSU) of evolution was estimated in MrModeltest 2.3 (Nylander 2008). Posterior Probabilities (PP) (Rannala and Yang 1996; Zhaxybayeva and Gogarten 2002) were determined by Markov Chain Monte Carlo sampling (MCMC) in MrBayes v. 3.2. Six simultaneous Markov chains were run for 10,000,000 generations and trees were sampled every 100$^{th}$ generation. The temperature values were lowered to 0.15, burn-in was set to 0.25 and the run was automatically stopped as soon as the average standard deviation of split frequencies reached below 0.01.

The phylogram was visualised in TreeView (Page 1996) and edited in Adobe Illustrator CS v. 5 (Adobe Systems Inc., USA). The finalised alignment and tree were deposited in TreeBASE, submission ID: 27401 (http://www.treebase.org).

## Results

### Phylogenetic analyses

The dataset for phylogenetic analysis comprised 64 strains, with *Marthamyces emarginatus* (Cooke & Massee) Minter selected as the outgroup taxon. This dataset consists of 2078 characters (including the gaps), of which 1205 are constant, 236 are variable parsimony-uninformative, while 637 characters are parsimony-informative. The most parsimonious tree showed with length of 2843 steps (CI = 0.480, RI = 0.759, RC = 0.364 and HI = 0.520). The best tree revealed by the MP analysis was selected to represent relationships amongst taxa (Fig. 1). The tree generated from Bayesian in-

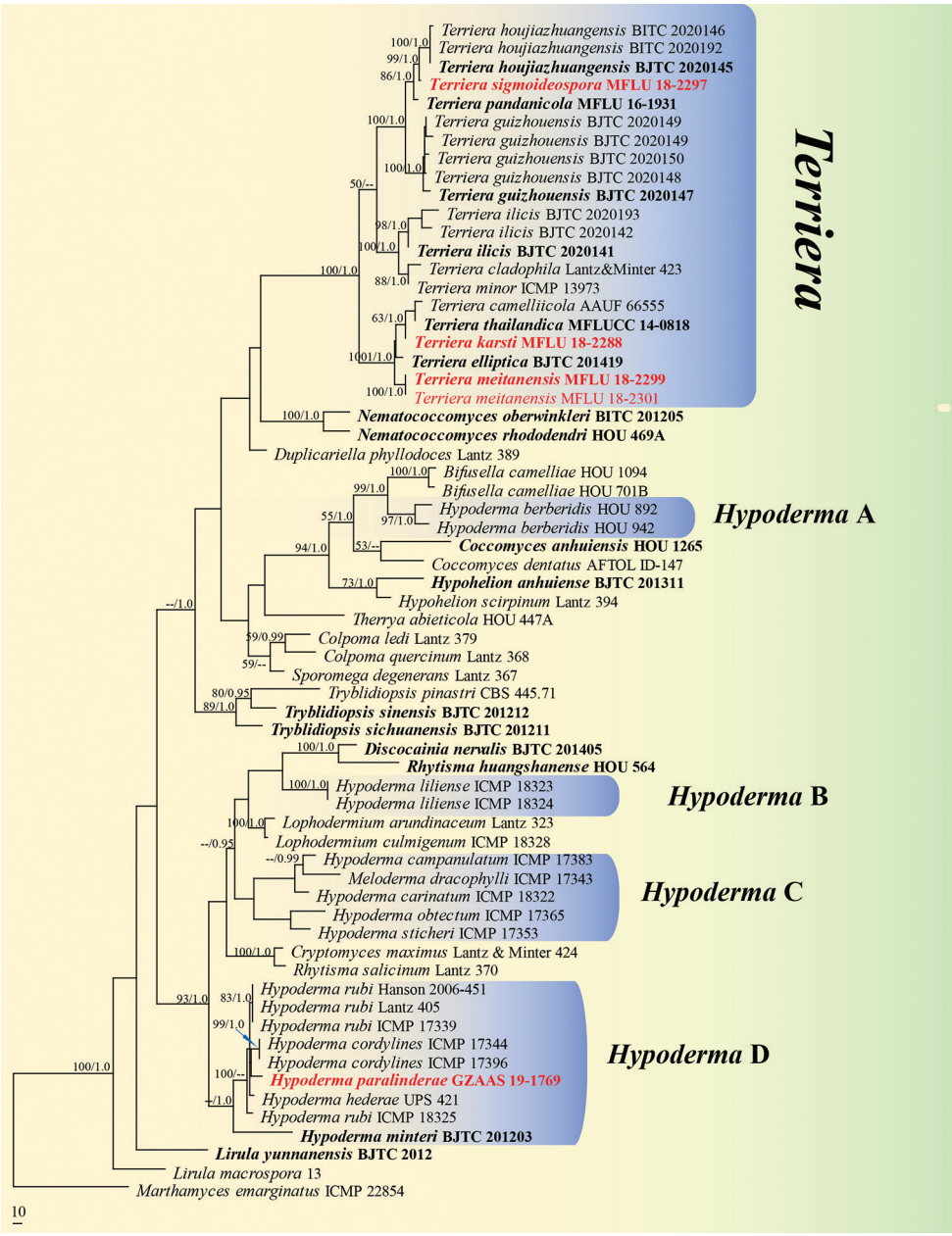


**Figure 1.** Phylogram of Rhytismataceae is presented as the best tree revealed by MP analysis, based on the concatenated LSU-ITS-mtSSU sequence dataset. MP bootstrap support values (MPBP ≥ 50%) and Bayesian inference posterior probabilities (BYPP ≥ 0.95) are shown near the nodes. The tree is rooted to *Marthamyces emarginatus* (ICMP 22854), the scale bar showing 10 changes. Type strains are indicated in bold and new sequences, generated in this study, are given in red.

ference analyses had similar topology. The phylogram (Fig. 1) shows that *Hypoderma* is non-monophyletic (Clade A, B, C and D), with *H. paralinderae* clusters with three existing species viz. *H. cordylines* P.R. Johnst., *H. hederae* (T. Nees ex Mart.) De Not. and *H. rubi* (Pers.) DC. In contrast, all of the *Terriera* species with available sequences (including the newly generated sequences) form a monophyletic clade with strong statistical support (MPBP 100% and BYPP 1.00). This corresponds to the phylogeny in Zhang et al. (2015). *Terriera meitanensis* and *T. karsti* group together with three reported species viz. *T. camelliicola* (Minter) Y.R. Lin & C.L. Hou, *T. elliptica* T.T. Zhang & C.L. Hou and *T. thailandica* Jayasiri & K.D. Hyde, while *T. sigmoideospora* is placed within another clade that comprises *T. houjiazhuangensis* C.L. Hou & S.R. Cai and *T. pandanicola* Tibpromma & K.D. Hyde.

## Taxonomy

***Hypoderma* De Not., G. bot. ital. 2(2): 13 (1847)**

De Candolle (1805) introduced *Hypoderma* to accommodate taxa resembling *Hysterium* Pers., but with apothecia that are immersed in host-plant tissue and the hymenia are exposed via a longitudinal split in the substratum. Subsequently, the nomenclature of *Hypoderma* was challenged by various authors (Chevallier 1822, 1826; Fries 1823; Wallroth 1833). De Notaris (1847) recognised the distinction between *Hypoderma* and *Lophodermium* Chevall. and separated them, based on the ascospore shapes. So far, there are 214 epithets included in Index Fungorum (2020), but around half of these species are synonymized under other genera, such as *Lophodermium*, *Meloderma* Darker and *Terriera*.

***Hypoderma paralinderae* J.F. Zhang & Z.Y. Liu, sp. nov.**
Index Fungorum number: IF556909
Facesoffungi Number No: FoF06797
Figure 2

**Etymology.** Referring to the morphological similarity with *Hypoderma linderae*.

**Holotype.** GZAAS 19-1769.

**Description.** *Apothecia* developing on dead stems, scattered, dark brown to black, shiny, long elliptical to slightly fusiform, straight or somewhat curved, ends rounded or obtuse, rising above the surface of the substrate, opening by a single longitudinal split. *Lips* moderately developed, pale brown (Fig. 2a, b). In median vertical section (Fig. 2c), apothecia subcuticular, 200–280 µm deep. *Covering stroma* (Fig. 2e) up to 38–45 µm thick near the opening, becoming to 12–18 µm thick towards the edges,

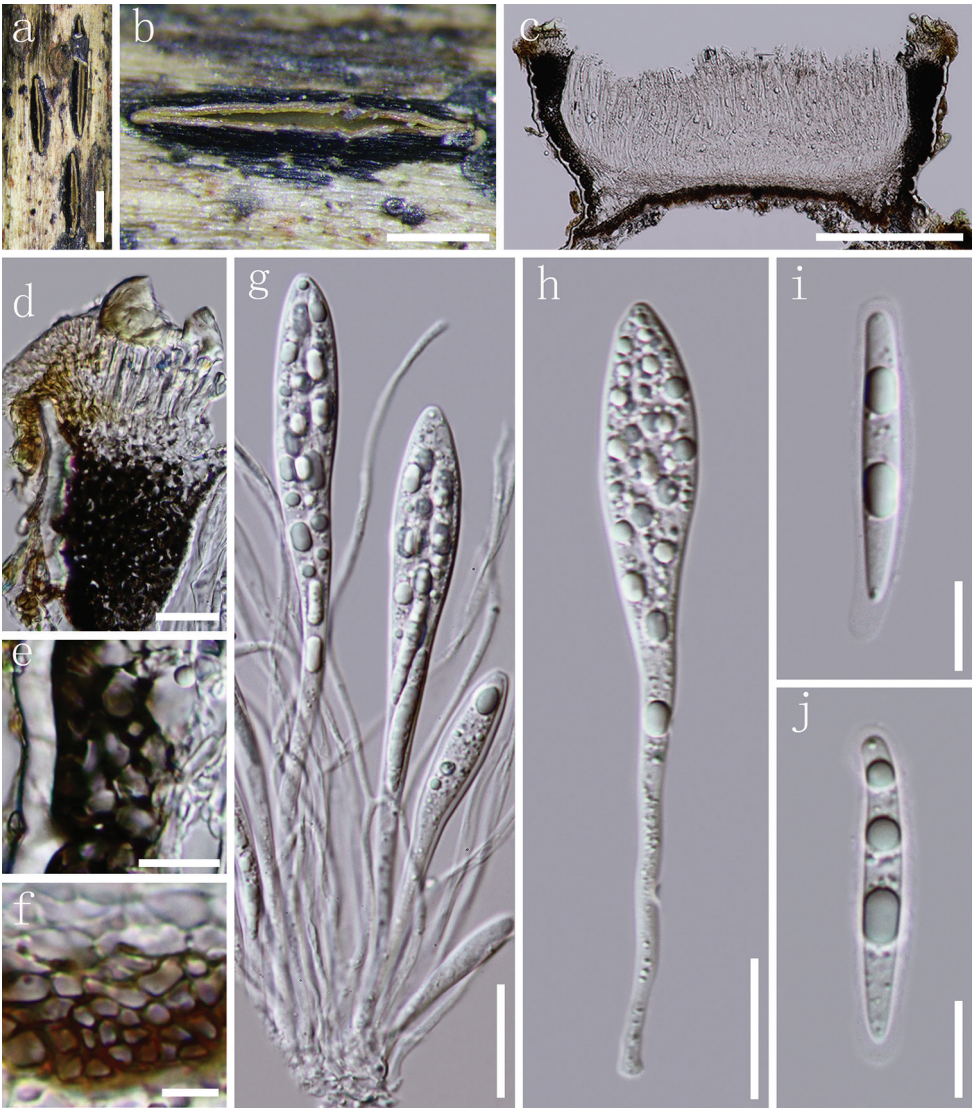


**Figure 2.** *Hypoderma paralinderae* **a, b** apothecia observed under a dissecting microscope in face view **c** vertical section through an apothecium **d** lips adjacent to the top of covering stroma **e** section of covering stroma **f** section of basal stroma **g** paraphyses and asci in various states of maturity **h** immature ascus **i, j** ascospores. Note: **c–j** mounted in water. Scale bar: 1 mm (**a**), 500 µm (**b**), 200 µm (**c**), 20 µm (**d, g, h**), 10 µm (**e, i, j**), 5 µm (**f**).

extending to the basal stroma, consisting of an outer layer of host cuticle and several layers of dark brown, thick-walled cells of *textura angularis*. *Lip cells* (Fig. 2d) clavate to cylindrical, 11–23 × 2–3 µm, thin-walled, hyaline to pale brown, 0–1-septate. *Basal stroma* (Fig. 2f) 10–16 µm thick, consisting of several layers of brown, thick-walled cells, arranged in *textura angularis*, becoming colourless, thin-walled cells of *textura*

*prismatica* towards the subhymenium. *Subhymenium* 19–27 µm thick, composed of several layers of hyaline, thin-walled cells of *textura angularis*. *Paraphyses* 1.5–2 µm, filiform, aseptate, unbranched, often curved, but not swollen at the apex, anastomosing at the base. *Asci* (81.5–)110–120(–129) × 10–14 µm ($\bar{x}$ = 108 × 12 µm, n = 25), 8-spored, unitunicate, cylindrical-clavate, round to subtruncate at the apex, with a 38–49 µm long stalk, thin-walled, J-, apical ring, without circumapical thickening. *Ascospores* 26–32.5 × 2.5–4.5 µm ($\bar{x}$ = 30.5 × 3.5 µm, n = 35, measured without the gelatinous sheath), multi-seriate and mostly arranged in the upper half of ascus, fusiform to slightly cylindrical, straight or lightly curved, apex rounded and tapering slightly to an acute base, aseptate, hyaline, guttulate, surrounded by a 0.5–1.5 µm thick gelatinous sheath (extending to 2.5 µm at the poles). *Asexual morph*: Not observed.

**Material examined.** CHINA, Guizhou Province, Leishan County, dead stems of unidentified herbaceous plants, 2 November 2017, J.F. Zhang, LS-21 (GZAAS 19-1769, ***holotype***).

**Notes.** Our phylogenetic analysis shows that *Hypoderma paralinderae* is placed in *Hypoderma* D clade (Fig. 1) and clustered with *H. cordylines*, *H. hederae* and *H. rubi*. Both *H. paralinderae* and *H. codylines* have similar sized asci (110–122.5 × 5.5–7 µm vs. 90–140 × 11–16 µm); however, they can be distinguished by the different shape and size of ascospores (fusiform to slightly cylindrical, 26–32.5 × 2.5–4.5 µm in *H. paralinderae* vs. elliptic, 14–21 × 4.5–6 µm in *H. cordylines*) (Johnston 1990). *Hypoderma paralinderae* shares similar-sized asci with *H. hederae*; however, it is differentiated from the latter by larger ascospores (26–32.5 × 2.5–4.5 µm vs. 18–22 × 3.5–4 µm) (Powell 1974). Moreover, *H. hederae* was described with oblong-cylindrical ascospores that are bluntly round on both ends; however, the ascospores in *H. paralinderae* are fusiform to cylindrical, but rounded at the apex and tapering slightly to an acute base (Powell 1974), while *H. paralinderae* differs from *H. rubi* by having obviously larger asci (110–122.5 × 5.5–7 µm vs. 60–100 × 10–12.5 µm) and ascospores (26–32.5 × 2.5–4.5 µm vs. 14–18 × 3.5–4.5 µm) (Hou et al. 2007). Besides, the recommendations of delineation taxa from Jeewon and Hyde (2016) are followed and comparisons of the ITS gene region between *H. paralinderae* and *H. cordylines* (ICMP 17344), as well as *H. paralinderae* and *H. rubi* (ICMP 17339) are processed. The results showed that there are 9/468 bp (1.9%) and 9/467 (1.9%) bp differences (including gaps) between them, respectively. According to the above evidence, *H. paralinderae* is introduced herein as new to science.

### *Terriera* B. Erikss., Symb. bot. upsal. 19(no. 4): 58 (1970)

*Terriera* was segregated from *Lophodermium* by Eriksson (1970) with *T. cladophila* as its type species. Johnston (2001) elucidated some distinctive morphological features (described as oblong to sublinear ascomata with single longitudinal opening slit, narrow-cylindrical asci and 1-septate ascospores that taper slightly at both ends and often becoming gently sigmoid on release and lacking a gelatinous sheath) for this genus and justified its monophyletic classification. There are 38 species accepted in *Terriera* (In-

dex Fungorum 2020) and around half of these species were discovered recently from China (Chen et al. 2011, 2013; Yang et al. 2011; Zheng et al. 2011; Gao et al. 2012; Song et al. 2012; Zhou et al. 2012; Li et al. 2015a, b; Lu et al. 2015; Wu et al. 2015; Cai et al. 2020). Here, we introduce three novel species. These three species share morphological characters typical of *Terriera* and cluster together with existing *Terriera* species in LSU-ITS-mtSSU phylogenetic analyses. In addition, a synopsis for *Terriera* species is also provided and listed in Table 2.

***Terriera karsti*** **J.F. Zhang & J.K. Liu, sp. nov.**
Index Fungorum number: IF556901
Facesoffungi Number No: FoF06799
Figure 3

**Holotype.** MFLU 18-2288.

**Etymology.** Refers to the karst landscape where the holotype was collected.

**Description.** *Apothecia* developing on dead branch, elliptical or oblong-elliptical in outline, ends slightly acute to obtuse. Apothecia surface black, matt or slightly glossy, moderately raising the substratum surface, opening by a single longitudinal split that extends to the ends of the apothecium (Fig. 3a, b). *Lips* absent. In median vertical section (Fig. 3d), apothecia deeply embedded in host tissue, with host cells becoming filled with fungal tissue as the apothecium develops. *Covering stroma* (Fig. 3c) 30–45 µm thick, composed of blackish-brown to black, thick-walled cells of *textura angularis* towards the exterior and several layers of pale to nearly hyaline, thin-walled cells towards the interior. Along the edge of the apothecial opening, there is a flattened, 12–20 µm thick extension adjacent to the covering stroma that is composed of strongly melanised tissue with no obvious cellular structure. *Basal stroma* 8–18 µm thick, dark brown or blackish-brown, composed of angular to globose, thick-walled cells, 2.5–4 µm diam. A triangular space between the covering stroma and basal stroma consists of thin-walled, nearly hyaline to grey-brown cells arranged in *textura prismatica*. *Paraphyses* 1–2 µm, filiform, hyaline, septate, gradually swollen or branching once at the apex, embedded in gelatinous sheaths. *Asci* (103–)110–122.5 × 5.5–7 µm ($\bar{x}$= 113 × 6 µm, n = 20), 8-spored, unitunicate, cylindrical, long stalk, thin-walled, apex truncate to somewhat round, J-, without circumapical thickening. *Ascospores* 55–66 × 1.5–2.0 µm ($\bar{x}$ = 61 × 1.8 µm, n = 25), fascicle, but not coiled, filiform, gradually tapering toward the ends, hyaline, aseptate, smooth-walled, straight or slightly curved, lacking gelatinous sheath. *Asexual morph*: Not observed.

**Culture characteristics.** Colonies on PDA reaching 51 mm after 14 days at 25 °C, irregular in shape, cottony with moderately dense, fluffy aerial mycelium. At first, white, becoming slightly greyish in the centre, reverse side bronze in the centre and pale towards the edge.

**Material examined.** CHINA, Guizhou Province, Guiyang, Yunyan District, dead branch of unidentified ligneous plants, 6 May 2016, J.F. Zhang, SH-06 (MFLU 18-2288, ***holotype***); *ibid.* (GZAAS 19-1720, ***isotype***); ex-type living culture, GZCC 19-0047.

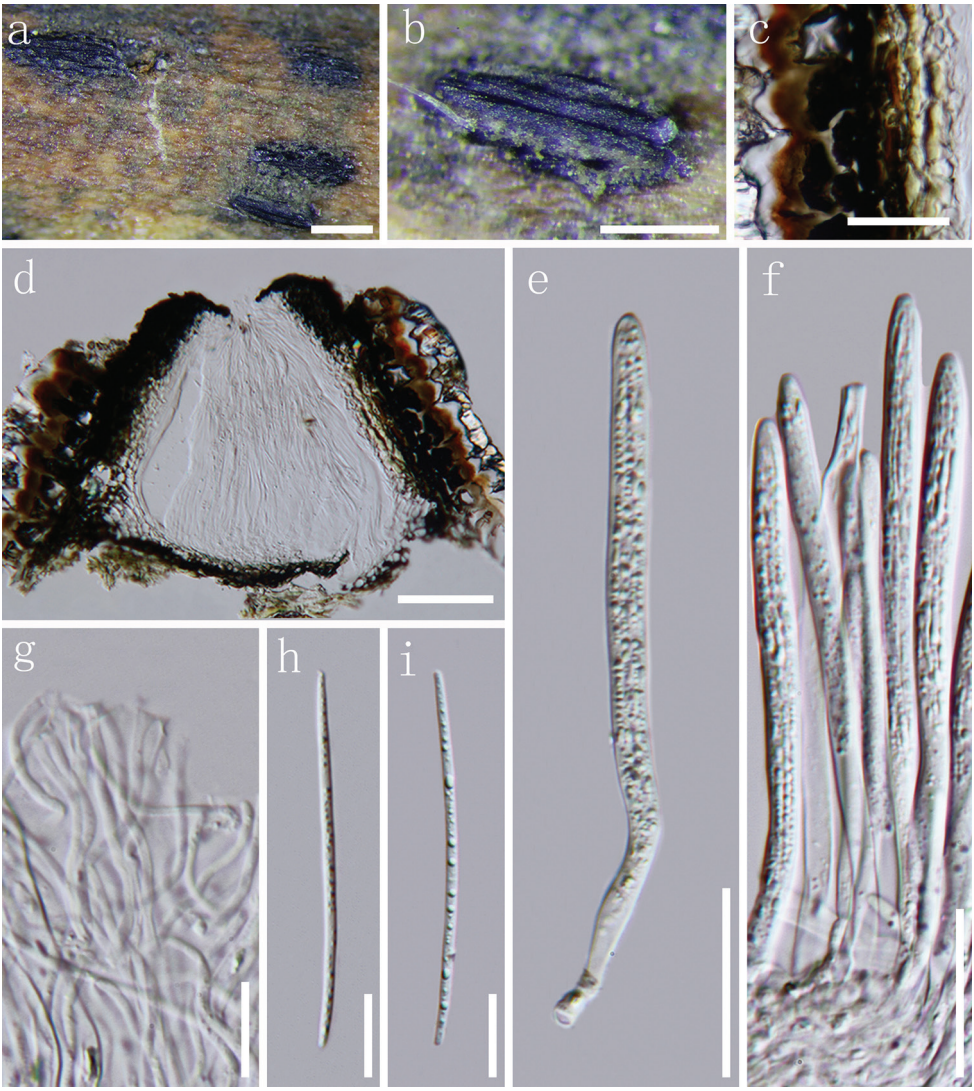


**Figure 3.** *Terriera karsti* **a, b** apothecia observed under the dissecting microscope **c** detail of covering stroma in vertical section **d** vertical section through an apothecium **e, f** asci in various states of maturity **g** apices of paraphyses **h, i** ascospores. Note: **c–i** mounted in water. Scale bar: 1 mm (**a**), 500 µm (**b**), 20 µm (**c, e, f**), 100 µm (**d**), 10 µm (**g, i**).

**Notes.** In the present study (Fig. 1), *Terriera karsti* is phylogenetically close to *T. camelliicola* and *T. thailandica* with moderate support (MPBP 63% and BYPP 1.00). *Terriera karsti* is not significantly distinguished from *T. camelliicola*, based only on morphological characters as they share similar-sized asci (110–122.5 × 5.5–7 µm vs. 85–120 × 5.5–6.5 µm) and ascospores (55–66 × 1.5–2 µm vs. 50–70 × 1 µm) (Johnston 2001). However, the ascospores of *T. camelliicola* are covered by a 0.5 µm wide gelatinous sheath, while this is not observed in *T. karsti* (Sharma 1982). In order

**Table 2.** Synopsis of *Terriera* species. The new species described in this study are indicated in bold.

| Species | Host | Appearance of apothecia | Asci | Ascospores | Origin | References |
|---|---|---|---|---|---|---|
| *Terriera aequabilis* | On dead leaves of *Photinia villosa* | Elliptical to sub-circular, straight or slightly curved to one side, ends rounded and opening by a single longitudinal split | 75–105 × 4.5–5.5 µm | 55–78 × 0.8–1 µm, filiform, aseptate, ends rounded, covered by a 0.3–0.5 µm wide gelatinous sheath | Jiangxi, China | Li et al. 2015b |
| *T. angularis* | On leaves of *Illicium simonsii* | Triangular to quadrangular, rarely elliptical and opening by 3–4 radial splits or a longitudinal split | 105–130 × 5.5–6.5 µm | 70–90 × 1–1.2 µm, filiform, aseptate, slightly tapering towards the round base, covered by a 0.8–1 µm wide gelatinous sheath | Hubei, China | Zhou et al. 2013 |
| *T. arundinacea* | On decomposed leaves of *Bambusa* sp. | Oblong to sublinear and opening by a single longitudinal split | 130–160 × 8–9 µm | 90–100 × 2–2.5 µm, slightly tapering towards the base, lacking gelatinous sheath | Java, Indonesia | Johnston 2001 |
| *T. asteliae* | On dead leaves of *Asterlia* sp. | Elliptical to oblong, ends rounded, opening by a single longitudinal slit | 75–105 × 8–10.5 µm | 45–70 × 2–2.5 µm, slightly tapering towards both ends and slightly constricted near the centre, aseptate or 1-septate, gently curved, lacking gelatinous sheath | Northland, New Zealand | Johnston 2001 |
| *T. breve* | On dead leaves of *Carex*, *Unicinia* and *Gahnia* spp. | Oblong-elliptical, ends rounded, often sublinear, with a single longitudinal opening slit | 110–135(–160) × 6–7 µm | (55–)60–75 × 1.5–2 µm, slightly tapering towards both ends, aseptate or 1-septate, gently curved or sigmoid, lacking gelatinous sheath | Campbell I, New Zealand | Johnston 2001 |
| *T. camelliae* | On fallen leaves of *Camellia* sp. | Subcircular to irregular bleached spots, elliptical or occasionally 3-lobed and opening by a longitudinal split | 85–120 × 5.5–6.5 µm | 52–80 × 1–1.2 µm, filiform, aseptate, covered by a ca. 0.5 µm wide gelatinous sheath. | Fuzhou, China | Chen et al. 2011 |
| *T. camelliicola* | On twigs of *Camellia sinensis* | Elliptical, occasionally fusing to form elongated elliptical, opening by a single longitudinal split | 80–110 × 5–7 µm | 50–70 × 1 µm, filiform, aseptate, covered by a 0.5 µm wide gelatinous sheath. | Assam, India | Minter and Sharma 1982 |
| *T. cladophila* | On dead twigs of *Vaccinium myrtillus* | Elliptical, rounded at the ends, with a longitudinal opening split | 75–100 × 5.5–8 µm | 60–70 × 1 µm, filiform, aseptate, lacking gelatinous sheath | Norway | Terrier 1942; Eriksson 1970 |
| *T. clithris* | On dead leaves of unidentified monocotyledon | Cylindrical to linear, with longitudinal opening slit | 110–120 × 6.5–7.0 µm | 60–80 × 1–1.5 µm, slightly tapering towards both ends, lacking gelatinous sheath | Rio Grande Do Sul, Brazil | Johnston 2001 |
| *T. coacervata* | On leaves of *Lithocarpus cleistocarpus* | Elliptical, sometimes branching into lobed or polygonal shapes, opening by a longitudinal split or by more than 3 lobes | 90–130 × 6.0–7.0 µm | 60–110 × 1.5–1.8 µm, filiform, aseptate, covered by a 1.0–1.5 µm wide gelatinous sheath | Anhui, China | Zheng et al. 2012 |
| *T. dracaenae* | On dead leaves or stems of *Dracaena* sp. | Oblong to oblong-elliptical, ends rounded, opening by a single longitudinal split | 130–140 (–160) × 6–7 µm | 100 × 2 µm, 1-septate, lacking gelatinous sheath | California, USA | Johnston 2001 |
| *T. elliptica* | On living twigs of *Rhododendron* sp. | Elliptical, ends rounded to subacute, opening by a longitudinal split | 135–175 × 7–9 µm | 60–85 × 1.5–2 µm, filiform, slightly tapering towards both ends, aseptate, covered by a 1–1.5 µm wide gelatinous sheath | Yunnan, China | Zhang et al. 2015 |
| *T. fici* | On dead leaves of *Ficus vasculosa* | Rounded or subrounded, with conspicuous edge and opening by a single longitudinal split | 90–115 × 4–5.5 µm | 65–80 × 0.8–1 µm, filiform, aseptate, rounded to obtuse at the apex, slightly tapering towards the rounded or subacute base, covered by a 0.5 µm wide gelatinous sheath | Hainan, China | Wu et al. 2016 |
| *T. fuegiana* | On dead leaves of *Rostkovia grandiflora* | Oblong elliptical to broad-elliptical, ends rounded, opening by a single, longitudinal slit | 75–95 × 7–10 µm | 60–65 × 1.5–2.5 µm, slightly tapering towards both ends, 1-septate, lacking gelatinous sheath | Tierra del Fuego, Argentina | Johnston 2001 |

| Species | Host | Appearance of apothecia | Asci | Ascospores | Origin | References |
|---|---|---|---|---|---|---|
| *T. fourcroyae* | On dead leaves of *Furcraea* sp. | Oblong-elliptical, ends rounded, with a single longitudinal opening slit | 95–110 × 5–6.5 µm | 60–70 × 1.5–2.5 µm, slightly tapering towards both ends, gently coiled or sigmoid, 1-septate, lacking gelatinous sheath. | Sri Lanka | Johnston 2001 |
| *T. guizhouensis* | On dead leaves of *Eriobotrya japonica* | Elliptical, occasionally curved, opening by a longitudinal split | 88–107 × 4–6 µm | 50–80 × 1–1.2 µm, filiform, slightly tapering towards both ends, aseptate, pluriguttulate, covered by a thin gelatinous sheath | Guizhou, China | Cai et al. 2020 |
| *T. houjiashanensis* | On dead leaves of *Ilex cornuta* | Elliptical, often curved, occasionally confluent, opening by a longitudinal split | 103–128 × 4–6 µm | 73–82 × 0.6–0.9 µm, filiform, slightly tapering towards both ends, aseptate, pluriguttulate, covered by an inconspicuous gelatinous sheath | Anhui, China | Cai et al. 2020 |
| *T. huangshanensis* | On leaves of *Eurya muricata* var. *huiana* | Elliptical, fusiform or subfusiform, straight or curved (lunate), sometimes 3-lobed or triangular, ends rounded to subacute, opening by a single longitudinal split | 100–120 × 5–7 µm | 58–90 × 1.5–2 µm, filiform, slightly tapering towards the base, aseptate, covered by a 1–1.5 µm thick gelatinous sheath | Anhui, China | Yang et al. 2011 |
| *T. ilicis* | On dead leaves of *Ilex pernyi* | Elliptical, occasionally curved, triangular or confluent, opening by a longitudinal split | 117–139 × 4–7 µm | 52–84 × ca. 1 µm, filiform, slightly tapering towards both ends, aseptate, pluriguttulate, covered by a thin gelatinous sheath | Hubei, China | Cai et al. 2020 |
| *T. illiciicola* | On dead leaves of *Lithocarpus cleistocarpus* | Subcircular to broad-elliptical, opening by a longitudinal split | 90–135 × 4.0–5.0 µm | 65–95 × 1 µm, filiform, aseptate, covered by an inconspicuous gelatinous sheath | Anhui, China | Zheng et al. 2011 |
| *T. intraepidermalis* | On fallen leaves of *Photinia prunifolia* | Widely elliptical, sometimes elliptical or subcircular, occasionally triangular, straight or curved to one side slightly, ends round to obtuse, opening by a single longitudinal split or by three radial splits | 90–135 × 5.5–7.5 µm | 70–105 × 1–1.5 µm, with upper end rounded to obtuse, slightly tapering towards the rounded base, covered by a 0.5 µm wide gelatinous sheath | Hunan, China | Lu et al. 2015 |
| *T. javanica* | On dead leaves of *Elettaria* sp. | Oblong-elliptical to sublinear, ends acute, opening by a single longitudinal slit | 85–95 × 5.5–7 µm | 50–60 × 1.5 µm, but the detailed morphological characters were not seen | Java, Indonesia | Johnston 2001 |
| ***T. karsti*** | **On dead branch of unidentified host** | **Elliptical or oblong-elliptical, ends slightly acute to obtuse, with a single longitudinal opening split** | **(103–)110–122.5 × 5.5–7 µm** | **55–66 × 1.5–2.0 µm, filiform, gradually tapering towards both ends, aseptate, lacking gelatinous sheath** | **Guihzou, China** | **In this study** |
| *T. latiascus* | On dead leaves of *Euterpe* and *Heliconia* spp. | Oblong-elliptical, with a single longitudinal opening slit | 80–95 × 7–8.5 µm | 40–50 × 2–2.5 µm, with 1(–3)-septate, slightly tapering to both ends | Amazonas, Brazil | Johnston 2001 |
| *T. longissima* | On dead leaves of Bambusaceae sp. | Oblong to sublinear, ends rounded, opening by a single, longitudinal slit | 175–210 × 6–6.5 µm | Approximately 120–130 µm long, but the detailed morphological characters were not seen | Potaro-Siparuni region VII, Guyana | Johnston 2001 |
| *T. mangiferae* | On dead leaves of *Aucuba japonica* and *Mangifera indica* | Ellipsoidal, with a longitudinal opening split | 80–90 × 5–6 µm | 70–80 × 1 µm, filiform, lacking gelatinous sheath | Java, Indonesia | Koorders 1907; Li et al. 2014 |
| ***T. meitanensis*** | **On dead culms of unidentified host** | **Elliptical to oblong-elliptical, ends slightly acute to obtuse, opening by a single longitudinal split** | **(98.5–)113–125.5(–131.5) × 6–7.5 µm** | **47–54.5 × 1.5–2.5 µm, filiform, gradually tapering towards both ends, aseptate, lacking gelatinous sheath** | **Guizhou, China** | **In this study** |

| Species | Host | Appearance of apothecia | Asci | Ascospores | Origin | References |
|---|---|---|---|---|---|---|
| *T. nematoidea* | On dead leaves of *Gahnia* sp. | Elliptical to sublinear, with a single longitudinal opening slit | 70–80 × 5–6.5 µm | 30–35 × 1 µm, slightly tapering towards both ends, gently curved or sigmoid, 1-septate, lacking gelatinous sheath | Northland, New Zealand | Johnston 2001 |
| *T. nitens* | On leaves of *Cyclobalanopsis myrsinifolia* | Suborbicular or broadly elliptical, straight or slightly curved, opening by a single longitudinal split | 95–150 × 1–1.2 µm | 68–115 × 0.8–1.2 µm, filiform, aseptate, round at the apex, slightly tapering towards the acute base, covered by a thin gelatinous sheath | Anhui, China | Chen et al. 2013 |
| *T. pandani* | On dead leaves of *Pandanus* sp. | Oblong to oblong-elliptical, ends rounded, opening by a single longitudinal slit | 100–120 × 5–6 µm | 50–70 × 1–1.5 µm, lacking gelatinous sheath | San Juan, Puerto Rico | Johnston 2001 |
| *T. pandanicola* | On dead leaves of *Pandanus* sp. | Elliptical, with rounded to subacute ends, opening by a longitudinal split | 50–66 × 4–5 µm | 55–78 × 1–2 µm, filiform, slightly tapering towards both ends, aseptate, lacking gelatinous sheath | Prachuap Khiri Khan, Thailand | Tibpromma et al. 2018 |
| *T. petrakii* | On fallen leaves of *Smilax bracteata* | Elongate-elliptical, strongly curved or triangular, often coalesced, opening by a longitudinal split | 85–110 × 4–5 µm | (60–)70–85 × 0.8 µm, filiform, aseptate, covered by a thin gelatinous sheath | Yunnan, China | Song et al. 2012 |
| *T. rotundata* | On fallen leaves of *Quercus* sp. | Elliptical, occasionally triangular, ends rounded, opening by a longitudinal split or occasionally by teeth | 90–120 × 4–5.5 µm | 70–90(–95) × 0.8–1 µm, filiform, aseptate, lacking gelatinous sheath | Yunnan, China | Song et al. 2012 |
| *T. sacchari* | On dead leaves and leaf bases of *Saccharum officinarum* | Narrow-oblong to sublinear, with a single longitudinal opening split | 90–100 × 5–7 µm | 50–60 × 1.5 µm, lacking gelatinous sheath | Hawaii, USA | Johnston 2001 |
| *T. samuelsii* | On dead leaves of unidentified monocotyledon | Oblong to sublinear, ends rounded, opening by a single longitudinal slit | 125–140 × 7–8 µm | (65–)75–90 × 2 µm, slightly tapering towards both ends, 1-septate, lacking gelatinous sheath | Amazonas, Brazil | Johnston 2001; 2003 |
| ***T. sigmoideospora*** | **On dead fallen leaves of unidentified host** | **Elliptical, ends rounded to subacute, opening by a single longitudinal split** | **(93.5–)102–121 × 5–6 µm** | **79–95 × 5–2 µm, filiform, slightly tapering towards both ends, aseptate, lacking gelatinous sheath** | **Guizhou, China** | **In this study** |
| *T. simplex* | On fallen leaves of *Trachelospermum jasminoides* | Elliptical to ovate, ends obtuse, rounded or slightly acute, opening by a single longitudinal split which is sometimes branched in the triangular ascomata | 72–95(–105) × 4.8–5.2 µm | (45–)56–82 × 1–1.2 µm, filiform, slightly tapering towards the rounded base, covered by a 0.8–1 µm wide gelatinous sheath | Anhui, China | Gao et al. 2012 |
| *T. stevensii* | On dead leaves of *Vincentia* sp. | Oblong, ends rounded, opening by a single longitudinal slit | 100–125 × 5–6 µm | 60–80 × 1.5–2 µm, lacking gelatinous sheath | Hawaii, USA | Johnston 2001 |
| *T. thailandica* | On dead branch of unidentified host | Elliptical, ends rounded to subacute, opening by a longitudinal split | 80–105 × 3.4–6.6 µm | 38–60 × 1–1.5 µm, filiform, slightly tapering towards both ends, aseptate, lacking gelatinous sheath | Chiang Rai, Thailand | Hyde et al. 2016 |
| *T. transversa* | On dead leaves of *Pandanus* sp. | Elliptical or oblong-elliptical, ends slightly acute to obtuse, opening by a single longitudinal split | 70–86 × 5–6 µm | 45–68 × 1–1.2 µm, filiform, slightly tapering towards both ends, aseptate, covered by a 0.5 µm wide gelatinous sheath | Hainan, China | Li et al. 2015a |

to clarify their affinity, the recommendations of species delineation from Jeewon and Hyde (2016) were followed and the comparison of each gene region between these two taxa is processed and showed that there are 9/840 bp (1%) and 10/694 bp (14.4%) differences in LSU and mtSSU regions, respectively, while *T. karsti* can be easily differentiated from *T. thailandica* by its larger asci (110–122.5 × 5.5–7 µm vs. 80–105 × 3.4–6.6 µm) and ascospores (55–66 × 1.5–2 µm vs. 38–60 × 1–1.5 µm) (Hyde et al. 2016). A comparison of the LSU gene region between these two taxa has also been processed and the result showed that there are 3/838 bp (base pair) differences. Based on phylogenetic analyses, coupled with morphological distinction, *Terriera karsti* is introduced herein as a new species.

***Terriera meitanensis*** **J.F. Zhang & Z.Y. Liu, sp. nov.**
Index Fungorum number: IF556900
Facesoffungi Number No: FoF06798
Figure 4

**Holotype.** MFLU 18-2299.

**Etymology.** Referring to the locality of the holotype, Meitan County, Guizhou Province, China.

**Description.** *Apothecia* developing on dead stems (Fig. 4a), semi-immersed to superficial, elliptical or oblong-elliptical, ends slightly acute to obtuse, surface black, matt, raising the substratum surface, opening by a single longitudinal split that extends nearly the entire length (Fig. 4b, c). In median vertical section (Fig. 4d), apothecia deeply embedded in host tissue, with host cells becoming filled with fungal tissue as the apothecium develops. *Covering stroma* (Fig. 4e) 33–42 µm thick, composed of blackish-brown, thick-walled cells that are fused with host tissue in the outermost layers, becoming pale pigmented or nearly colourless towards the hymenium, thin-walled cells, arranged in *textura angularis* or *textura globulosa.* Along the upper edge of the apothecial opening, there is a flattened, 19–34 µm thick extension adjacent to the covering stroma that is composed of strongly melanised tissue with no obvious cellular structure. *Basal stroma* (Fig. 4g) 8–18 µm thick, dark-brown or blackish-brown, composed of angular to globose, thick-walled cells, 2.5–4 µm diam. Where the covering stroma meets the basal stroma, there is a triangular-shaped, 35–60 µm thick, tissue composed of thin-walled, hyaline to pale brown cells forming a *textura prismatica* (Fig. 4f). *Subhymenium* 12–16 µm thick, consisting of hyaline *textura angularis* to *textura intricata*. *Paraphyses* 1–2 µm, filiform, hyaline, septate, gradually swollen or branching once at the apex, embedded in gelatinous matrix, anastomosing at the base. *Asci* (98.5–)113–125.5(–131.5) × 6–7.5 µm ($\bar{x}$ = 117 × 6.5 µm, n = 20), 8-spored, unitunicate, cylindrical, somewhat long-stalked, thin-walled, apex generally truncate, J-, without circumapical thickening. *Ascospores* 47–54.5 × 1.5–2.5 µm ($\bar{x}$ = 50.5 × 2 µm, n = 35), fascicle, filiform, gradually tapering towards the ends, hyaline, aseptate, smooth-walled, straight or slightly curved, lacking a gelatinous sheath. *Asexual morph*: Not observed.

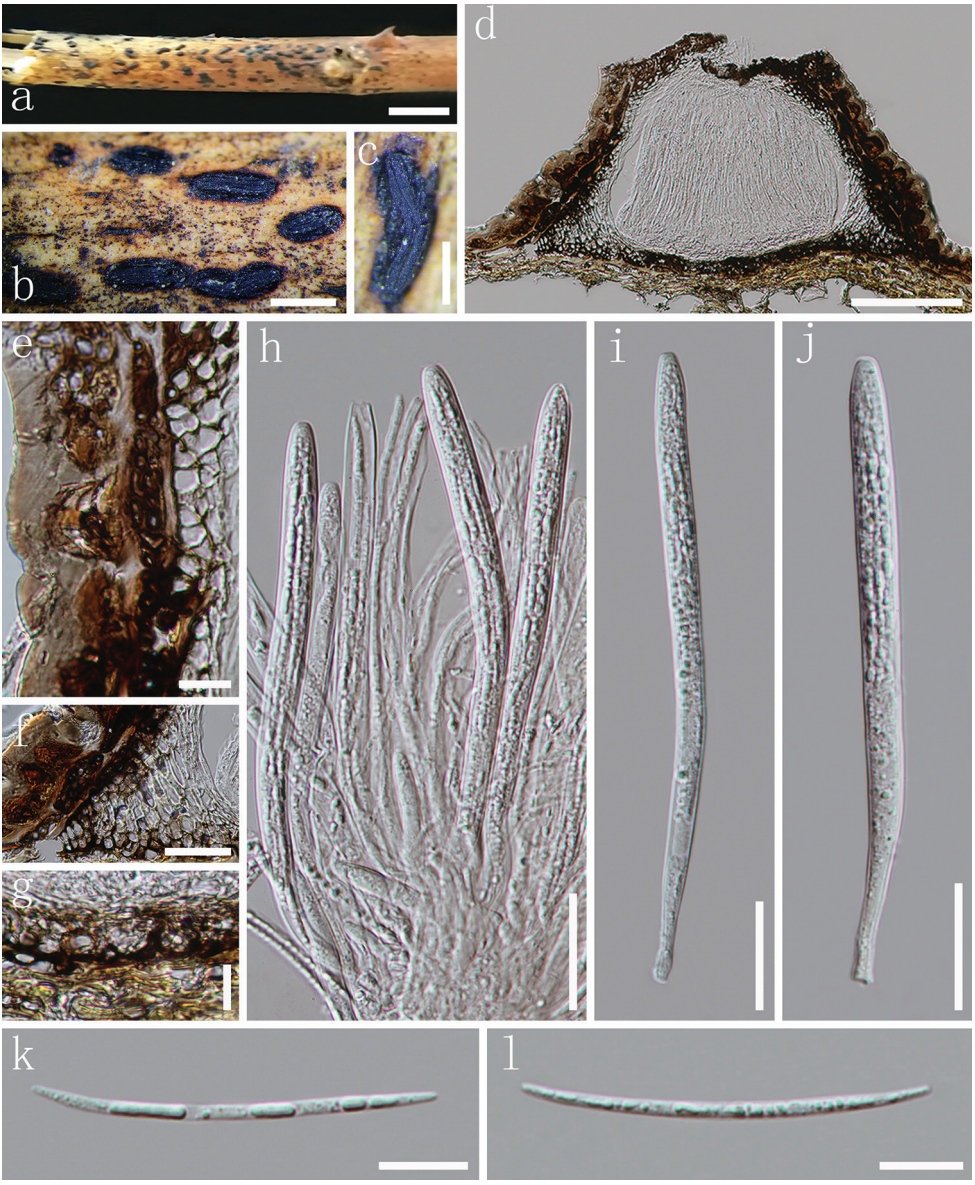


**Figure 4.** *Terriera meitanensis* **a** habit of apothecia on substrate **b, c** apothecia observed under the dissecting microscope in face view **d** vertical section through an apothecium **e** covering stroma **f** triangular space in section between the covering stroma and basal stroma **g** basal stroma **h** paraphyses with anastomoses amongst asci in various states of maturity **i, j** immature asci **k, l** ascospores. Note: **d–l** mounted in water. Scale bar: 1 cm (**a**), 1 mm (**b**), 500 µm (**c**), 100 µm (**d**), 10 µm (**e, g, k, l**), 30 µm (**f**), 20 µm (**h–j**).

**Material examined.** CHINA, Guizhou Province, Zunyi, Meitan County, dead stems of unidentified host, 28 August 2017, J.F. Zhang, MT-1 (MFLU 18-2299, ***holotype***); *ibid.* (GZAAS 19-1731, ***isotype***).

**Notes.** In our phylogenetic analysis (Fig. 1), *Terriera meitanensis* is placed in a robust clade with *T. camelliicola*, *T. elliptica*, *T. karsti* and *T. thailandica* by strong statistical support (MPBP 100% and BYPP 1.00). *Terriera meitanensis* has larger asci than *T. camelliicola* and *T. thailandica*, while the ascospores of *T. meitanensis* are smaller (Johnston 2001; Hyde et al. 2016). Both *T. meitanensis* and *T. karsti* share similar-sized asci, but *T. karsti* has larger ascospores (47–54.5 × 1.5–2.5 µm vs. 55–66 × 1.5–2.0 µm). *Terriera meitanensis* differs from *T. elliptica* by its obviously smaller asci (113–122.5 × 6–7.5 µm vs. 135–175 × 7–9 µm) and ascospores (47–54.5 × 1.5–2.5 µm vs. 60–85 × 1.5–2 µm) (Zhang et al. 2015). Moreover, the ascospores of *T. camelliicola* and *T. elliptica* are enveloped by a gelatinous sheath, respectively, while this is not observed in *T. meitanensis*. In addition, the comparison of the ITS gene region is processed between *T. meitanensis* and its closest species *T. elliptica*, based on the recommendations from Jeewon and Hyde (2016) and the results showed that there are 15/489 bp (3%) differences. Therefore, we introduce *T. meitanensis* herein as a new species, based on morphological and molecular evidence.

***Terriera sigmoideospora*** **J.F. Zhang & K.D. Hyde, sp. nov.**
Index Fungorum number: IF556902
Facesoffungi Number No: FoF06800
Figure 5

**Holotype.** MFLU 18-2297.

**Etymology.** Refers to its sigmoidal ascospores.

**Description.** *Apothecia* developing on fallen leaves, scattered, dark brown to black, matt, elliptical, sometimes 3-lobed or triangular, straight or slightly curved, ends rounded to subacute, strongly raising the surface of the substrate at maturity, opening by a single longitudinal split that extends almost the whole length of the apothecium (Fig. 5a, b). Immature apothecia appearing as a single dark brown protrusion, circular to slightly elongated. In median vertical section (Fig. 5d), apothecia 185–220 µm deep. *Covering stroma* (Fig. 5c) 20–25 µm thick near the centre of the apothecium, consisting of an outer layer of host cuticle, remains of epidermal and hypodermal cells filled with thick-walled, angular fungal cells and an inner layer of *textura angularis* to *textura globulosa* with 4–7 µm diam., dark brown, thick-walled cells, slightly thinner towards the edges, extending to the basal stroma, but conspicuously thicker towards the apothecial opening, with a 15–27 µm thick extension comprising highly melanised tissue with no obvious cellular structure. *Excipulum* moderately developed, closely adhering to the covering stroma and the extension, arising from the marginal paraphyses, becoming thinner towards the base. *Basal stroma* concave, 12–15 µm thick, composed of dark brown, thick-walled, angular cells. A triangular space between the covering stroma and basal stroma is composed of thin-walled, colourless cells that are vertically arranged in rows. *Subhymenium* 6–9 µm thick, flat, consisting of hyaline cells of *textura intricata*. *Paraphyses* filiform, hyaline, septate, gradually or suddenly swollen to

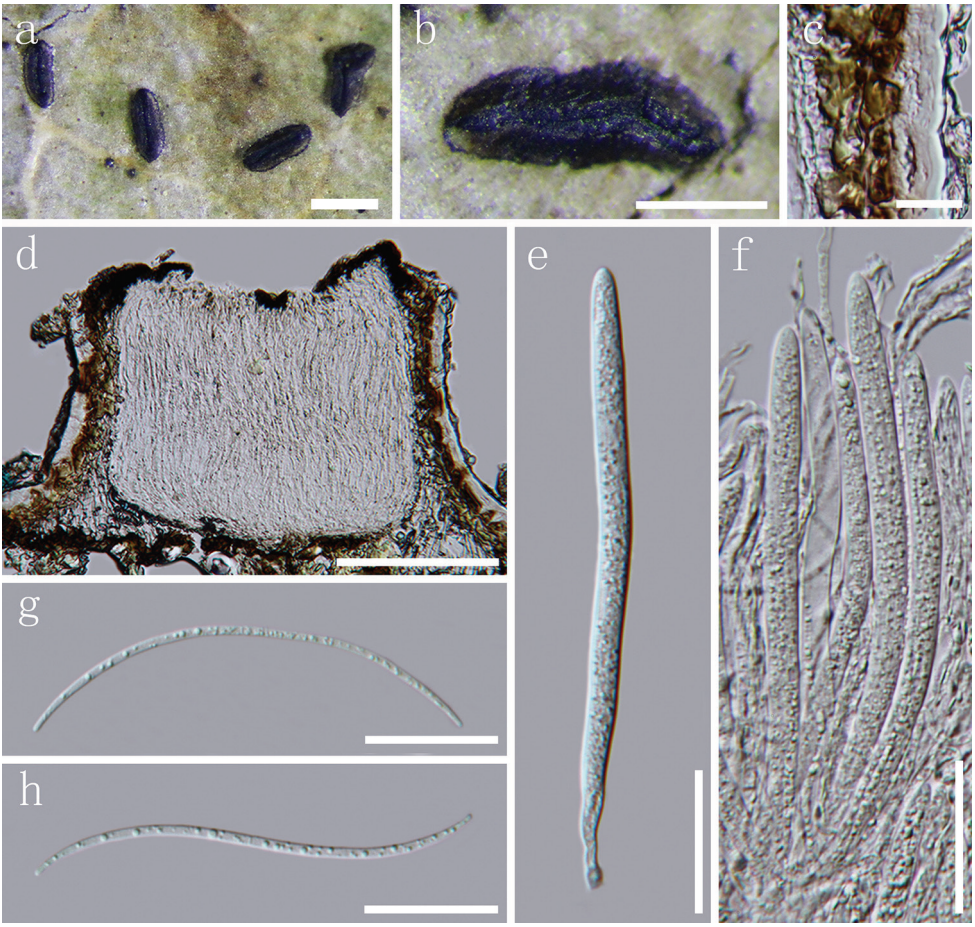


**Figure 5.** *Terriera sigmoideospora* **a, b** apothecia observed under the dissecting microscope **c** section of covering stroma **d** median vertical section through an apothecium **e** immature ascus **f** paraphyses and asci in various states of maturity **g, h** ascospores. Note: **c–h** mounted in water. Scale bar: 1 mm (**a**), 500 µm (**b**), 100 µm (**c**), 20 µm (**d–h**).

2.5 µm near the apex, covered by a thin gelatinous sheath, forming a 4–8 µm thick epithecium. *Asci* (93.5–)102–121 × 5–6 µm ($\bar{x}$ = 108.5 × 5.5 µm, n = 20), 8-spored, unitunicate, cylindrical, apex tapering to round, thin-walled, J-, without circumapical thickening. *Ascospores* 79–95 × 1.5–2 µm ($\bar{x}$ = 89.5 × 1.9 µm, n = 30), fascicle, filiform, sigmoid, tapering slightly towards the ends, hyaline, aseptate, guttulate, gelatinous sheath not observed. *Asexual morph*: Not observed.

**Material examined.** CHINA, Guizhou Province, Guiyang, dead leaves of unidentified host, 5 October 2016, J.F. Zhang, GZ-28 (MFLU 18-2297, ***holotype***); *ibid.* (GZAAS 19-1729, ***isotype***).

**Notes.** In the present phylogenetic analysis (Fig. 1), *Terriera sigmoideospora* is placed within *Terriera* and is related to *T. houjiazhuangensis* C.L. Hou & S.R. Hou

by strong statistical support (MPBP 99% and BYPP 1.00). *Terriera sigmoideospora* shares similar-sized asci with *T. houjiazhuangensis* (102–121 × 5–6 µm vs. 103–128 × 4–6 µm), but has larger ascospores (79–95 × 1.5–2 µm vs. 73–82 × 0.6–0.9 µm) (Cai et al. 2020). Besides, the ascospores of *T. houjiazhuangensis* are enveloped by an inconspicuous gelatinous sheath, while this is not observed in *T. sigmoideospora*. In addition, the comparison of the ITS gene region between these two taxa has been processed and showed that there are 19/815 (2.3%) bp differences. *Terriera pandanicola* is sister to the above two taxa; however, it is significantly distinguished from *T. sigmoideospora* as its obviously smaller asci (50–66 × 4–5 µm vs. 102–121 × 5–6 µm) and ascospores (55–78 × 1–2 µm vs. 79–95 × 1.5–2 µm) (Tibpromma et al. 2018).

## Discussion

The diversity of microfungi in many parts of the world is understudied. This is evident from the numerous new species being described from Asia and South America (Hyde et al. 2018, 2019a, 2020). With this in mind, we are studying the fungi of the Karst regions in China and Thailand, where we are also finding numerous new species (Zhang et al. 2016, 2017a, b, 2018, 2019). Our study is contributing to the knowledge of fungal diversity in the region, where species may also have biotechnological potential (Hyde et al. 2019b). Additionally, as Rhytismataceae is a relatively poorly studied group, we report on one new species from *Hypoderma* and three new *Terriera* species, thereby illustrating the diversity and potential for new discoveries of these fungi in Asia.

*Hypoderma*, a large genus in Rhytismataceae, is a complicated group. There are only a few species in this genus with sequence data, but these have shown the group to be polyphyletic (Lantieri et al. 2011; Wang et al. 2013). This is also true of the phylogenies in this study (Fig. 1). *Hypoderma* is morphologically similar to *Lophodermium* and they mainly differ on the basis of ascospore shape as the former have elliptical to cylindrical-fusiform ascospores, while the latter has filiform ascospores (Powell 1974). However, there are no molecular studies that provide a natural classification for these two genera, even though more than 35 species have been synonymized under *Lophodermium* (Index Fungorum 2020). Fresh collections and molecular sequences are required to move toward a revision of these genera.

*Terriera* is one of the few genera in Rhytismataceae that can be considered a monophyletic group, based on distinctive morphology and phylogenetic characterisation (Zhang et al. 2015). Our molecular analyses corroborate this. However, there are only nine taxa with available sequences in GenBank and most of *Terriera* species were established, based only on morphological features (Yang et al. 2011; Gao et al. 2012; Song et al. 2012; Zhou et al. 2012; Chen et al. 2013; Li et al. 2015b; Lu et al. 2015; Zhang et al. 2015; Cai et al. 2020). In the latest study (Cai et al. 2020), *T. pandanicola* was distant from *Terriera* in ITS analysis, but included in this group on the basis of concatenated LSU-mtSSU sequence data. Cai et al. (2020) indicated that this taxon should

be revised in a future study. Based on their suggestion, we checked the sequence data of *T. pandanicola* and found that the ITS sequence of this species is misidentified as it is not a related *Terriera* or even a Rhytismataceae species in BLASTn results. However, the newly generated available sequences (ITS and mtSSU) of *T. pandanicola* have been uploaded in GenBank and included in our phylogenetic analysis and the results indicated that it is a unique species in *Terriera* in the present study (Fig. 1).

## Acknowledgements

Kevin D. Hyde thanks the Thailand Research grants entitled "The future of specialist fungi in a changing climate: baseline data for generalist and specialist fungi associated with ants, *Rhododendron* species and *Dracaena* species" (Grant No. DBG6080013) and "Impact of climate change on fungal diversity and biogeography in the Greater Mekong Subregion" (Grant No. RDG6130001). Jason M. Karakehian is thanked for revising the manuscript. Dr. Shaun Pennycook (Manaaki Whenua Landcare Research, New Zealand) is gratefully thanked for advising on the fungal names. Dr. Saowaluck Tibpromma is thanked for updating the new sequences of *T. pandanicola*. Jin-Feng Zhang would like to thank Dr. Peter R. Johnston for providing literature and suggestions.

## References

Cai SR, Wang SJ, Lv T, Hou CL (2020) Three new species of Terriera (Rhytismatales, Ascomycota) from China. Mycological Progress 19: 825–835. https://doi.org/10.1007/s11557-020-01594-4

Cannon PF, Minter DW (1986) The Rhytismataceae of the Indian subcontinent. Mycological Papers 155: 1–123.

Chen JL, Lin YR, Hou CL, Wang SJ (2011) Species of Rhytismataceae on *Camellia* spp. from the Chinese mainland. Mycotaxon 118: 219–230. https://doi.org/10.5248/118.219

Chen L, Minter DW, Wang SJ, Lin YR (2013) Two new species of Rhytismataceae on fagaceous trees from Anhui, China. Mycotaxon 126: 109–120. https://doi.org/10.5248/126.109

Chevallier FF (1822) Essai sur les Hypoxylons lichenoides. Journ. Phys. Chim. Hist. Nat. 94: 28–61.

Chevallier FF (1826) Flore Generale des Environs de Paris. 1: 439–440.

Darker GD (1967) A revision of the genera of the Hypodermataceae. Botany 45: 1399–1444. https://doi.org/10.1139/b67-145

De Candolle AP (1805) Flore Francaise, edn 3, vol. 2, Paris, 600 pp.

De Notaris G (1847) Prime linee di una nuova disposizione dei Pirenomicete Isterni. Giornale Botanico Italiano 2: 5–52.

Ekanayaka AH, Hyde KD, Gentekaki E, McKenzie EHC, Zhao Q, Bulgakov TS, Camporesi E (2019) Preliminary classification of Leotiomycetes. Mycosphere 10: 310–489. https://doi.org/10.5943/mycosphere/10/1/7

Eriksson B (1970) On Ascomycetes on Diapensiales abd Ericales in Fennoscandia. I. discomycetes. Symbolae Botanicae Upsalienses 19: 1–71.

Ford DC, Williams P (2007) Karst Hydrogeology and Geomorphology. Wiley, Chichester 562 pp. https://doi.org/10.1002/9781118684986

Fries EM (1823) Systema mycologicum, sistens fungorum ordines, genera et species. 2. Gryphiswaldiae: Sumtibus Ernesti Mauritti, 610 pp.

Gao XM, Zheng CT, Lin YR (2012) *Terriera simplex*, a new species of Rhytismatales from China. Mycotaxon 120: 209–213. https://doi.org/10.5248/120.209

Gardes M, Bruns TD (1993) ITS primers with enhanced specificity for basidiomycetes-application to the identification of mycorrhizae and rusts. Molecular Ecology 2: 113–118. https://doi.org/10.1111/j.1365-294X.1993.tb00005.x

Gernandt DS, Platt JL, Stone JK, Spatafora JW, Holst-Jensen A, Hamelin RC, Kohn LM (2001) Phylogenetics of Helotiales and Rhytismatales based on partial small subunit nuclear ribosomal DNA sequences. Mycologia 93: 915–933. https://doi.org/10.2307/3761757

Hall TA (1999) BioEdit: a user-friendly biological sequence alignment editor and analysis program for Windows 95/98/NT. Nucleic Acids Symposium Series 41: 95–98.

Hernández MC, Johnston PR, Minter DW (2014) Rhytismataceae (Ascomycota) in Cuba. Willdenowia 44: 65–75. https://doi.org/10.3372/wi.44.44110

Hou CL, Lin YR, Piepenbring M (2005) Species of Rhytismataceae on needles of *Juniperus* spp. from China. Botany 83: 37–46. https://doi.org/10.1139/b04-149

Hou CL, Liu L, Piepenbring M (2007) A new species of *Hypoderma* and description of *H. rubi* (Ascomycota) from China. Nova Hedwigia 84: 487–493. https://doi.org/10.1127/0029-5035/2007/0084-0487

Hou CL, Piepenbring M (2009) New species and new records of Rhytismatales from Panama. Mycologia 101: 565–572. https://doi.org/10.3852/08-216

Huang QH, Cai YL (2006) Assessment of karst rocky desertification using the radial basis function network model and GIS technique: a case study of Guizhou Province, China. Environmental Geology 49: 1173–1179. https://doi.org/10.1007/s00254-005-0162-4

Hyde KD, Hongsanan S, Jeewon R, Bhat DJ, McKenzie EMC, Jones EBG, Phookamsak R, Ariyawansa HA, Boonmee S, Zhao Q, Abdel-Aziz FA, Abdel-Wahab MA, Banmai S, Chomnunti P, Cui BK, Daranagama DA, Das K, Dayarathne MC, de Silva NI, Dissanayake AJ, Doilom M, Ekanayaka AH, Gibertoni TB, Góes-Neto A, Huang SK, Jayasiri SC, Jayawardena RS, Konta S, Lee HM, Li WJ, Lin CG, Liu JK, Lu YZ, Luo ZL, Manawasinghe IS, Manimohan P, Mapook A, Niskanen T, Norphanphoun C, Papizadeh M, Perera RH, Phukhamsakda C, Richter C, Santiago ALCMA, Drechsler-Santos ER, Senanayake IC (2016) Fungal diversity notes 367–490: taxonomic and phylogenetic contributions to fungal taxa. Fungal Diversity 80: 1–270.

Hyde KD, Jeewon R, Chen YJ, Bhunjun CS, Calabon MS, Jiang HB, Lin CG, Norphanphoun C, Sysouphanthong P, Pem D, Tibpromma S, Zhang Q, Doilom M, Jayawardena RS, Liu JK, Maharachchikumbura SSN, Phukhamsakda C, Phooksmsak R, Al-Sadi AM, Thongklang N, Wang Y, Gafforov Y, Jones EBG, Lumyong S (2020) The numbers of fungi: is the descriptive curve flattening? Fungal Diversity 103: 219–271. https://doi.org/10.1007/s13225-020-00458-2

Hyde KD, Norphanphoun C, Chen J, Dissanayake AJ, Doilom M, Hongsanan S, Jayawardena RS, Jeewon R, Perera RH, Thongbai B, Wanasinghe DN, Wisitrassameewong K, Tibpromma S, Stadler M (2018) Thailand's amazing diversity – up to 96% of fungi in northern Thailand are novel. Fungal Diversity 93: 215–239. https://doi.org/10.1007/s13225-018-0415-7

Hyde KD, Tennakoon DS, Jeewon R, Bhat DJ, Maharachchikumbura SSN, Rossi W, Leonardi M, Lee HB, Mun HY, Houbraken J, Nguyen TTT, Jeon SJ, Frisvad JC, Wanasinghe DN, Lücking R, Aptroot A, Cáceres MES, Karunarathna SC, Hongsanan S, Phookamsak R, de Silva NI, Thambugala KM, Jayawardena RS, Senanayake IC, Boonmee S, Chen J, Luo ZL, Phukhamsakda C, Pereira OL, Abreu VP, Rosado AWC, Bart B, Randrianjohany E, Hofstetter V, Gibertoni TB, da Silva Soares AM, Plautz Jr. HL, Sotão HMP, Xavier WKS, Bezerra JDP, de Oliveira TGL, de Souza-Motta CM, Magalhães OMC, Bundhun D, Harishchandra D, Manawasinghe IS, Dong W, Zhang SN, Bao DF, Samarakoon MC, Pem D, Karunarathna A, Lin CG, Yang J, Perera RH, Kumar V, Huang SK, Dayarathne MC, Ekanayaka AH, Jayasiri SC, Xiao YP, Konta S, Niskanen T, Liimatainen K, Dai YC, Ji XH, Tian XM, Mešic A, Singh SK, Phutthacharoen K, Cai L, Sorvongxay T, Thiyagaraja V, Norphanphoun C, Chaiwan N, Lu YZ, Jiang HB, Zhang JF, Abeywickrama PD, Aluthmuhandiram JVS, Brahmanage RS, Zeng M, Chethana T, Wei DP, Réblova M, Fournier J, Nekvindová J, Barbosa RN, dos Santos JEF, de Oliveira NT, Li GJ, Ertz D, Shang QJ, Phillips AJL, Kuo CH, Camporesi E, Bulgakov TS, Lumyong S, Jones EBG, Chomnunti P, Gentekaki E, Bungartz F, Zeng XY, Fryar S, Tkalčec Z, Liang J, Li GS, Wen TC, Singh PN, Gafforov Y, Promputtha I, Yasanthika E, Goonasekara ID, Zhao RL, Zhao Q, Kirk PM, Liu JK, Yan JY, Mortimer PE, Xu JC (2019a) Fungal diversity notes 1036–1150: taxonomic and phylogenetic contributions on genera and species of fungal taxa. Fungal Diversity 96: 1–242. https://doi.org/10.1007/s13225-019-00429-2

Hyde KD, Xu JC, Rapior S, Jeewon R, Niego AGT, Abeywickrama PD, Alithmuhandiran JVS, Brahamanage RS, Brroks S, Chaiyasen A, Chethana KWT, Chomnunti P, Chepkirui C, Chuankid B, de Silva NI, Doliom M, Faulds C, Gentekaki E, Gopalan V, Kakumyan P, Harishchandra D, Hemachandran H, Hongsanan S, Karunarathna A, Karunarathna SC, Khan S, Kumla J, Jayawardena RS, Liu JK, Liu NG, Luangharn T, Macabeo APG, Marasinghe DS, Meeks D, Mortimer PE, Mueller P, Nadir S, Nataraja KN, Nontachaiyapoom S, O'Brien M, Penkhrue W, Phukhamsakda C, Ramanan US, Rathnayaka AR, Sadaba RB, Sandargo B, Samarakoon BC, Rathnayaka AR, Sadaba RB, Sandargo B, Samarakoon BC, Tennakoon DS, Siva R, Sriprom W, Suryanarayanan TS, Sujarit K, Suwannarch N, Suwunwong T, Thongbai B, Thongklang N, Wei DP, Wijesinghe SN, Winiski J, Yan JY, Yasanthika E, Stadler M (2019b) The amazing potential of fungi: 50 ways we can exploit fungi industrially. Fungal Diversity 97: 1–136. https://doi.org/10.1007/s13225-019-00430-9

Jayasiri SC, Hyde KD, Ariyawansa HA, Bhat DJ, Buyck B, Cai L, Dai YC, Abd-Elsalam KA, Ertz D, Hidayat I, Jeewon R, Jones EBG, Bahkali AH, Karunarathna SC, Liu JK, Luangsa-ard JJ, Lumbsch HT, Maharachchikumbura SSN, McKenzie EHC, Moncalvo J, Ghobad-Nejhad M, Nilsson H, Pang KL, Pereora OL, Phillips AJL, Raspé O, Rollins AW, Romero AI, Etayo J, Selcuk F, Stephenson SL, Suetrong S, Taylor JE, Tsui CKM, Vizzini A, Abdel-Wahab MA, Wen TC, Boonmee S, Dai DQ, Daranagama DA, Dissanayake AJ, Ekanayaka AH, Fryar SC, Hongsanan S, Jayawardena RS, Li WJ, Perera RH, Phookamsak R, de Silva N, Thambugala KM, Tian Q, Wijayawardene NN, Zhao RL, Zhao Q, Kang

JC, Promputtha I (2015) The Faces of Fungi database: fungal names linked with morphology, phylogeny and human impacts. Fungal Diversity 74: 3–18. https://doi.org/10.1007/s13225-015-0351-8

Jeewon R, Hyde KD (2016) Establishing species boundaries and new taxa among fungi: recommendations to resolve taxonomic ambiguities. Mycosphere 7: 1669–1677. https://doi.org/10.5943/mycosphere/7/11/4

Johnston PR (1986) Rhytismataceae in New Zealand 1. Some foliicolous species of *Coccomyces* de Notaris and *Propolis* (Fries) Corda. New Zealand Journal of Botany 24: 89–124. https://doi.org/10.1080/0028825X.1986.10409723

Johnston PR (1990) Rhytismataceae in New Zealand 3. The genus *Hypoderma*. New Zealand Journal of Botany 28(2): 159–183. https://doi.org/10.1080/0028825X.1990.10412355

Johnston PR (2001) Monograph of the monocotyledon-inhabiting species of *Lophodermium*. Mycological Papers 176: 1–239.

Johnston PR, Park D (2007) Revision of the species of Rhytismataceae reported by Spegazzini from south America. Boletín de la Sociedad Argentina de Botánica 42: 87–105.

Johnston PR, Quijada L, Smith CA, Baral H-O, Hosoya T, Baschien C, Pärtel K, Zhuang WY, Haelewaters D, Park D, Carl S, López-Giráldez F, Wang Z, Townsend JP (2019) A multigene phylogeny towards a new phylogenetic classification of Leotiomycetes. IMA Fungus 10: 1–22. https://doi.org/10.1186/s43008-019-0002-x

Koorders SH (1907) Botanische Untersuchungen. Verhandelingen Koninklijke Nederlandse Akademie van Wetenschappen Afdeling Natuurkunde 13: 1–263.

Lantieri A, Johnston PR, Park D, Lantz H, Medardi G (2011) *Hypoderma siculum* sp. nov. from Italy. Mycotaxon 118: 393–401. https://doi.org/10.5248/118.393

Lantz H, Johnston PR, Park D, Minter DW (2011) Molecular phylogeny reveals a core clade of Rhytismatales. Mycologia 103: 57–74. https://doi.org/10.3852/10-060

Li Q, Wang SJ, Chen YX, Tang YP, Lin YR (2015a) *Terriera transversa* sp. nov. from Hainan, China. Mycotaxon 130: 893–898. https://doi.org/10.5248/130.893

Li Q, Wu Y, Lu DD, Xu YF, Lin YR (2015b) A new species of *Terriera* (Rhytismatales, Ascomycota) on *Photinia villosa*. Mycotaxon 130: 27–31. https://doi.org/10.5248/130.27

Li ZJ, Cao N, Chen HF, Taylor JE, Hou CL (2014) New species and new records of Rhytismataceae from Japan. Mycological Progress 13: 951–958. https://doi.org/10.1007/s11557-014-0979-x

Liu B, Zhang M, Bussmann WR, Liu HM, Liu YY, Peng YD, Zu KL, Zhao YM, Liu ZB, Yu SX (2018) Species richness and conservation gap analysis of karst areas: A case study of vascular plants from Guizhou, China. Global Ecology and Conservation 16: e00460. https://doi.org/10.1016/j.gecco.2018.e00460

Lu DD, Yang MS, Wang SJ, Lin YR (2015) *Terriera intraepidermalis* sp. nov. on *Photinia prunifolia* from China. Mycosystema 34(6): 1025–1030. https://doi.org/10.13346/j.mycosystema.140169

Lumbsch HT, Huhndorf SM (2007) Outline of Ascomycota-2007. Myconet 13: 1–58.

Minter DW, Sharma MP (1982) Three Species of *Lophodermium* from the Himalayas. Mycologia 74: 702–711. https://doi.org/10.1080/00275514.1982.12021576

Nylander J (2008) MrModeltest2 version 2.3 (program for selecting DNA substitution models using PAUP*). Evolutionary Biology Centre, Uppsala, Sweden

Page RDM (1996) Tree View: An application to display phylogenetic trees on personal computers. Bioinformatics 12: 357–358. https://doi.org/10.1093/bioinformatics/12.4.357

Powell PE (1974) Taxonomic studies in the genus Hypoderma. Thesis (Ph.D.) Cornell University, Ithaca.

Rannala B, Yang Z (1996) Probability distribution of molecular evolutionary trees: a new method of phylogenetic inference. Journal of Molecular Evolution 43: 304–311. https://doi.org/10.1007/BF02338839

Ronquist F, Teslenko M, van der Mark P, Ayres DL, Darling A, Höhna S, Larget B, Liu L, Suchard MA, Huelsenbeck JP (2012) MrBayes 3.2: efficient Bayesian phylogenetic inference and model choice across a large model space. Systematic Biology 61: 539–542. https://doi.org/10.1093/sysbio/sys029

Song JF, Liu L, Li YY, Hou CL (2012) Two new species of *Terriera* from Yunnan Province, China. Mycotaxon 119: 329–335. https://doi.org/10.5248/119.329

Species Fungorum (2020) CABI Databases. http://www.speciesfungorum.org/ [Accessed December 2020]

Swofford DL (2002) PAUP 4.0 b10: Phylogenetic analysis using parsimony. Sinauer Associates, Sunderland.

Tanney JB, Seifert KA (2017) *Lophiodermium resinosum* sp. nov. from red pine (*Pinus resinosa*) in Eastern Canada. Botany 95: 773–784. https://doi.org/10.1139/cjb-2017-0012

Terrier CA (1942) Essai sur la systématíque des Phacidiaceae (Fr.) sensu Nannfeldt (1932). Matériaux Flore Crytogamique Suise 9: 1–99.

Tian HZ, Yang Z, Wang S, Hou CL, Piepenbring M (2013) A new species and phylogenetic data for *Nematococcomyces*. Botany 91: 592–596. https://doi.org/10.1139/cjb-2012-0306

Tibpromma S, Hyde KD, McKenzie EHC, Bhat DJ, Phillips AJL, Wanasinghe DN, Samarakoon MC, Jayawardena RS, Dissanayake AJ, Tennakoon DS, Doilom M, Phookamsak R, Tang AMC, Xu JC, Mortimer PE, Promputtha I, Maharachchikumbura SSN, Khan S, Karunarathna SC (2018) Fungal diversity notes 840–928: micro-fungi associated with Pandanaceae. Fungal Diversity 93: 1–160. https://doi.org/10.1007/s13225-018-0408-6

Wallroth FG (1833) Flora Cryptogamica Germaniae. Pars posterior. Norimbergiae, 923 pp.

Wang S, Taylor JE, Hou CL (2013) Species of Rhytismatales on *Berberis* from China. Mycological Progress 12: 629–635. https://doi.org/10.1007/s11557-012-0868-0

White TJ, Bruns T, Lee S, Taylor J (1990) Amplification and direct sequencing of fungal ribosomal RNA genes for phylogenetics. In: Innis MA, Gelfand DH, Shinsky JJ, White TJ (Eds) PCR protocols: a guide to methods and applications. Academic Press, New York, 315–322. https://doi.org/10.1016/B978-0-12-372180-8.50042-1

Wijayawardene NN, Hyde KD, Al-Ani LKT, Tedersoo L, Haelewaters D, Rajeshkumar KC, Zhao RL, Aptroot A, Leontyev DV, Saxena RK, Tokarev YS, Dai DQ, Letcher PM, Stephenson SL, Ertz D, Lumbsch HT, Kukwa M, Issi IV, Madrid H, Phillips AJL, Selbmann L, Pfliegler WP, Horváth E, Bensch K, Kirk PM, Kolaříková K, Raja HA, Radek R, Papp V, Dima B, Ma J, Malosso E, Takamatsu S, Rambold G, Gannibal PB, Triebel D, Gautam AK, Avasthi S, Suetrong S, Timdal E, Fryar SC, Delgado G, Réblová M, Doilom M, Dolatabadi S, Pawłowska JZ, Humber RA, Kodsueb R, Sánchez-Castro I, Goto BT, Silva DKA, de Souza FA, Oehl F, da Silva GA, Silva IR, Błaszkowski J, Jobim K, Maia LC, Barbosa FR, Fiuza

PO, Divakar PK, Shenoy BD, Castañeda-Ruiz RF, Somrithipol S, Lateef AA, Karunarathna SC, Tibpromma S, Mortimer PE, Wanasinghe DN, Phookamsak R, Xu J, Wang Y, Tian F, Alvarado P, Li DW, Kušan I, Matočec N, Mešić A, Tkalčec Z, Maharachchikumbura SSN, Papizadeh M, Heredia G, Wartchow F, Bakhshi M, Boehm E, Youssef N, Hustad VP, Lawrey JD, Santiago ALCMA, Bezerra JDP, Souza-Motta CM, Firmino AL, Tian Q, Houbraken J, Hongsanan S, Tanaka K, Dissanayake AJ, Monteiro JS, Grossart HP, Suija A, Weerakoon G, Etayo J, Tsurykau A, Vázquez V, Mungai P, Damm U, Li QR, Zhang H, Boonmee S, Lu YZ, Becerra AG, Kendrick B, Brearley FQ, Motiejūnaitė J, Sharma B, Khare R, Gaikwad S, Wijesundara DSA, Tang LZ, He MQ, Flakus A, Rodriguez-Flakus P, Zhurbenko MP, McKenzie EHC, Stadler M, Bhat DJ, Liu JK, Raza M, Jeewon R, Nassonova ES, Prieto M, Jayalal RGU, Erdoğdu M, Yurkov A, Schnittler M, Shchepin ON, Novozhilov YK, Silva-Filho AGS, Gentekaki E, Liu P, Cavender JC, Kang Y, Mohammad S, Zhang LF, , Xu RF, Li YM, Dayarathne MC, Ekanayaka AH, Wen TC, Deng CY, Pereira OL, Navathe S, Hawksworth DL, Fan XL, Dissanayake LS, Kuhnert E, Grossart HP, Thines M (2020) Outline of fungi and fungus-like taxa. Mycosphere 11: 1060–1456. https://doi.org/10.5943/mycosphere/11/1/8

Wijayawardene NN, Hyde KD, Lumbsch HT, Liu JK, Maharachchikumbura SSN, Ekanayaka AH, Tian Q, Phookamsak R (2018) Outline of Ascomycota: 2017. Fungal Diversity 88: 167–263. https://doi.org/10.1007/s13225-018-0394-8

Wu Y, Wang SJ, Meng YQ, Tang YP, Lin YR (2015) *Terriera fici* sp. nov. on *Ficus vasculosa* from Hainan Province, China. Mycotaxon 130: 1111–1116. https://doi.org/10.5248/130.1111

Yang ZZ, Lin YR, Hou CL (2011) A new species of *Terriera* (Rhytismatales, Ascomycota) from China. Mycotaxon 117: 367–371. https://doi.org/10.5248/117.367

Zhang JF, Liu JK, Hyde KD, Chen YY, Liu YX, Liu ZY (2017a) Two new species of *Dyfrolomyces* (Dyfrolomycetaceae, Dothideomycetes) from karst landforms. Phytotaxa 313: 267–277. https://doi.org/10.11646/phytotaxa.313.3.4

Zhang JF, Liu JK, Hyde KD, Liu YX, Bahkali AH, Liu ZY (2016) *Ligninsphaeria jonesii* gen. et. sp. nov., a remarkable bamboo inhabiting ascomycete. Phytotaxa 247: 109–117. https://doi.org/10.11646/phytotaxa.247.2.2

Zhang JF, Liu JK, Hyde KD, Yang W, Liu ZY (2017b) Fungi from Asian Karst formations II. Two new species of *Occultibambusa* (Occultibambusaceae, Dothideomycetes) from karst landforms of China. Mycosphere 8: 550–559. https://doi.org/10.5943/mycosphere/8/4/4

Zhang JF, Liu JK, Jeewon R, Wanasinghe DN, Liu ZY (2019) Fungi from Asian Karst formations III. Molecular and morphological characterization reveal new taxa in Phaeosphaeriaceae. Mycosphere 10: 202–220. https://doi.org/10.5943/mycosphere/10/1/3

Zhang JF, Liu JK, Ran HY, Khongphinitbunjong K, Liu ZY (2018) A new species and new record of *Lophiotrema* (Lophiotremataceae, Dothideomycetes) from karst landforms in southwest China. Phytotaxa 379: 169–179. https://doi.org/10.11646/phytotaxa.379.2.5

Zhang TT, Tong X, Lin YR, Hou CL (2015) A new species and a new combination of *Terriera* based on morphological and molecular data. Mycological Progress 14: 1–6. https://doi.org/10.1007/s11557-015-1078-3

Zhaxybayeva O, Gogarten JP (2002) Bootstrap, Bayesian probability and maximum likelihood mapping: exploring new tools for comparative genome analyses. BMC Genomics 3: 1–4. https://doi.org/10.1186/1471-2164-3-4

Zheng Q, Lin YR, Yu SM, Chen L (2011) Species of Rhytismataceae on *Lithocarpus* spp. from Mt Huangshan, China. Mycotaxon 118: 311–323. https://doi.org/10.5248/118.311

Zhou F, Wang XY, Zhang L, Lin YR (2012) *Terriera angularis* sp. nov. on *Illicium simonsii* from China. Mycotaxon 122: 355–359. https://doi.org/10.5248/122.355

Zoller S, Scheidegger C, Sperisen C (1999) PCR primers for the amplification of mitochondrial small subunit ribosomal DNA of Lichen-forming Ascomycetes. The Lichenologist 31: 511–516. https://doi.org/10.1006/lich.1999.0220

## Supplementary material 1

**Dataset for molecular analyses**

Authors: Jin-Feng Zhang, Jian-Kui Liu, Kevin D. Hyde, Anusha H. Ekanayaka, Zuo-Yi Liu

Data type: phylogenetic

Explanation note: The dataset of combined of LSU_ITS_mtSSU to build the phylogenetic tree.



Link: https://doi.org/10.3897/mycokeys.76.58465.suppl1